Technical note TN-2009-00150

Issued: 04/2009

Event related (de-)synchronization patterns in actual and imagined hand movements

BCI application

A. Espinosa Manzanal

G. Garcia Molina and Ferran Marqués

Philips Research Eindhoven

Concerns: Interim Report

Period of Work: September 2008 - April 2009

Notebooks: None

Authors' address A. Espinosa Manzanal arnau.espinosa@philips.com

G. Garcia Molina gary.garcia@philips.com

Title: Event related (de-)synchronization patterns in actual and imagined hand movements

Author(s): A. Espinosa Manzanal ; G. Garcia Molina and Ferran Marqués

Reviewer(s): Vojkan Mihajlovic

Technical Note: TN-2009-00150

Subcategory:

Project: Body & Mind Enhancers for Relaxation, Sleep and Performance (2008-0359)
http://www.philips.com

Customer: Philips Research

Keywords: Brain Computer Interface (BCI), Electroencephalogram (EEG), Motor imagery, Event-Related Desynchronization/Synchronization (ERD/ERS), Common Spatial Patterns (CSP), Principal Component Analysis (PCA), Neural Network.

Abstract: This project presents different signal processing techniques, such as Principal Component Analysis (PCA) and Common Spatial Patterns (CSP), applied to characterize the reactivity of central rhythms in the alpha and beta bands during self paced voluntary and imaginary movement. The idea is to allow people to control devices, or interact with machines by simply thinking. To do so, we monitor the brain activity using electroencephalogram (EEG) measurements which record the signals from electrodes positioned on the scalp.

The objective is to use motor imagery signals to build a brain computer interface, able to learn from data analyzed before, using the properties of neural networks. The possibility of designing an intuitive communication system between a brain and a computer, available to be operated by everyone, even by people with severe motor impairments, is the main objective of this study.

Conclusions: The study of Common Spatial Patterns (CSP) offer a great pathway to the brain computer interfaces over electroencephalogram (EEG) signals. Mental activity of real and imaginary hand movements can be used to extract significant patterns from different subjects. Principal Component Analysis (PCA) and CSP method allows maximizing a mental state population over another different mental state population; a neural network is used to differentiate between both populations.

The conclusions of this thesis are:

(a) Motor imagery movement of hands have tested and verified the actual theory of ERS/ERD. Real movement too.

(b) Principal component analysis reduces the correlation between EEG signals from two mental states.

(c) The CSP method is used for spatial analysis of EEG signals. The spatial filters designed in accordance with common spatial patterns, for the reactive frequency bands, represent a great ability to deal with multi channel EEG signals. This method gives features that characterize the ERD.

(d) Single layer neural network allows to make an optimal extraction of information and is an adaptive system that can be used in online analysis of the data.

(e) Variance analysis allows founding the interactions of the algorithm that are more significant and allows to study the significance of this result.

The final conclusion in this project is that the suggested techniques have shown great potential, and further research on this topic is recommended.

Als meus pares, Josep i Rosa,
pel seu amor incondicional,

a la meva germana, Júlia, per
aguantar-me i animar-me,
conscient i inconscientment,
encara que no ho demani,

al nen que vaig ser,
per acompanyar-me sense
demanar gaires explicacions.

Contents

List of Figures

List of Tables

Acknowledgments

"You've had a hard time?
I've been here five years,
they only hung me the
right way up yesterday."
Monty Python, Life of Brian

BEFORE START, I want to explain the use of more than one language, in my defense I just say that the following words are *From the Heart*, and they speak more than one idiom.

This report documents the Master Thesis research work of 8 months in the Brain Computer Interface project at Philips Research on the High Tech Campus in Eindhoven, Netherlands. It has been a long way to arrive there and it would never have been possible for me to accomplish without the help, support and encouragement from many people.

First of all I wish to express my gratitude to Dr. Gary Nelson Garcia Molina for giving me the opportunity to do this MSc project in the Experience Processing group of Philips, under his tutelage and supervision. For entrusting and introducing me in the Brain Computer Interfaces world, allowing me to star in this discipline that is rather new and offers therefore a broad range of unexplored topics. For his support and guidance to tackle the problems that have appeared during the elaboration and the ideas that make possible finish this work. I got the same words for Dr. Vojkan Mihajlovic who introduced me in his demo and provide me the possibility of participating in a real application of BCI.

Furthermore, I'd want to thank Dr. Dmitri Chestacov and, for extension, all the people that work in Philips research, without their clusters meetings and discussions the result would have not been the same. And, of course, I'm thankful to my colleagues who volunteered to participate as test subjects in this study.

I am especially grateful to Dr. Ferran Marqués, my project's supervisor, tutor and teacher of Technical University of Catalonia. To offer the challenge to make my MSc project in Spain in Philips and to his never ending encouragement words and his passion in teaching and researching that were a source of inspiration for me.

Eindhoven, April 2009
Arnau ESPINOSA

Resumen

LA TECNOLOGÍA ACTUAL no permite a las personas controlar periféricos o interactuar con máquinas mediante el uso del cerebro. Los sistemas actuales diseñados para facilitar la vida a personas incapacitadas no permiten controlar una silla de ruedas o un ratón de ordenador, o a personas con discapacidad cerebral controlar un sintetizador vocal usando el pensamiento, o simplemente estados mentales.

De todos modos, la tecnología permitirá estos avances pronto. Investigaciones realizadas por científicos en las pasadas décadas muestran que el uso de bioseñales puede mejorar la cualidad y la eficiencia de los diagnósticos de una enfermedad. Al mismo tiempo que los científicos avanzan en el desarrollo de la ciencia neuronal, el cerebro humano sigue siendo desconocido. Avances recientes en neurociencia, psicología, procesado de señal y inteligencia artificial están haciendo posible desarrollar sistemas directos de conexión mente-ordenador. Un interfaz cerebro-ordenador, BCI en siglas en inglés, es un sistema que permite a las personas interactuar con su entorno sin usar actividad muscular.

Este proyecto se enmarca en el campo de los BCI y presenta diferentes técnicas de procesados de señal aplicadas para investigar la reacción de ritmos centrales en las bandas de frecuencia cerebral alpha y beta durante movimiento real e imaginario de las extremidades. El objetivo a largo plazo de este proyecto es construir un sistema de comunicación intuitivo, capaz de ser usado por cualquiera, incluso por personas con problemas de movilidad.

La idea es permitir el control de periféricos o la interacción con máquinas mediante simple pensamiento. Para hacer esto se monitoriza la actividad cerebral usando medidas de electroencefalograma (EEG) extraídas de electrodos situados en el cuero cabelludo. El objetivo es usar señales del motor imaginario, que podemos definir como, pensar en mover una extremidad, por ejemplo una mano, un pie, o la lengua, pero sin ejecutar el moviendo real de la extremidad.

Abstract

CURRENT TECHNOLOGY does not allow people to control devices, or interact with machines by simply thinking. The current systems for making the life easier to disabled people do not permit to control a wirehair or a computer mouse, or to people with mental disease to control a vocal synthesizer just using their brain, or some mental states.

Even though, knowledge will permit this soon. Scientific research over the past decades has shown that recordings of bio-physiological signals may help in the improvement of the quality and efficiency for disease diagnosis. At the same time that the scientific advance in neuroscience, the human brain is less unknown. Recent advances in neuroscience, psychology, signal processing and machine learning have made possible to develop direct brain-computer communication systems. A brain computer interface, BCI, is a technical system that allows a person to be connected with the external world without relying on muscle activity.

This Master's Thesis has been carried out within the context of BCI and presents different signal processing techniques applied to investigate the reactivity of central rhythms in the alpha and beta bands during self paced voluntary and imaginary movement. The long-term goal of the project is to build an intuitive communication system that everyone would be able to use, even by people with severe motor impairments.

The idea is to allow people to control devices, or interact with machines by simply thinking. To do so, we monitorize the brain activity using electroencephalogram (EEG) measurements which record the signals from electrodes positioned on the scalp. The objective is to use motor imagery, in other words, to think about moving a limb, for instance the hands, the feet, or the tongue but without executing the movement. This study explains the details of the algorithms used to identify motor imagery patterns from the EEG.

To achieve this task, the design and implementation of a Matlab algorithm has been carried out. It can be divided in tree different parts: signal preprocessing, features extraction and decision.

The objective of the first main part, preprocessing, is the conversion of the continuous RAW_EEG recordings into artifact-free trials of spontaneous EEG signal, to prepare the signals for further processing. For each subject used in the experiments, continuous EEG recordings are structured into short-time trials and, after artifact rejection step, advanced digital signal processing techniques are used to extract ERS/ERD features, personalized for the brain frequency bands, from the multi channel EEG.

Common processing is performed in the second part of the algorithm. The different features from subjects are combined to detect and quantify intra-trial epochs of significant differences between mental states. Based in Principal Component Analysis (PCA) and Common Spatial Patterns (CSP) theory, the filtered EEG signal in the frequency of interest is processed to maximize the patterns that are unique for a mental state and minimize all the others. A set of training signals, chosen in the preprocessing part, is required for training the algorithm and the CSP technique, making possible that the algorithms learn and compute automatically patterns of new data cases.

The enrolling process for new cases is the aim of the third part of the algorithm. Based in a neural network, the machine learning method is the tool for the online analysis of single-trial brain data.

The results of the study indicate that the EEG signals contain extractable information that characterize the performed movements. The methods are prove to be effective and provide evidence for the existence of the distinct reactivity patterns which are the basis of the feature extraction.

Keywords: Brain Computer Interface (BCI), Electroencephalogram (EEG), Alpha rhythms, Beta rhythms, Motor imagery, Event-Related Desynchronization/Synchronization (ERD/ERS), Common Spatial Patterns (CSP), Principal Component Analysis (PCA), Neural Network.

Section 1

Introduction

1.1 Introduction to Brain Computer Interfaces

HUMANS HAVE BEEN ALWAYS FASCINATED by the mystery of life, and have tried to understand better and better how the human body works. During the last centuries, the medicine made great progress in the field of the human body, now we know how the body works and our knowledge about the mechanisms that make it possible, are continuously growing up.

Figure 1.1: Plato (left) and Aristotle (right), a detail of *The School of Athens*, a fresco by Raphael. Aristotle gestures to the earth, representing his belief in knowledge through empirical observation and experience, while holding a copy of his *Nicomachean Ethics* in his hand, whilst Plato gestures to the heavens, representing his belief in *The Forms*.

During many years mankind has investigated and discovered that some electrical phenomena is involved in human physiology [9]. Since Aristotle (1.1), about 340 B.C., wrote: *"The torpedo narcotizes the creatures that it want to catch overpowering them by the strength of a shock that is resident in its body"*, introducing the fact that have existed electrical phenomena associated with living tissues. Until the first signal recorded by Alexander Muirhead, in 1869, from the electrical current induced in the vicinity of the heart, the way has been long, and we still are in an embryonic stage.

Over time, and with the invention of high gain amplifiers, it became finally possible to record currents from the scalp. In 1929, the German psychiatrist Hans Berger (1.2) was the first to use scalp electrodes and found that existed some rhythmic in these recorded current fluctuations, particularly in the back of the head [10]. He called this pattern the alpha-rhythm, shown in figure 1.3.

Figure 1.2: Hans Berger, *(May 21, 1873 - June 1, 1941)*, is known as the first to record electroencephalograms from human subjects and is the discoverer of the rhythmic Alpha brain waves.

More recently, in the last part of 20th century, the incorporation of computers for research purposes and their high computational power made our possibilities increase, not only in the knowledge, even in the relation between the human and the world that is between us. A new option appears, the communication between a human brain and a machine. The new possibilities offered by this field, called bioinformatics, seem to be unlimited and have opened the way to new degrees of understanding.

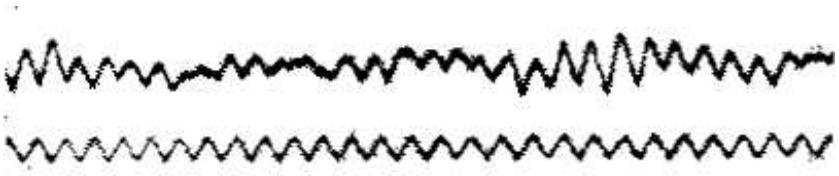

Figure 1.3: This image is one of the first EEGs, appearing in Berger's First Report. It is a portion of fig. 13 from Berger's first publication on EEG: [1] Archives für Psychiatrie. 1929.

Now, with the help of computers, and with the appearance of advanced techniques in digital signal processing [11] and pattern recognition [12], it becomes possible to start to extract relevant information from Electroencephalogram signals recorded from the human brain. However, neuroscience is a rather new discipline, and our knowledge about the mechanisms in the brain is still very low, but it helps to understand better how mechanisms work in the body. Nowadays, medical signal processing opens a new broad range of technological applications which can help researchers, clinicians and surgeons in their work, and can also lead to the creation of everyday-life objects like brain computer interfaced (BCI) systems [13].

1.2 The study

Recent advances in neuroscience, psychology, signal processing, machine learning and hardware equipment made possible to develop direct brain-computer communication systems. A Brain-Computer Interface (BCI) is a communication system in which the messages or commands that the subject sends to the external world do not pass through the normal brain output pathways of peripheral nerves and muscles [14]. As any communication system a BCI is provided with inputs (electrophysiological signals resulting from brain activity monitoring), outputs (actions executed on an active device), elements that take and transform the data between inputs and outputs, and a protocol that determines its operation. BCI applications include cursor positioning, spelling programs, and control of external devices [15], as well as many other applications.

In the figure 1.4 we show a detailed scheme of the processing steps used in the first part of the system, it helps to have a global vision of the parts that interact in the algorithm. In fact, the RAW_EEG_class 1 or 2, used as input data coming from a recording system called Biosemi 32, which performs implicitly a pre-band pass filter, and takes the scalp signal with a sample frequency of 2048 Hz.

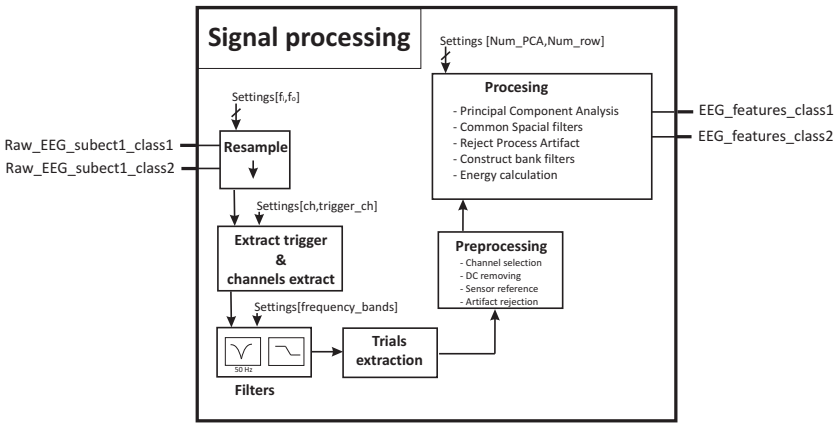

Figure 1.4: Detailed scheme of the processing steps used in the first part of the system. It provides a global vision of the parts that interact in the algorithm for each subject.

From this "raw" signal we have to extract the trigger signal add it in one of the additional channels of the data and select the channels that we will use in the study. The trigger can be either an acoustic or visional signal recorded from external sensor. Thereby we can study the differences between visual or audio evoked potentials in the motor cortex. The channel extraction permits to differ between data channels or auxiliary channels that bring additional data like the trigger channel.

The study of the brain frequency bands, alpha and beta, provides the most important features, for this reason we will focus our study on them both, [7]. We use an infinite impulse response filter to extract these bands for each subject. These personalized bands are calculated using Fourier [11] systems and is one of the settings that personalize the algorithm for each subject.

Using the trigger signal we extract the trials from the raw data, obtaining a matrix of trials

that contain the recorded brain activity data in the moment of interest, usually real or imaginary movements. Afterwards, we make a channel selection using a preprocessing block with different analysis techniques, such as a Direct Current (DC) removing, we take a sensor reference and apply an artifact rejection. These actions, permits focussing the analysis on the motor cortex or any brain zone that we consider relevant for the study, without artifact and implicit data or brain signals that do not contribute to extract useful information. These features, extracted from each subject of the two classes of brain states, will later be combined to recognize some significant differences between the two sets and a classifier with a neuronal network will be created.

1.2.1 Project motivation

Maybe the most interesting and important application of the BCI technology today is medical rehabilitation and increasing life applications for people with severe motor impairments. As the operation of a true brain computer interface does not require any muscle activity, a communication system based on BCI techniques could be used by everyone.

The purpose of a brain computer interface in this case is to capture those signals directly from the brain and convert them into a form that can be understood by a computer or other device. The signals could then be used to operate for example a wheelchair, an artificial limb or a word processor, thereby providing the patient with communication channels previously cut-off by the disease.

This project aims to present different signal processing techniques, like Principal Component Analysis (PCA) and Common Spatial Patterns (CSP), and understand their application in the field of BCIs. Furthermore, we will use the acquired knowledge to investigate the reactivity of central rhythms in the alpha and beta bands of different subject during self paced voluntary and imaginary movement. The goal is to allow people to control devices, or interact with machines by simply thinking. To do so, we monitor the brain activity using a Biosemi system that takes the electroencephalogram (EEG) signals recorded from electrodes positioned on the scalp.

EEG signal processing represents a newer promising way for the development of practical BCIs [11]. The analysis of EEG signals, their multivariate nature and relatively low signal - to - noise ratio, is a real challenge. This thesis aims at identifying the key features characterizing the EEG signals that result from the performance of typical mental tasks used in BCI systems. To do that, appropriate tasks must be carried out to encourage the brain to generate reproducible stable patterns of activity, like brain oscillations (ERD/ERS) patterns. Those patterns are associated with cortical areas and connected to the brains normal motor output channels.

1.2.2 Objectives

The main challenges of this thesis can be summarized as follows:

- Design a preprocessing step for recording EEG data, filtered in interested bands for each subject, and clean of any artifacts.

- Demonstrate the theory of variant alpha peak for different subject and age. Detect for all the subjects the reactive frequency bands of their brains.
- Verification of the ERS/ERD theory, the right brain hemisphere controls the left part of the body and vice versa.
- Characterization of the ERD/ERS patterns in the frequency bands found in the previous step.
- Finding a linear combination of the electrodes for each subject and thus providing a spatial analysis of the EEG signals, using Principal Component Analysis (PCA) and Common Spatial Patterns (PCA).
- Design a Neuronal Network able to differentiate the kinds of features extracted from different EEG signals and show the results. Make the system capable for an online analysis and to learn from data analyzed previously.
- Focus the study in the brain activity created by real movement action and motor imagery. Extract the most relevant and common (between different subjects) patterns and characteristics. Perform the experiments on 4 male subjects with different ages and record their electroencephalograms signals.
- Elaborate a compilation of theoretical aspects of CSP in motor imagery and demonstrate the usefullness of CSP and PCA in processing EEG signals and BCIs.
- Finally, the main objective of this study is to design a communication system between a brain and a computer, available to everyone, even by people with severe motor impairments.

1.2.3 Organization

In this section the organization of this report is shown, it is divided into four main steps:

- In the first section, the necessary theory to understand our research is described. It first starts with a brief explanation of the mechanisms involved in the brain to finally explain how it is possible to understand the recorded signals to infer conclusions about these mechanisms.
- In the second section, the designed methods, using advanced signal processing techniques, are used in order to extract, from the recorded EEG signals, possible relevant features from each subject. These features are combined to detect and quantify relevant differences between mental states. Using CSP algorithms some filter banks are created for maximizing the variance of one class of mental state while minimizing the others.

  When the transform matrices have been created, a neural network is trained to automatically quantify patterns in new cases. Using the same signal processing techniques than in training data, features are extracted from new EEG recorded signals and their values are used as input for the classifier, detecting to which class of mental state it belongs.

- Finally, in the last part, analysis of results are shown like the characteristics of different subjects during cognitive task which could be useful for researchers to understand better the human brain and its process.

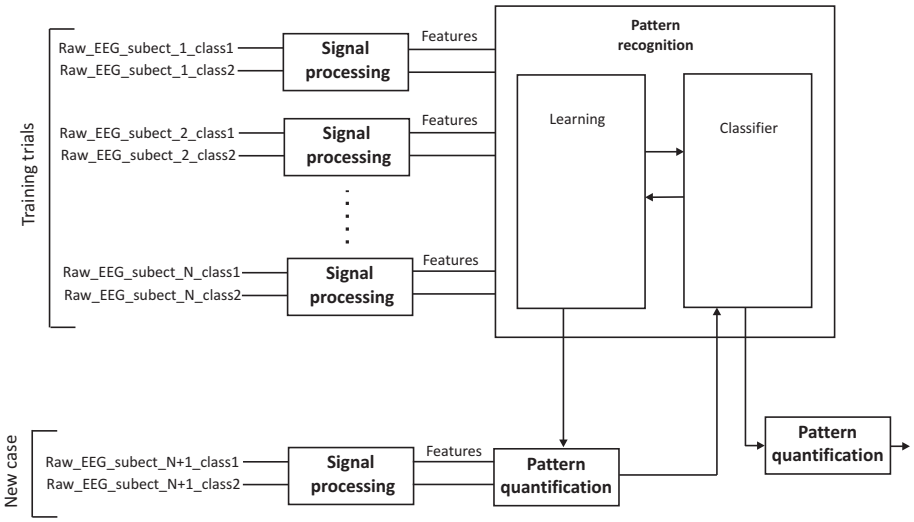

Figure 1.5: General description of the organization of our algorithm that contains all the steps named before.

Section 2

Background

THE LAST FRONTIER of the biological sciences is to understand the biological basis of consciousness and the mental process by which we perceive, act, learn, and remember. In the last two decades it has become possible to establish a general plan for the function of cells, a plan that provides a common conceptual framework for all the cell biology, including cellular cells.

Such a comprehensive approach depends on the view that all behavior is the result of a brain function. What we commonly call the mind is a set of operations carried out by the brain. The actions of the brain underlie not only relatively simple motor behaviors such as walking or eating, but all the complex cognitive actions that we believe are quite essentially human, such as thinking, speaking, and creating works of art. As a corollary, all the behavioral disorders that characterize psychiatric illness are disturbances of the brain function.

Figure 2.1: Hypothetic representation of the brain.

Background is necessary to introduce the reader to some concepts, definitions and conventions about the organization of the nervous system and the operations of the brain. This chapter is focused in this background and the electrical nature of the human nervous system. We would start our description from a macroscopic point of view to finally concentrate on the microscopic phenomena, focusing in background information related to brain computer interfaces in motor imagery. Specifically focus on the information related to the physiology of movements recorded by EEG and that describe the changes that occur in the EEG rhythm within specific frequency bands and location of cortex, namely *Event Related Desynchronisation/Synchronisa-*

tion (ERD/ERS).

Central Nervous System	Brain	Prosencephalon	Telencephalon	Rhinencephalon, Amygdala, Hippocampus, Neocortex, Lateral ventricles	
			Diencephalon	Tectum, Cerebral peduncle, Pretectum, Mesencephalic duct	
		Brain stem	Mesencephalon	Metencephalon	Pons, Cerebellum
			Rhombencephalon	Myelencephalon	Medulla oblongata
	Spinal cord				

Figure 2.2: Parts that form the Central Nervous System.

2.1 Macroscopic architecture of the brain

The human brain is considered to be the most complex organ in the body and together with the spinal cord, form the central nervous system (CNS). This central nervous system mainly initiates, manages and coordinates thoughts, movements or general control actions. It is a huge network, composed of several entities, which process, in real-time, many number of signals to maintain the body in a healthy state and to perform specific tasks.

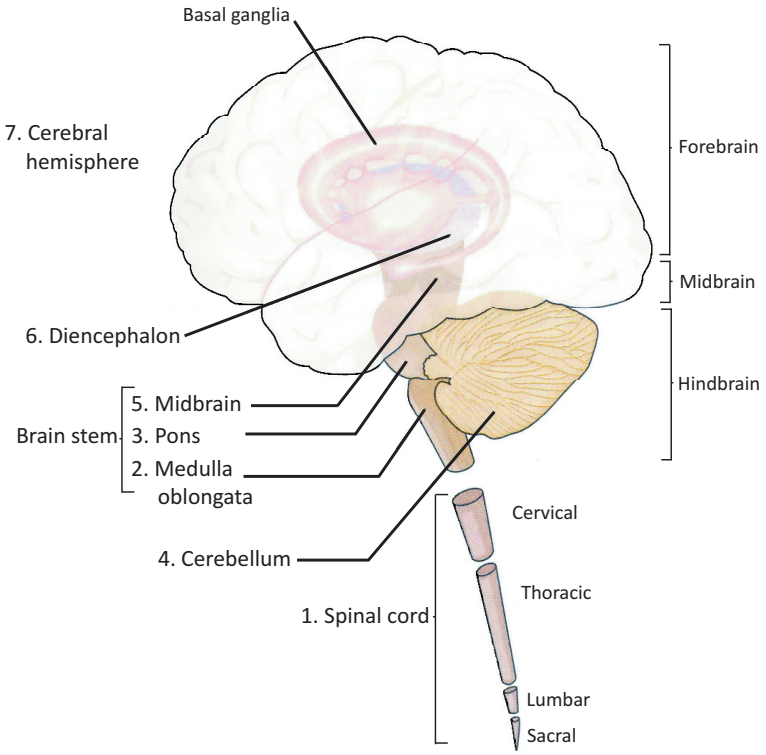

Figure 2.3: The Central Nervous System can be divided into seven main parts. From [2]

The central nervous system is a bilateral and essentially symmetrical structure with seven main parts: the spinal cord, medulla oblongata, pons, cerebellum, midbrain, diencephalon, and the cerebral hemispheres (figure 2.3), [2]. Radiographic imaging techniques have made it possible to visualize these structures in living subjects. Through a variety of experimental methods,

such images of the brain can be obtained while the subjects are engaged in specific tasks, which then can be related to the activities of discrete regions of the brain. As a result, Gall's original idea that different regions are specialized for different functions is now accepted as one of the cornerstones of modern brain science.

As we shall see below, many sensory, motor, and cognitive functions are served by more than one neural pathway. When one functional region or pathway is damaged, other may be able to compensate partially for the loss, thereby obscuring the behavioral evidence for localization. Nevertheless, the neural pathways for certain higher functions have been precisely mapped in the brain. For example, the cerebral hemispheres are associated with higher level of processing, like thoughts or voluntary movements. Moreover, EEG recordings are performed directly above the cerebral cortex (figure 2.4).

2.1.1 Cerebral cortex & Functional areas

The brain operations responsible for our cognitive abilities occur primarily in the cerebral cortex - the furrowed gray matter covering the cerebral hemispheres. In each of the brain's two hemispheres the overlying cortex is divided into four anatomically distinct lobes: frontal, parietal, temporal, and occipital (see figure 2.4), originally named for the skull bones that encase them.

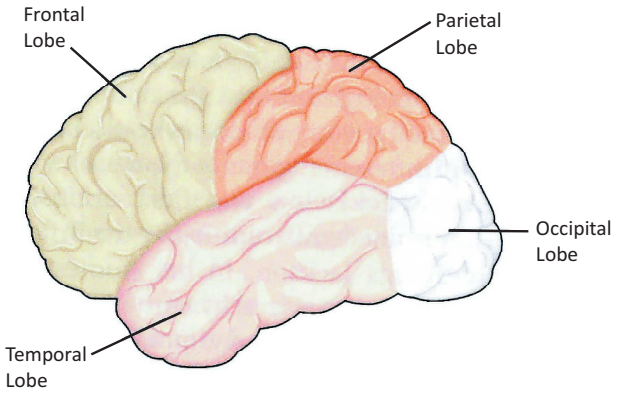

Figure 2.4: The four lobes of the cerebral cortex.

These lobes have specialized functions. The frontal lobe is largely concerned with planning future action and with the control of movement; the parietal lobe with somatic sensation, with forming a body image, and with relating onet's body with vision; the temporal lobe with hearing; and through its deep structures-the hippocampus and the amygdaloid nuclei- with aspects of learning, memory, and emotion. Each lobe has several characteristics deep infolding (a favored evolutionary strategy for packing in more cells in a limited space). The crests of these convolutions are called gyri, while the intervening grooves are called sulci or fissures. The more prominent gyri and sulci are quite similar in everyone and have specific names. For example, the central sulcus separates the precentral gyrus, which is dedicated to motor function, from the postcentral gyrus, which is concerned with sensory function (figure 2.5 and 2.6).

The organization of the cerebral cortex is characterized by two important features. The first are, each hemisphere is concerned primarily with sensor and motor processes on the contralat-

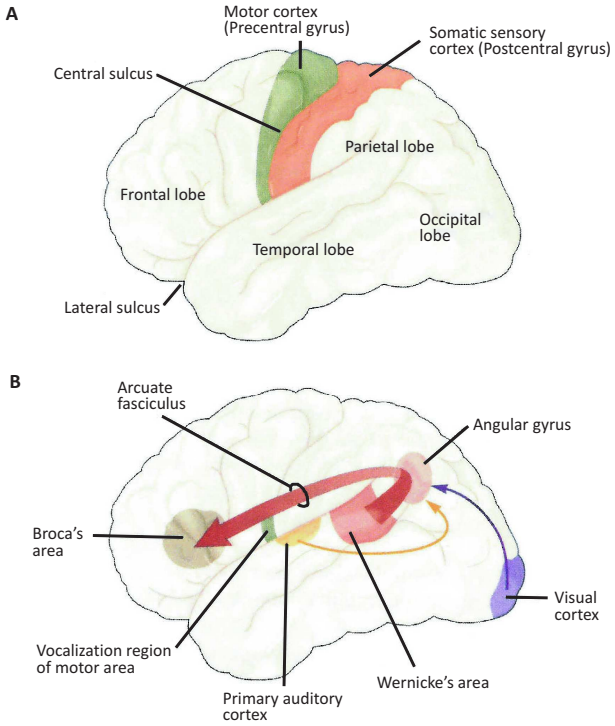

Figure 2.5: The major areas of the cerebral cortex are shown in this lateral view of the left hemisphere. **A.** Outline of the left hemisphere. **B.** Areas involved in language. From [2].

eral (opposite) side of the body. Thus sensory information that arrives at the spinal cord from the left sided of the body-from the left hands, for example- crosses over to the right side of the nervous system (either within the spinal cord or in the brain stem) on its way to the cerebral cortex. Similarly, the motor areas in the right hemisphere exert control to the movements of the left half of the body. Second, although the hemispheres are similar in appearance, they are not completely symmetrical in structure or equivalent in function.

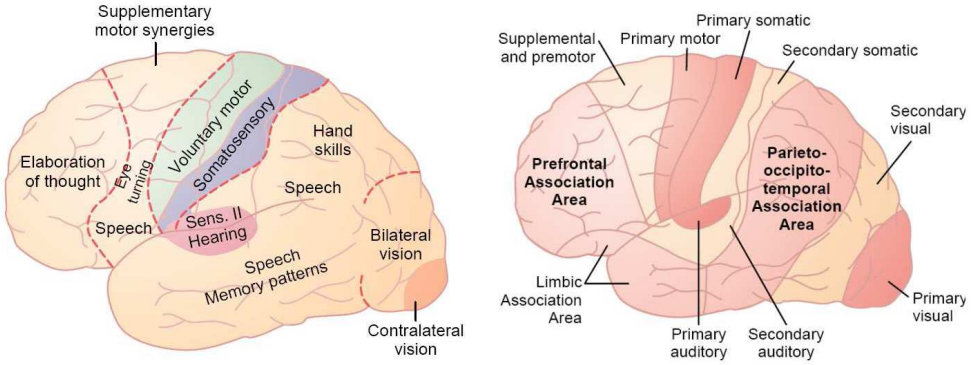

Figure 2.6: Functional areas of the human cerebral cortex (right) and the functions they are related with (left). From [3].

2.2 Inner mechanisms

Humans are vastly superior to other animals in their ability to exploit their physical environment. The remarkable range of human behavior -indeed, the complexity of the environment humans have been able to create for themselves- depend on a sophisticated array of sensory receptors connected to a highly flexible neural machine -a brain- that is able to discriminate an enormous variety of events in the environment. The continuous stream of information from these receptors is organized by the brain into perceptions and then into appropriate behavioral responses. All of this is accomplished by the brain using nerve cells and the connections between them.

2.2.1 Microscopic description of the cortex

Individual nerve cells, the basic unit of the brain, are relatively simple in their morphology. Although the human brain contains an extraordinary high number of these cells (on the order of 10 exp10 neurons), which can be classified into thousands of different types, all nerve cells share the same basic architecture. The complexity of the human behavior depends less on the specialization of individual nerve cells and more on the fact that many of these cells form precise anatomical circuits. One of the key organizational principles of the brain, therefore, is that nerve cells with basically similar properties can nevertheless produce quite different actions because of the way they are connected between them and with the sensory receptors and muscle.

There are two main classes of cells in the nervous system: nerve cells (*neurons*) and glial cells (*glia*):

Glia cells far outnumber neurons - there are between 10 and 50 times more glia than neurons in the central nervous system of vertebrates. Glia surrounds the cell bodies, axons, and dendrites of neurons. As far as is known, glia are not directly involved in information processing, glial cells provide support and protection for neurons. They are thus known as the "glue" of the nervous system. The four main functions of glial cells are: to surround neurons and hold them in place, to supply nutrients and oxygen to neurons, to insulate one neuron from another, and to destroy pathogens and remove dead neurons. Glia cells also modulate neurotransmission [16], but there is no evidence that glia cells are directly involved in electrical signaling. Signaling is the function of nerve cells, the neurons.

A typical neuron has four morphologically defined regions: the cell body, dendrites, the axon and presynaptic terminals (see figure 2.7). Each of these regions has a distinct role in the generation of signals and the communication of signals between nerve cells.

The cell body (*soma*) is the metabolic center of the cell. It contains the nucleus, which stores the genes of the cell, as well as the endoplasmic reticulum, an extension of the nucleus where the cell's proteins are synthesized. The cell body usually gives rise to two kinds of processes: several short, *dendrites*, and one, long, tubular, *axon*. Dendrites branch out in tree-like fashion and are the main apparatus for receiving incoming signals from other nerve cells. In contrast, the axon extends away from the cell body and is the main conducting unit for carrying the signal to other neurons, figure 2.8. An axon can conduct electrical signals to long distances, ranging from 0.1 mm to 3m. These electrical signals are called *action potentials*, figure 2.9.

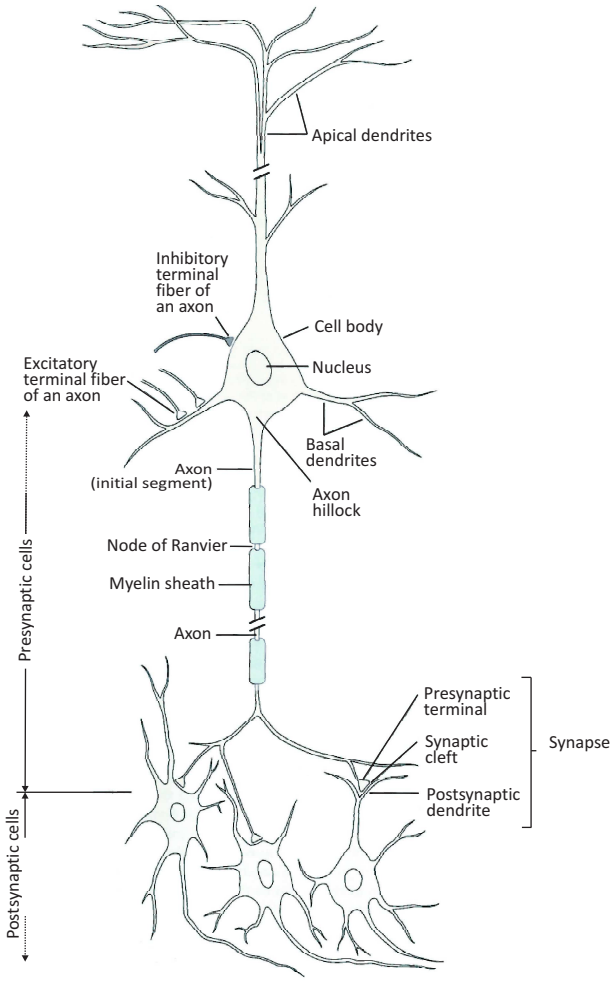

Figure 2.7: Structure of a neuron with the four morphologically defined regions: the cell body, dendrites, the axon and presynaptic terminals.

2.2.2 Action potentials & Cerebral processes

Action potentials constitute the signals by which the brain receives, analyzes, and conveys information. These signals are highly stereotyped throughout the nervous system, even though they are initiated by a great variety of events in the environment that impinge on our bodies -from lights to mechanical contact, from odorant to pressure waves. Thus, the signals that convey information about vision are to those that carry information about vision odors. Then, the information conveyed by an action potential is determined, not by the form of the signal, but by the pathway the signal travels in the brain.

When the skin is excited by an external stimulus, sensory neurons enter the spinal cord to relay the electrical signal from the skin to the brainstem. This brainstem plays an important role in the regulation of cardiac and respiratory function. It also regulates the central nervous system, and it is pivotal in maintaining consciousness and regulating the sleep cycle. There, the information is modulated with other signals, coming from other stimuli and being relevant to the previously mentioned cases, to be transmitted to the thalamus. The thalamus is an important

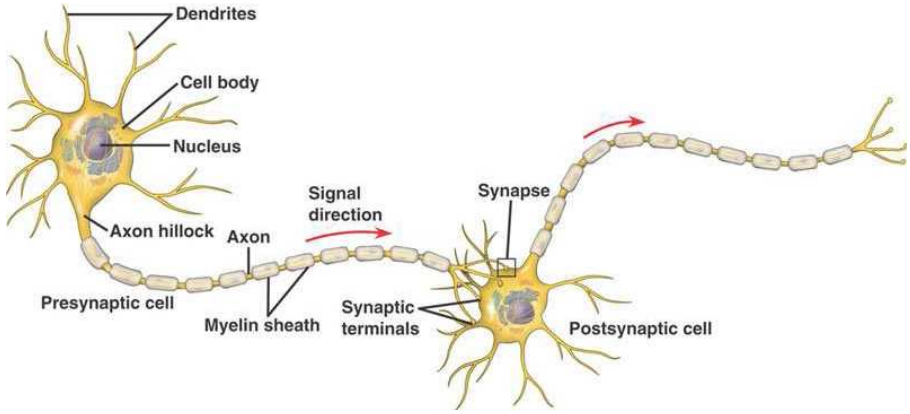

Figure 2.8: The axon conducts electrical impulses away from the neuron's cell body (or soma) while the dendrites conduct the electrical stimulation received from other neural cells toward the cell body.

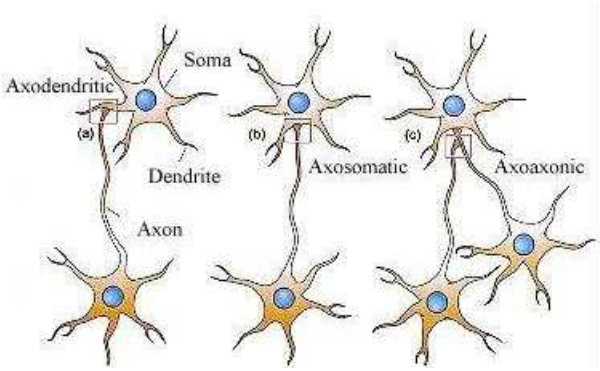

Figure 2.9: Electric potentials are produced at the synaptic junctions which can be localized over the dendrites (axodendritic synapse), the soma (axosomatic synapse) or the axon (axoaxonic synapse).

structure to relay information from the brainstem to specific areas of the cortex. The thalamus plays an important role in regulating states of sleep and wakefulness, and also processes the information to select the level of attention to stimuli.

This transfer of information to areas of the cortex is realized via thalamus-cortical relay neurons, or TCR neurons. In the cortex, highest level of processing functions as well as cognitive tasks is performed. From figure 2.10, different areas of cortex execute specific functions and return some of their outputs to other regions which execute other specific tasks. In practice, current insights are that specific higher cognitive functions are realized by parallel simultaneous processing of information in multiple cortical areas which are not necessary closely located to each other. In this way, other neurons may project back again the electrical signal onto the cerebral cortex, introducing large feedback loops. Those loops are important in the generation of rhythmical components in EEG.

It exists feedback loops between the thalamus and the cerebral cortex, that play key roles in the generation of rhythmical patterns in the EEG, as explained in the following section.

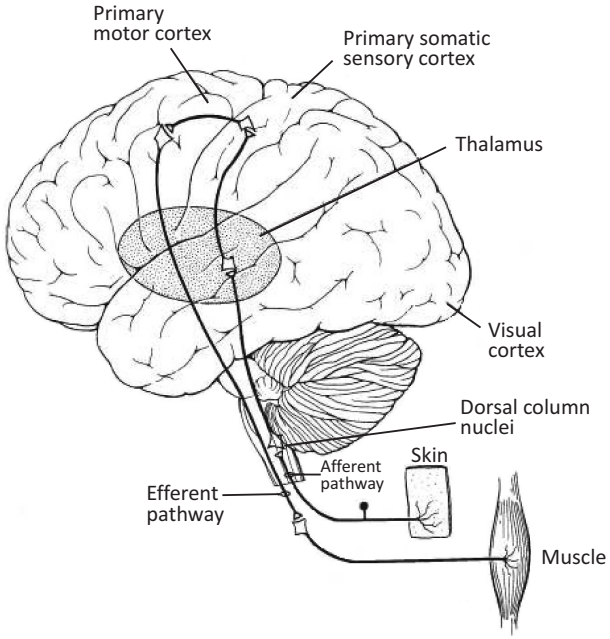

Figure 2.10: Illustration of how neurons can interact with each other to relay and process information, from [2].

2.3 Electroencephalogram (EEG)

Post-synaptic potentials generate the EEG signal, it is not possible for a scalp EEG to determine the activity within a single dendrite or neuron. Thus, the EEG recording from one electrode is the summation of the synchronous activity of thousands of neurons that have similar spatial orientation, radial to the scalp. The appearance of EEG rhythmic activity results from the coordinated activation of neuron groups, whose summed synaptic events become sufficiently large. Also, currents that are tangential to the scalp are not registered by the EEG. Because voltage fields fall off with the fourth power of the radius, activity from deep sources is more difficult to detect than currents on the cortex [17], [18], [19] and [20].

However, EEG was chosen for some important reasons. Mainly, for its simplicity: the electrodes are placed on a cap which does not impose the subjects to stay motionless. This type of recording system is shown in figure 2.11. More technically, EEG has a high temporal resolution and a reasonable spatial one depending on the number of electrodes used. Moreover, this is a noninvasive technique: the recording is done on the scalp.

2.3.1 EEG recordings system

Inner bioelectrical phenomena can be detected thanks to the appearance of ionic currents on the scalp. The conversion of these currents into electric voltages is performed via metal-electrolyte interfaces, called electrodes. Nevertheless, even if it is possible to record, in theory, very deep electrical activity, these electrodes will mainly record cortical activity, according to the decrease property of electrical fields with the distance.

Figure 2.11: A practical way to record EEG is to place the electrodes on a helmet. Picture taken in Philips Research laboratories.

Clinical electroencephalography is the recording of electrical potentials on the scalp: however, it provides a highly limited view of cerebral activity because of inherently poor spatial resolution and insensitivity to electrical fields that are either not perpendicular to the scalp's surface or distant from it. The spatial resolution limitation partly results from the electrical field insensitivity. To have an amplitude that is detectable at the level of the scalp, neuronal potentials must be sufficiently synchronized with neighboring neuronal potentials over distances of several square centimeters. Nevertheless, electroencephalography has excellent temporal resolution, which is in millisecond order of magnitude, [4].

Recording the low-amplitude cerebral potentials, especially in the context of the larger amplitude potentials of muscle and ambient electrical noise, requires differential recording, which is also called common mode rejection. This technique produces an EEG wave by subtracting the electrical field detected by one electrode from the field detected by another electrode; a differential amplifier is show in the figure 2.12. Because the substraction cancels any electrical field that is present at both electrodes, extra cerebral electrical noise is minimized and cerebrally generates fields that are local to one electrode that remains visible despite of its lower voltage. A typical adult human EEG signal is about $10\mu V$ to $100\mu V$ in amplitude when measured from the scalp. For this reason the amplification between the active electrode and the reference, are typically about 1.000 to 100.000 times, or 60 to 100 dB of voltage gain.

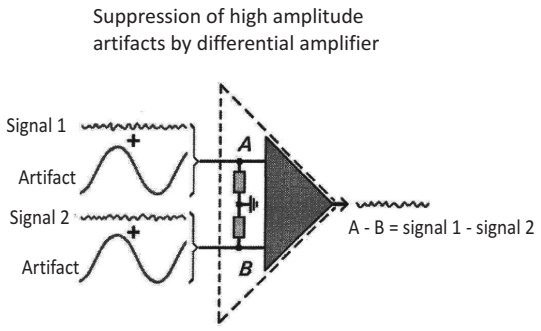

Figure 2.12: Differential amplifiers have the ability to remove the common noise.

However, the cancelation of artifacts using differential systems is nonspecific and, therefore, also minimizes the amplitude of any broad cerebrally generated activity that is identical at the two electrode locations. The other major limitation of this technique is the absence of any ex-

ternal reference against which the field of one electrode may be compared. Without an external reference, every wave represents a combination of focal activities. Thus, viewing the activity with multiple pairs of electrodes is necessary to best understand its location.

However, the cancelation of artifacts using differential systems is nonspecific and, therefore, also minimizes the amplitude of any broad cerebrally generated activity that is identical at the two electrode locations. The other major limitation of this technique is the absence of any external reference against which the field of one electrode may be compared. Without an external reference, every wave represents a combination of focal activities. Thus, viewing the activity with multiple pairs of electrodes is necessary to understand its location.

Since different regions of the cortex have different functionalities, the electrical activity recorded by electrodes on the scalp can vary depending on the position of the electrodes. A standard system for the placement of electrodes was developed by a group of neurophysiologists in 1947 [5]. For reasons of standardization, the locations of the electrodes used in recording EEGs are defined by international agreement as the "10-20 system" of electrode placement (figure 2.13). This system uses measurements of the head referenced to visible anatomic landmarks to minimize the variation in electrode placement among recording technologies and to provide the maximum uniformity in electrode to brain structure correspondence among patients.

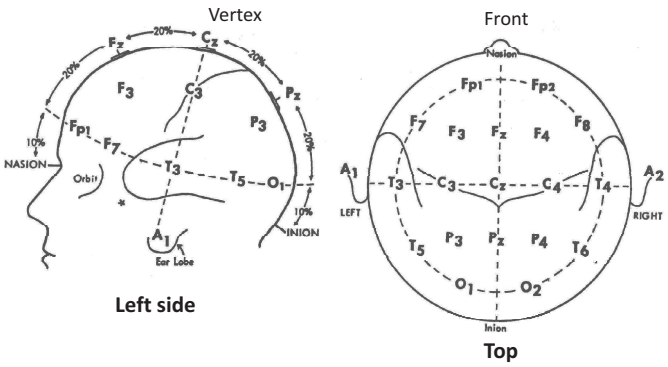

Figure 2.13: The International 10-20 System of Electrode Placement, from [4].

In the 10-20 system each electrode is coded by a letter to identify the lobes and by a number to identify the hemisphere location. The smaller the number, the closer the position of the electrode site to the midline or axis of the skull. F, T, C, P, and O stand for Frontal, Temporal, Central, Parietal and Occipital locations of the brain. Even numbers refer to the right hemisphere and odd numbers refer to the left hemisphere. The midline of the head is defined as the line connecting the nasion (the point between the forehead and nose) and the inion (the bump at the back of the skull). Along this line five points are marked as depicted in figure 2.13 and 2.14. The first point is called the frontal pole (Fp) and is placed at 10% of the nasion-inion distance from the nasion. The next four points: F, C, P, and O are positioned 20% of the distance from each other with the O-point 10% away from the inion. A similar segmentation in the same 10-20 way is done to the line between the preauricular points which are small pieces of cartilage near the opening of the auditory canal in the ear. The following electrodes are placed along two lines between the frontal and occipital point.

A top view of the scalp illustrating 32 electrode positions according to the 10-10 system

shown in figure 2.14.

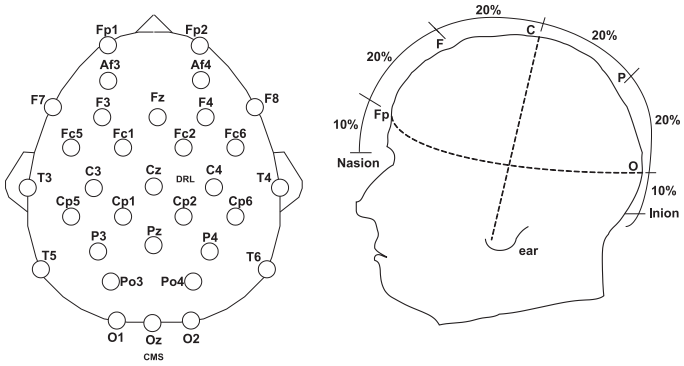

Figure 2.14: 10-20 System of Electrode Placement, form [5].

2.3.2 Distortions and artifacts

Although EEG is designed to record cerebral activity, it also used to record electrical activities arising from sites other than the brain. The recorded activity that is not of cerebral origin is termed artifact and can be conveniently divided into physiologic and extraphysiologic artifacts. *Physiologic* artifacts are generated by the body but arise from sources other than the brain. *Extraphysiologic* artifacts are from outside the body (i.e., equipment, environment).

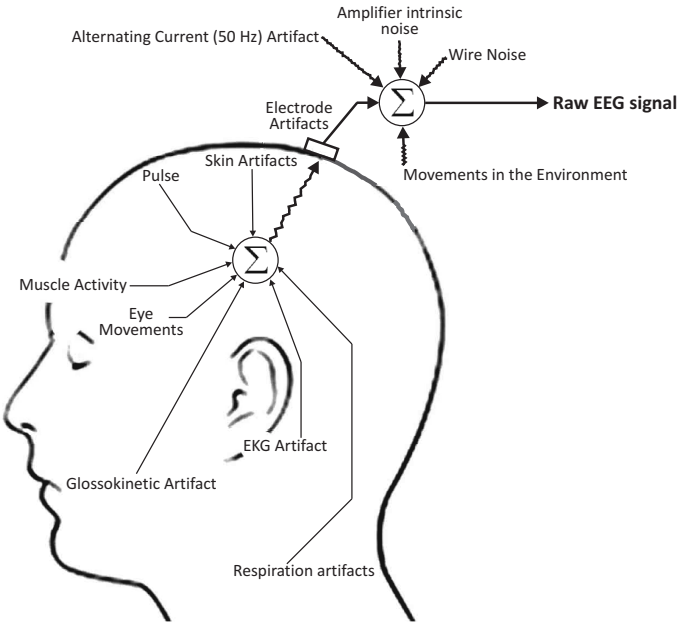

Figure 2.15: Model of the artifacts that are involved in the raw EEG signals.

Physiologic Artifacts

Physiological artifacts are generated from the patient itself and include cardiac, glossokinetic, muscle, eye movement, respiratory and pulse artifact among many others.

- **Muscle (Electromyogram) Activity**
  Myogenic potentials are probably the most common artifacts and are seen on virtually all EEG performed in clinical practice. Frontalis and temporalis muscles (e.g., clenching of jaw muscles) are particularly common. As a general rule, the potentials generated in the muscles are of shorter duration than those generated in the brain and are identified easily on the basis of duration, morphology, and high frequency of 50-100Hz (figure: A.1 and A.7). A particular type of muscle artifact is chewing, characterized by rhythmic burst of muscle maximum in the temporal chains (figure: A.2).

- **Glossokinetic Artifact**
  In addition to muscle activity, the tongue works as a dipole, with the tip negative with respect to the base. In this case the tip of the tongue is the most important part because it is more mobile. The artifact produced by the tongue has a broad potential field that drops from frontal to occipital areas, although it is less steep than the are produced by eye movement artifacts. The amplitude of the potentials is much lower than in the delta range and occurs synchronously when the patient says "Lah-lah-lah-lah", which can be verified by the technologist. Chewing and sucking (pacifier) can produce similar artifacts.

- **EKG Artifact**
  Some individual variations in the amount and persistence of EKG artifact are related to the field of the heart potentials over the surface of the scalp. Generally subjects with short and wide necks have the largest EKG artifacts on their EEG recordings. The voltage and apparent surface of the artifact vary from derivation to derivation and, consequently, from montage to montage. The artifact is observed best in referential montages using ear electrodes (A1 and A2). EKG artifact is recognized easily by its rhythmicity and coincidence with the EKG tracing (figure A.1). The situation becomes difficult when abnormal cerebral activity (e.g., sharp or slow waves) appears intermixed with EEG artifact.

- **Pulse**
  Pulse artifact occurs when an EEG electrode is placed over a pulsating vessel. The pulsation can cause slow waves that may simulate EEG activity. A direct relationship exists between EKG and the pulse waves. The QRS complex (i.e., electrical component of the heart contraction) happens slightly ahead of the pulse waves 200-300msec delay after EKG.

- **Eye Movements**
  Eye movements are observed on all EEG recordings and are useful in identifying sleep stages. The eyeball acts as a dipole with a positive pole anteriorly (cornea) and a negative pole posteriorly (retina). When the globe rotates about it axis, it generates a large amplitude that alternate the current field, which is detectable by any electrodes near the eye. The other source of artifact comes from EMG potentials from muscle in and around the orbit. Vertical eye movements typically are observed with blinks (i.e., Bell's phenomenon). A blink causes the positive pole (i.e., cornea) to move closer to frontpolar (FP1-Fp2) electrodes, producing symmetric downward deflections. During downward eye movement the positive pole (i.e., cornea) of the globe moves away from frontpolar electrodes, producing an upward deflection best recorded in channels 1 and 5 in the bipolar longitudinal montage. Lateral eye movement affects lateral frontal electrodes F7 and F8 (which are just

about where "eye electrodes" of the PSG would be). During a left lateral eye movement, the positive pole of the globe moves toward F7 and away from F8. Using a bipolar longitudinal montage, there is a maximum positivity in electrode F7 and maximum negativity simultaneously in electrode F8 (figure: A.3) A so-called lateral rectus spike (figure: A.4) may be present in electrode F7. With right lateral eye movement, the opposite occurs.

- **Respiration artifacts**
  Respiration can produce two kinds of artifacts. One type is in the form of slow and rhythmic activity, synchronous with the body movements of respiration and mechanically affecting the impedance of (usually) one electrode. The other type can be slow or sharp waves that occur synchronously with inhalation or exhalation and involve those electrodes on which the patient is tying. Several commercially available devices to monitor respiration can be coupled to the EEG machine. As with the EKG, one channel can be dedicated to respiratory movements.

- **Skin Artifacts**
  Biological processes may alter impedance and cause artifacts. Sweat is a common cause (figure: A.5). Sodium chloride and lactic acid from sweating react with metals of the electrodes and produce large and very slow (usually ~ 0.5 Hz) baseline sways.

Extraphysiologic Artifacts

Common extraphysiologic artifacts include those generated by monitoring devices, infusion pumps and suctioning devices though electrical devices like mobile phones may also degrades the EEG record.

- **Electrode Artifacts**
  The most common electrode artifact is the electrode "pop". Morphologically this appears as single or multiple sharp waveforms due to abrupt impedance change. It identified easily by its characteristic appearance (i.e., abrupt vertical transient that does not modify the background activity) and it usual distribution, which is limited to a single electrode (figure: A.6). In general, sharp transients that occur at a single electrode (i.e., no field) should be considered artifacts until proved otherwise. At other time, the impedance change is less abrupt, and the artifact may mimic a low-voltage arrhythmic delta wave.

- **Alternating Current (50 Hz) Artifact**
  Adequate grounding on the patient has almost eliminated this type of artifact from power lines. The problem arises when the impedance of one of the active electrodes becomes significantly large between the electrode and the ground of the amplifier. In this situation, the ground becomes an active electrode that, depending on its location, reproduces the 50 Hz artifact. The artifact has the exact frequency of 50 Hz and is easily identified by increasing the time base (figure: A.7).

- **Movements in the Environment**
  Movement of other persons round the patient can generate artifacts, usually of capacitive or electrostatic origin. The artifact produced by respirators varies widely in morphology and frequency. Monitoring the ventilator rate in a separate channel helps to identify this type of artifact. Interference from high-frequency radiation from radio, TV, hospital paging systems, and other electronic devices can overload EEG amplifiers. The cutting

or coagulating electrode used in the operating room also generates high-voltage high-frequency signals that interfere with the recording system. Touching or hitting electrodes can produce odd waveforms, and, for example, repetitive head movements can produce rhythmic artifacts (figure: A.8).

2.4 Spontaneous EEG and static patterns

As seen before, artifacts are involved in recorded signals from the scalp, but there are more factors that affect the mental activity of these signals, i.e. the evoked potentials. An evoked potential is the electrical response of the brain to a sensory stimulus. It is possible to demonstrate that the brain attained a steady-state regime in which the amplitude and phase of the harmonics (frequency components) of the response were approximately constant over time. By analogy, with the steady-state response of a resonant circuit that follows the initial transient response the defined an idealized steady-state evoked potential (SSEP) as a form of response to repetitive sensory stimulation in which the constituent frequency components of the response remain constant with time in both amplitude and phase.

Sensory evoked potentials (SEP) are recorded from the central nervous system following stimulation of sense organs (for example, visual evoked potentials elicited by a flashing light or changing pattern on a monitor; auditory evoked potentials by a click or tone stimulus presented through earphones) or by tactile or somatosensory evoked potential (SSEP) elicited by tactile or electrical stimulation of a sensory or mixed nerve in the periphery.

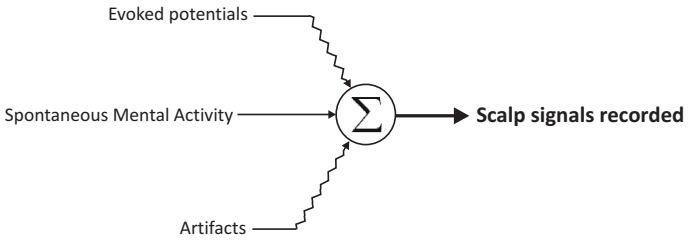

Figure 2.16: A simple model of the components involved in the recorded scalp signals

Knowing this, only the spontaneous EEG components seem to be interesting. This will imply the estimation and the suppression of the evoked components from the EEG signals. Therefore, this will be an important part of the signal processing task.

2.5 Band signals and Event Related (De-)synchronization

2.5.1 Brain frequency bands

As seen before, feedback loops generate rhythmical electrical activity in the brain. Nevertheless, to be able to notice significant rhythmical activity on the scalp, and therefore in the EEG, many brain cells have to be excited in synchrony. This is the basic concept of EEG analysis because different rhythms can be detected in EEG and these are correlated with different brain states, functions or pathologies. These rhythmical waves are usually categorized based on their

frequency content as it follows:

- **Delta**
  Delta wave is a high amplitude brain wave with a frequency of 0.5-3 Hz and is usually associated with slow-wave sleep. Delta wave activity occurs most frequently during stage 4 slow-wave sleep (SWS), accounting for 50% or more of the EEG record during this stage. These waves are believed to originate in the thalamus in coordination with the reticular formation. This rhythms tends to be the highest in amplitude, sometimes over $100\mu V$.

- **Theta**
  The theta rhythm is seen normally in young children and adults in light sleep. In the awake adult, high theta activity is considered abnormal and it is related to different brain disorders. Most of the waves can be found in the parietal and temporal regions and their amplitude is usually less than $100\mu V$.

- **Alpha**
  With Hans Berger's 1929 publication on the human electroencephalogram (EEG), the Alpha rhythm (AR) was the first EEG pattern to be described, and it continues to be the most commonly noted rhythm in clinical EEG interpretation because it is reproducible and easily recognized (figure: A.9). Alpha appears during wakefulness, under relaxation with eyes closed and mental inactivity conditions. The waves are mostly found in the occipital region, at the back of the head. During sleep, the alpha waves disappear completely. The normal alpha rhythm has the following characteristics:

  - Frequency of 8-12Hz: Lower limit of normal generally accepted in adults and children older than 8 years is 8 Hz.
  - Location: Posterior dominant: occasionally, the maximum may be little more anterior, and may be more widespread.
  - Morphology: Rhythmic, regular, and waxing and waning.
  - Amplitude: Generally $20 - 100\mu V$.
  - Reactivity: Best with eyes closed; attenuates with eye opening.

- **Mu rhythm**
  Is an alpha-range activity that is seen over the sensorimotor cortex (figure: A.10). It characteristically attenuates with movement of the contralateral arm (or mental imagery of movement of the contralateral arm). Characteristics of mu rhythm are as follows:

  - Frequency of 7-11 Hz: Generally in alpha frequency band (8-12Hz).
  - Location: Centroparietal area.
  - Morphology Arch-like shape or like an "m"; most often asymmetric and asynchronous between the two sides and may be unilateral.
  - Amplitude: Generally low to medium and comparable to that of the alpha rhythm.

  - Reactivity: mu rhythm attenuates with contralateral extremity, the thought of a movement, or tactile stimulation.

- **Beta**
  It is often associated with active thinking and concentration. It is the dominant rhythm in subjects who are alert or anxious or who have their eyes open. The beta rhythm are usually seen in parietal and frontal regions (figure: A.11) and has the following characteristics:

  - Frequency (by definition) greater than 13 Hz, typically 18-25 Hz.
  - Location: Mostly frontocentral but somewhat variable; some describe various types according to location and reactivity -generalized, percentral, and posterior.
  - Morphology: Usually rhythmic, waxing, and waning, and symmetric.
  - Amplitude: Usually in the range of $5 - 20\mu V$.
  - Reactivity: Most common 18-25 Hz beta activity enhanced during stages 1 and 2 sleep and tends to decrease during deeper sleep stages; central beta activity may be reactive (attenuates) to voluntary movements and proprioceptive stimuli; in infants older than 6 months, onset of sleep marked by increased beta activity in central and postcentral regions.

- **Gamma**
  A gamma wave is a pattern of brain waves, associated with perception and consciousness. Gamma waves are produced when masses of neurons emit electrical signals at the rate of around 40 times a second (40 Hz), but can often be between 26 and upwards of 70 Hz. By one definition, gamma waves manifest at 24 Hz and higher, though researchers have recognized that higher level cognitive activities occur when lower gamma waves suddenly double into the 40 Hz range. Gamma waves are involved in higher mental activity; these rhythms represent binding of different populations of neurons together into a network for the purpose of carrying out a certain cognitive or motor function. Because of the filtering properties of the skull and scalp, gamma rhythms can only be recorded from electrocorticography[1].

For more information see [21].

2.5.2 ERD/ERS and attention activity

As seen before, for each part of the human body it exists a corresponding region in the primary motor and primary somatosensory area of the neocortex, and the appearance of EEG rhythmic activity results from the coordinated activation of neuron groups is related with actions and emotions that occur in the patient. The brain activity during resting wakefulness contains distinct rhythms located over various brain areas; the moment-to-moment amplitude fluctuations of these local rhythms reflect variable functional states of the underlying neuronal cortical networks and can be used for brain computer interfacing.

[1] Electrocorticography (ECoG) is the practice of using electrodes placed directly on the exposed surface of the brain to record electrical activity from the cerebral cortex.

Specifically, the pericentral and mu rhythms are diminished, or even almost completely blocked, by movements of the somatotopically corresponding body part, independent of their active, passive or reflexive origin. Blocking effects are visible bilateral but with a clear predominance contralateral to the moved limb. This attenuation of brain rhythms is termed event-related desynchronization (ERD), see [22], [23], [8] and [18].

An event related EEG response can occur either in the form of an amplitude increase or an amplitude decrease. The decrease of power within the alpha frequency band is called ERD. The following increase in power after the event was named ERS. ERD and ERS are highly frequency specific, ERD being mostly present in the alpha and lower beta bands while ERS is found in the alpha, beta and gamma [24].

The alpha band rhythm of the EEG is characteristic for inactive cortical fields. Thus alpha desynchronization is an indicator of an activated brain state and can be seen as an electrophysiological correlate of activated cortical neurons. The neuronal agglomerations tend to work independently and the EEG displays low amplitudes. A synchronized activity within the alpha band can be interpreted as an electrophysiological correlate of decreasecortical excitability. In this case, neural populations display synchronized behavior and the EEG displays high amplitudes.

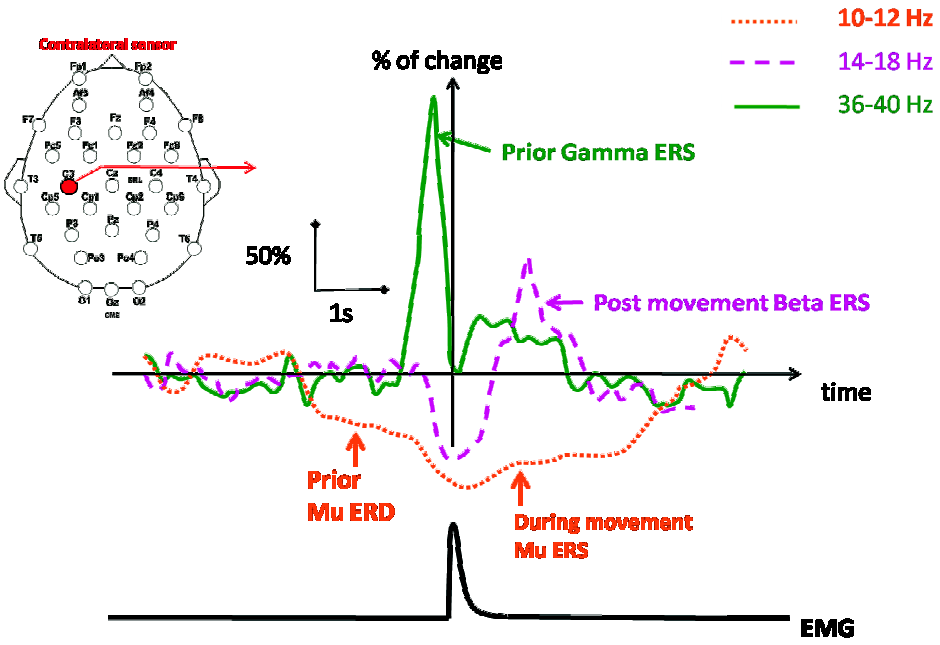

Figure 2.17: Event-Related Synchronization (ERS) and Desynchronization (ERD) during finger movement of right hand, from [6].

Self-paced movement can be divided into three phases: planning, execution and recovery. The planning phase starts about two seconds before the movement onset over the contralateral side and is manifested as a unilateral desynchronization of mu and central beta rhythms. During the execution of the movement, ERD is bilateral symmetrical. After the termination of movement ERD recovers slowly within 2-3 seconds in the alpha (mu) band and relatively quicker in

the beta band (within 1 sec) showing a transient postmovement power increase the characteristic of an ERS [25] and [24]. Therefore, in the case of voluntary movement there are at least three characteristic EEG patterns:

- A contralateral dominant mu and beta ERD prior to movement.
- A bilateral ERD during movement.
- A contralateral dominant beta ERS after movement.

[22] had also stated that beta desynchronization is more widespread than synchronization. This observation is not surprising taking into account that in performing a special task there are always more cortical areas in a processing mode than in an idling mode and therefore EEG desynchronization is dominating over EEG synchronization.

This concept of ERS/ERD will play a key role all along this study and was suggested to be an indicator of high-level of processing activity or cognitive tasks in the referenced used this chapter.

2.6 Motor Imagery

Motor imagery can be defined as thinking about moving a limb, for instance the hands, the feet, or the tongue but without executing the movement. It is believed that motor imagery is based on similar processes to those which are involved in planning actual movements.

The main difference between performance and imagery is that in the latter case execution would be blocked at some cortico-spinal level. [22] and [26] show similar cortical activity over the contralateral hand area during execution and imagination of movement. Accordingly, both real and imaginary movements should elicit similar patterns of cortical activation in relevant brain regions. The activation of hand area neurons either by the preparation for a real hand movement or by imagination of a hand movement is accompanied by a circumscribed ERD over the hand area.

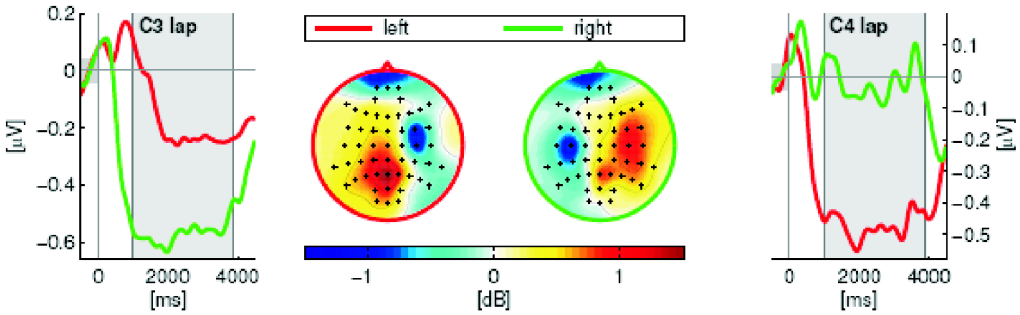

Figure 2.18: Event-Related Desynchronization (ERD) during motor imagery of the left and the right hand, from [7].

It was observed that the prominent changes in the EEG were localized in the hand area sensorimotor cortex. A similar ERD has been found on the contralateral side during the motor imagery as is usually found during the preparation of real movement. An example of ERD distribution during motor imagery, mapped on the reconstructed cortical surface of one subject is shown in figure 2.18.

During an execution of a real movement, the initially contralateral ERD develops a bilateral distribution whereas in case of imagined movement it seems to be more concentrated on the contralateral side only.

Section 3

Description of the algorithm

3.1 Introduction

IN THE PREVIOUS CHAPTER we expose a review of the physiological and electromagnetic principles of the brain and its internals process. In this chapter we present the architecture of a BCI algorithm based on scalp recorded electroencephalogram that consists in a recording procedure, the methods used for removing external noise and artifacts, and the equations applied for extracting concrete features of raw brain signals. The first main part of the algorithm consists, using the data from training populations, to extract meaningful characteristics about the state of the functional activity in the brain of subjects during a continuous performance task, usually hand real movement or imaginary movement.

We base the first part of the study in the Alfa and Beta bands personalized for each subject, using this subjective band to extract the most useful features, the ERS/ERD curves that we explain in section two. To compute these features, preprocessing and estimations of the spontaneous EEG components have to first be performed according to rational technics and physiological considerations. We have to consider that the RAW_EEG signal is corrupt by external noise and subject generated and electrode artifacts. Most sources of external noise can be avoided by the appropriate control of the environment of the laboratory when we make the experiments, thus, the power line noise can be easily deleted by a notch well-balanced filter in the frequency of the line, 50Hz in Europe.

In the figure 3.1 we show a detailed scheme of the preprocessing steps used in the first part of the system, it helps to have a global vision of the parts that interact in this chapter. In fact, the RAW_EEG_class 1 or 2 used as input data comes from a recording system called Biosemi 32, which makes a pre-band pass filter that is implicit in the amplifier between 0.5 to 100 Hz, and obtains the scalp signal with a sample frequency of 2048 Hz. Using this sample frequency we obtain so many samples, that consume much time and resources, for this reason the first step is downsampling it to 256 Hz in order to reduce the computation amount complexity of the data. From this "raw" signal we have to extract the trigger signal, added in one of the additional channels of the data, and select the channels that will be implicated in the study. The trigger can be from an acoustic or sight signal recorded from an external sensor, thereby we can study the differences between visual or audio evoked potentials in the motor cortex. The channel extraction permits to differ between data channels or auxiliary channels that bring additional data, as is the case of the trigger channel. As we explain in the second section, the study of the brain frequency

bands alpha and beta provide the most important features. Therefore, our study will be focused on them. To extract these bands for each subject we will use an infinite impulse response filter. These personalized bands have been calculated using Fourier systems what is one of the settings that personalize the algorithm for each subject. The notch filter used is to remove the external noise added from the power lines. Using the trigger signal we extract the trials from the raw data, obtaining a matrix of trials that contain the recorded brain activity data in the moment of interest, usually real or imagery movement. After this part, we will use a preprocessing block with different analysis techniques, to make a channel selection, in order to make a Direct Current (DC) removing, to obtain a sensor reference and to apply an artifact rejection. These actions such as the channel selection permit to focus the analysis in the motor cortex or any brain zone that we consider relevant for the study, removing artifact and implicit data or brain signals that do not contribute to extract useful information. These features, extracted from each subject of the two brain states classes, will be combined to recognize some significant differences between the two sets and a classifier with a neuronal network will be created.

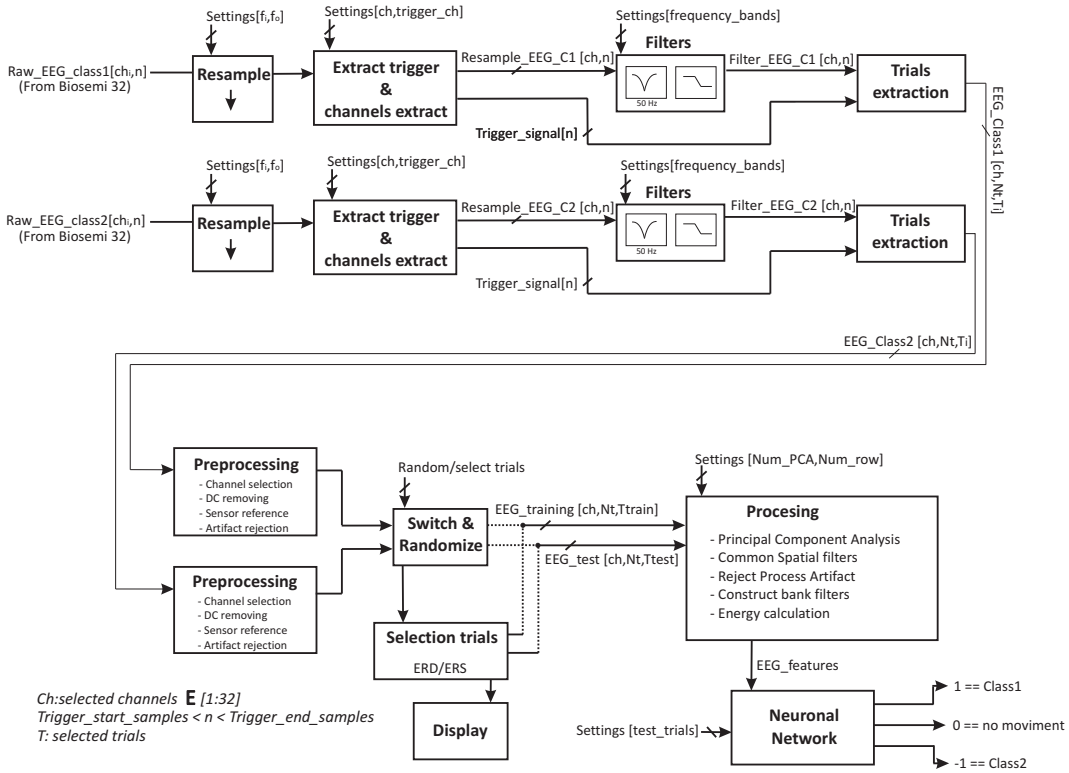

Figure 3.1: A detailed scheme of the first main part of the algorithm. Digital signal processing techniques are applied to each subject in order to estimate meaningful ERS/ERD features.

The main part of the algorithm is focused on the processing part, where, through a selection based in the study of the ERD & ERS curves for each trial, we apply different digital processing signals techniques with the idea of obtaining the difference between brain states. With this objective, we use a set of techniques that include the Principal Component Analysis (PCA), the Common Spatial Patterns (CSP), a reject process artifact, a bank filters and an energy calculation. Each of these techniques are explained in this chapter. However, the practical aspects discussed in the previous chapters are not neglected and through this chapter, we try to discuss,

from a theoretical and practical point of view, the different decisions taken.

3.2 Recording procedure

The first step of this system is to obtain the brain activity from different subjects. For each subject we record two main files during the experiment, named *RAW_EEG_CLASS 1* and *RAW_EEG_CLASS 2*, containing each of them the EEG data of all channels, directly recorded from the amplifier outputs with the format *.bdf*. Electrophysiological data was recorded using a BIOSEMI Active-Two amplifier system with 32 pin-type silver chloride active (Ag/AgCl) electrodes (see figure 3.2). The electrodes were placed on the scalp at positions defined by the 10-20 International System: electrodes FP1, FP2, F7, F3, Fz, F4, F8, C3, Cz, C4, P7, P3, Pz, P4, P8, T7, T8, O1, Oz, and O2. The remaining electrodes were from a 10-10 system: electrodes AF3, AF4, FC1, FC2, CP1, CP2, PO3, PO4, FC5, FC6, CP5, and CP6. The electrodes share a common connector with 140cm cable length which is connected to an AD-box. The electrical contact is very important to obtain correct results in the recording. Thus electrode gel was used to increase conduction between electrodes and the scalp. The EEG data was collected at a sampling rate of 2048 Hz.

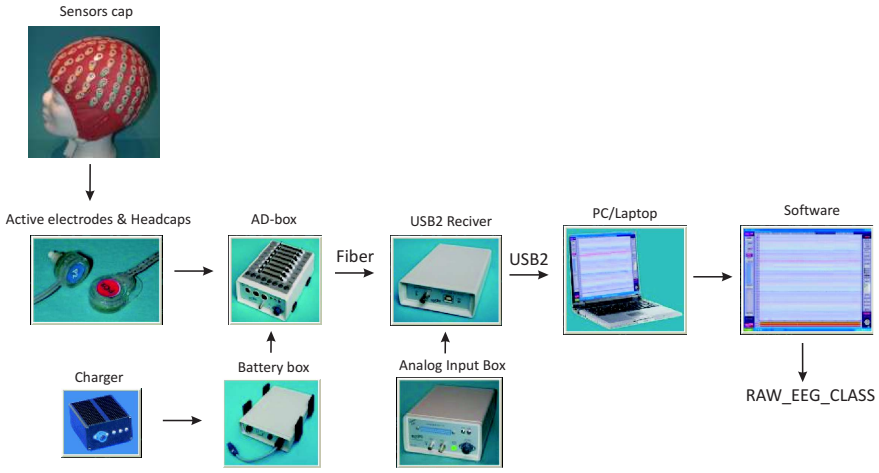

Figure 3.2: A detailed scheme of BioSemi recording system.

BioSemi replaces the "ground" electrodes which are used in conventional systems with two separate electrodes: Common Mode Sense (CMS) active electrode and Driven Right Leg (DRL) passive electrode. These 2 electrodes form a feedback loop, which drives the average potential of the subject (the Common Mode voltage) as close as possible to the ADC reference voltage in the AD-box (the ADC reference can be considered as the amplifier "zero"). The CMS reference electrode was mounted approximately 3cm below the Oz electrode, near the inion, and the DRL was placed between Cz and C3 (see figure 3.3). Usually, the standard position for CMS is between Cz and C4. However, since changes of oscillatory activity during hand movement are expected in the primary motor cortex (see Section 2.1.1), the standard CMS location was placed far from the source of movement.

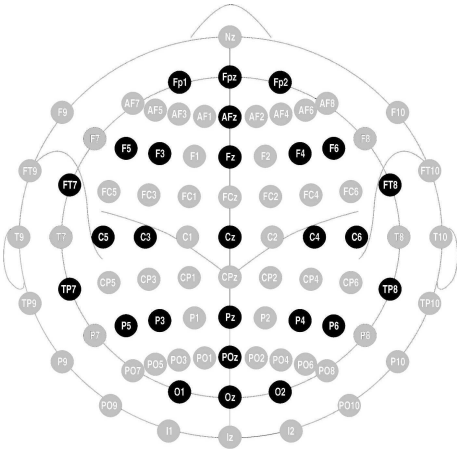

Figure 3.3: Sensor position using the 10-10 system and the 10-20 system.

3.3 Preprocessing

The objective of this part is the conversion of the continuous RAW_EEG recordings into artifact-free trials of spontaneous EEG. The processes involved are embedded in the generic name of preprocessing and are described below.

3.3.1 Resample

This technique, also called downsampling, consists in the sample reducion of the signal as we can see in the figure 3.4. As we saw previously, the BioSemi output obtains a signal of 2048 Hz, this frequency is very high, so will consume many time and resources, for this reason and the first step is a down sampling to 256 Hz that reduces the computation complexity of the data. We use a downsampling factor of M=8 to reduce the data selecting every M^{th} sample:

$$Signal\_out(k) \; = \; Signal\_in(M \cdot k) \tag{3.1}$$

The resample function applies an anti-aliasing (lowpass) FIR filter to the input signal during the resampling process, that compensates the filter's delay. The filter is designed using a Matlab function called FIRLS. In its filtering process, the function assumes that the samples at times before and after the given samples in the signal are equal to zero. Thus large deviations from zero at the end points of the input sequence can cause inaccuracies in output signal at its final points.

3.3.2 Filter selection

Brain frequency bands

Population of neurons are the origin of the brain oscillatory frequencies, the frequency experiments some oscillations decreases with an increase of the number of synchronized neuronal assembles. As we expose in the chapter 2, the usual classification of the main EEG rhythms based on their frequency ranges is as follows: delta (2 to 4 Hz), theta (4 to 8 Hz), alpha (8 to 13 Hz), beta (12 to 30 Hz) and gamma (higher than 30 Hz). For its characteristics, the alpha band,

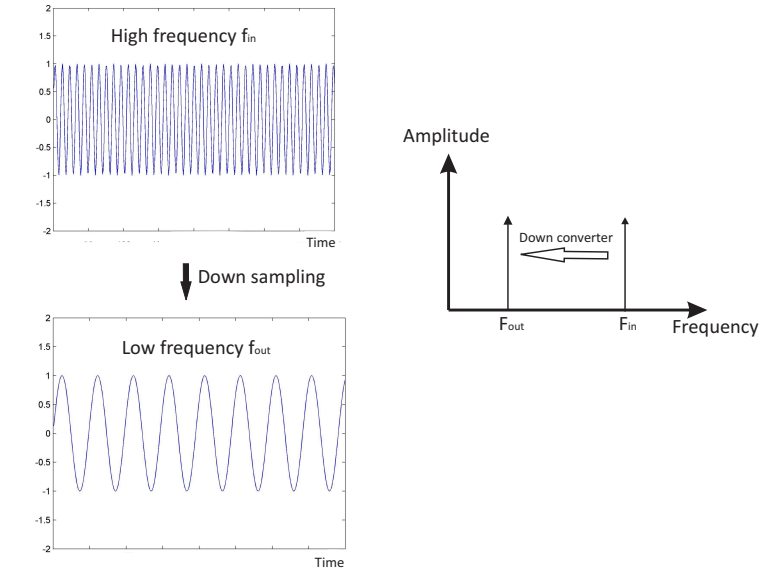

Figure 3.4: Downsample explication in frequency.

that appears during wakefulness, under relaxation with eyes closed and mental inactivity conditions, and the beta band that is associated with the active thinking and concentration, provide interesting information, moreover, the theta band give information of the states of still alertness. We focus our attention in these bands and also the mu band as it is an alpha-range activity that is seen over the sensor motorcortex. Mu band characteristically attenuates with movement of the contralateral arm (or mental imagery movement of the contralateral arm). An oscillatory component is defined by the presence of a rhythmic activity in the EEG which is manifested by a "peak" in spectral analysis.

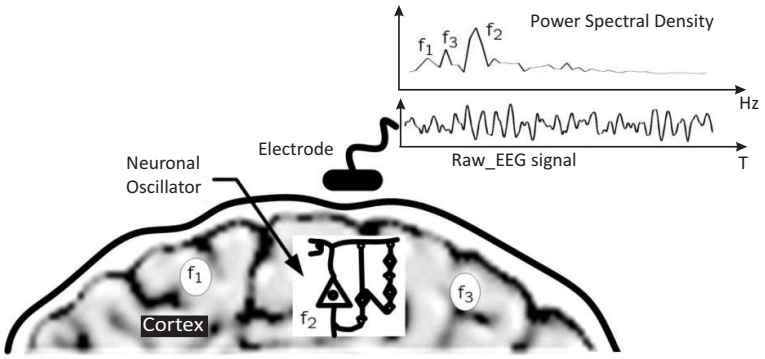

Figure 3.5: Spectral Analysis Scheme for detecting the peak frequencies.

In contrast to theta, alpha is the dominant rhythmic activity, and it is characterized by a sinusoidal waveform. In the human EEG of young healthy adults there are at least two other oscillatory components, the mu rhythm and the third rhythm. The mu rhythm has an arch-shaped wave morphology, that appears over the motor area and becomes suppressed (desynchronized) during motor related task demands. This attenuation of brain rhythms is termed event-related desynchronization (ERD), see [27], [24].

Since a focal ERD can be observed over the motor or sensory cortex even when a subject is only imagining a movement or sensation in the specific limb, this feature can also be used for BCI control: The discrimination of the imagination of the movements of left hand vs. right hand or vs. foot can be based on the somatotopic arrangement of the attenuation of the alpha and/or beta rhythms. [28]

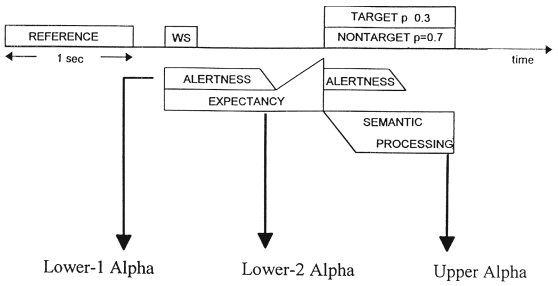

Figure 3.6: Brain states relation with Alpha subbands.

As [8], our main findings related to the alpha frequency range is that alpha desynchronization is not a unitary phenomenon. If different frequency bands are distinguished within the range of the extended alpha band, two distinct patterns of desynchronization can be observed. Lower alpha (see the figure 3.7) desynchronization, in the range of about 6-10 Hz, is obtained in response to a variety of non-task and non-stimulus specific factors. Upper alpha (see the figure 3.7) desynchronization, in the range of about 10-12 Hz, is topographically restricted and it is developed during the processing of sensory-semantic information. This is shown in figure 3.6.

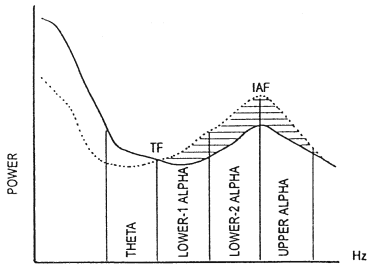

Figure 3.7: Frequency alpha subbands. From [8].

In [8] it is explained that the EEG oscillations of the alpha frequency show large interindividual differences which are related to age (figure 3.8) and memory performances. For this reason, it is necessary to calculate the alpha and beta frequencies for each subject.

To focus the study in these frequency bands of each subject we filter the signal using an Infinite Impulse Response (IIR) band-pass filter personalized. A band-pass filter passes frequencies within a certain range and rejects frequencies outside that range. An ideal band-pass filter would have a completely flat pass-band (e.g. with no gain/attenuation signal after the filter) and would completely attenuate all frequencies outside the pass-band. Additionally, the transition out of the pass-band would be immediate in frequency. In practice, it does not exist an ideal band-pass filter ideal.

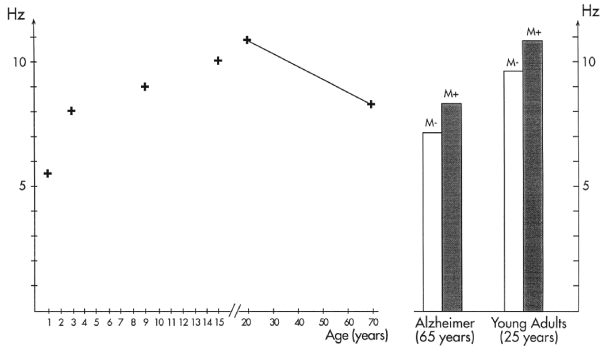

Figure 3.8: Interindividual differences in alpha frequency are large and vary with age and memory performance. From [8].

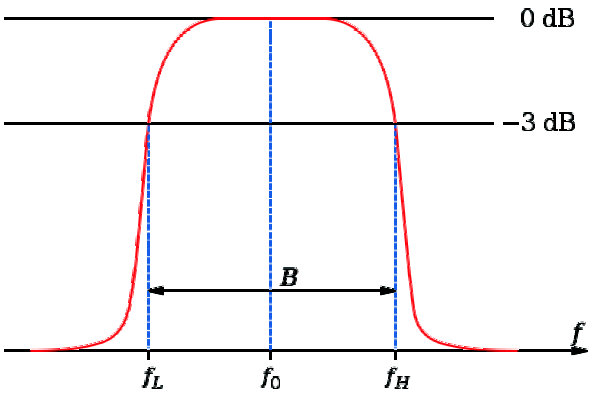

Figure 3.9: A diagram showing the definition of bandwidth (B) for a bandpass filter. f_0 is the center frequency, f_h is the higher cut-off frequency, and f_l is the lower cut-off frequency. The 0 dB level is the level of the peak of the bandpass response, which is not necessarily located at the center frequency.

In this study we use several bands to obtain the most significant results of the algorithm, however, we are focused in the alpha and beta bands. Therefore it is necessary to know in which frequencies every subject operates and to focus the filters to them. Several methods for the exact alpha band calculation have been studied, like autocorrelation analysis [29], Fourier transforms (FT), Fast Fourier Transforms [30], Adaptive Auto-Regressive (AAR)[30], among others. We could prove that for each subject the peak of his alpha frequency is not stable, therefore, the frequency alpha peak changes for each person, also the peak is not stable between different trials separated in time.

At last, we use a manual system to choose the subject alpha peak frequency, based in the Discrete Fourier Transform (DFT). After some experiments we extracted a mean frequency of all the 32 the sensors used. In the table 3.1 we can see the different mean alpha frequencies for each subject of the experiment. These results fit with [8], but we can not guarantee it because our study do not use a large population, without a large population is not possible to extract any axiom. In appendix C we can see all the peak frequencies for each subject.

Table 3.1: Subject Alpha frequencies

Subject	Alpha dominant Pitch	Std between trials	Std between sensors
S1	10.94 Hz	0.33	0.33
S2	11.01 Hz	0.688	0.477
S3	12.24 Hz	0.759	0.814
S4	9.29 Hz	0.95	0.77

Power line noise filtering

A frequently occurring linear data filtering application occurs when one tries to process a signal of the form:

$$u(n) = s(n) + A\sin(w_0 \cdot n) \tag{3.2}$$

Our main goal is to remove the additive sinusoidal component, $A\sin(w_0 \cdot t)$, without seriously adding distortion the desired signal $s(t)$. This situation occurs with the power line that adds a noise in a single frequency (a 50Hz sinusoidal wave) to the EEG signal, and it can be filtered using a notch filter [31].

The ideal filter for the above application would have a response $s(t)$ to the input $u(t)$. In the frequency domain, the required linear filter would show a gain of one for all frequencies except at w_0 where its gain is zero, but how the ideal notch filter is not physically realizable, we must implement a notch filter approximation. From [32] and [33] we obtain that transfer function of digital notch filter characterized by:

$$H(z) = \frac{B(z)}{A(z)} = \frac{1 + a_2 - 2a_1 Z^{-1} + (1 + a_2)Z^{-2}}{1 - a_1 Z^{-1} + a_2 Z^{-2}} \tag{3.3}$$

where

$$a_1 = \frac{2\cos(\omega_0)}{1 + \tan\left(\frac{BW}{2}\right)}$$

$$a_2 = \frac{1 - \tan\left(\frac{BW}{2}\right)}{1 + \tan\left(\frac{BW}{2}\right)}$$

ω_0 is the center frequency of $H(z)$ and BW is the $3dB$ bandwidth of $H(z)$. Within the frequency band inside BW all signal component are attenuated by more than 3 dB.

From equation 3.3 and [31] we obtain a difference equation of $y(t)$ that denotes the values of the filter's output signals for 3.2:

$$y(n) - a_1 y(n-1) + a_2 y(n-2) = (1 + a_2)u(n) - 2a_1 u(n-1) + (1 + a_2)u(t-2) \tag{3.4}$$

In the figure 3.10 we show the frequency response of a Notch filter of order 2 centered in a 50 Hz frequency and it's phase variation. This filter is used in the first part of the preprocessing to remove the power line noise.

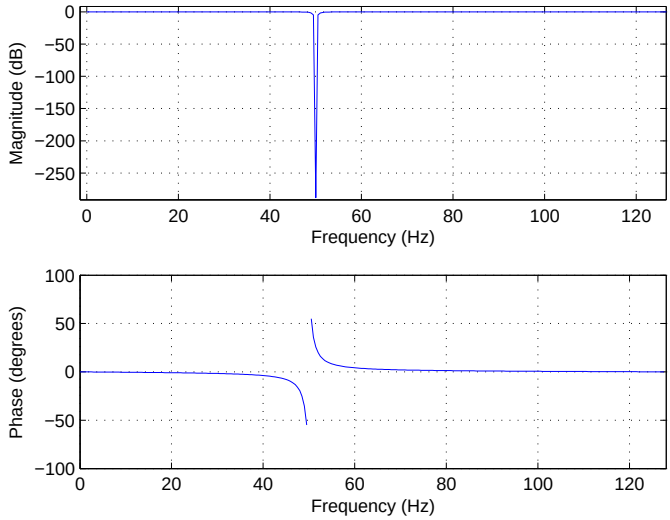

Figure 3.10: Notch filter transfer function and phase variation.

For more information see [34].

3.3.3 Trial selection

The two main files recorded during a typical experiment on a given subject are the RAW_EEG files, containing the EEG data of all the channels[1], directly recorded from the amplifier outputs and, a *Trigger_signal*, containing the absolute time of the screen blink as well as the absolute time of the subject responses[2]. Therefore the purpose is to divide this continuous recording into *Trials* and to keep only those corresponding to correct responses. See the figure 3.11.

The trial duration is chosen in the moment of the record of the brain activity, at this moment the recording Matlab function allows to choose the reference period (time and duration), the movement duration (4 seconds for the experiments) and the relaxation time, usually 2 seconds more, enough to detect the ER synchronization event. This system is based on [28]. The trigger signal that synchronizes the recorded data with the mental activity in the correct time can be visual or acoustic, each external signal indicates the moment when the subject realizes the mental activity corresponding at the state under study.

The literature [22] shows that the trials are usually synchronized with the trigger and we follow the same choice. It is made in accordance with other authors and allows us to get insights into the mental preparation even after the computation of the power reference period, as we will

[1] 32+8 channels were recorded.
[2] Time of auditory or visual marker.

see later.

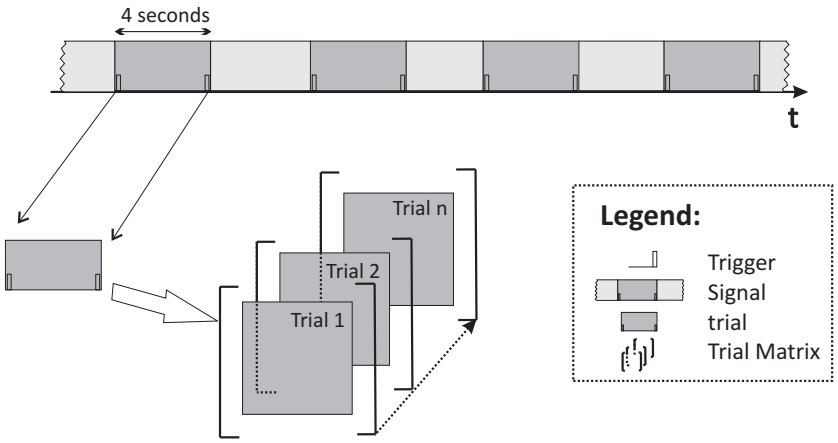

Figure 3.11: A simple scheme to explain the trial selection process.

3.3.4 The reference period

The EEG signals are processed in segments (EEG-trials) in which the BCI tries to recognize the mental activity, this process is contained in the processing part. Through the EEG_CLASS, signals are referenced to one sensor or a mean of all of them, previously, the raw eeg-trial signal is referenced to the average of the EEG channels in order to discard continues data that does not provide important contributions of information (see equation 3.5 and cite [22]). Therefore, the mean of the data is zero.

$$\sum_{n=0}^{Nt-1} EEG\_Class[ch, n, Ti] = 0 \tag{3.5}$$

where:

$$ch = 1, ..., Num\_channels \ \ and \ \ Ti = 1, ..., Num\_trials \tag{3.6}$$

So a reference period is used in the calculation of the ERS/ERD (equation 3.7), in function of the channel, therefore the signals are centered in zero, see the figure 3.12.

$$ERD(ch, j) = \frac{EEG\_Power[ch, n] - Ref(ch)}{Ref(ch)} \tag{3.7}$$

The reference period is taken 2 seconds before the mental activity starts as it is possible to observe in figure 3.13, and reference the energy of the EEG signal of 1 second. Consequently, this reference period is a sample of the background activity of the brain, since the brain activity is not stable and fluctues in time, a calculation of the reference period is allowed in every trial, using the trigger signal to determinate the correct position of the reference period.

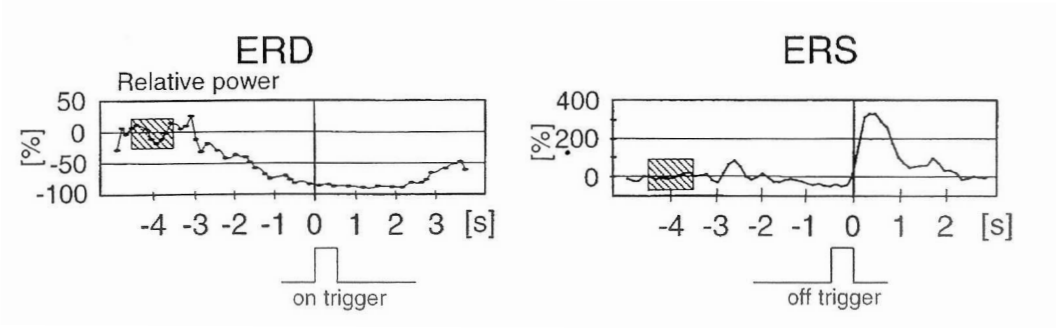

Figure 3.12: Reference period market in the grated square.

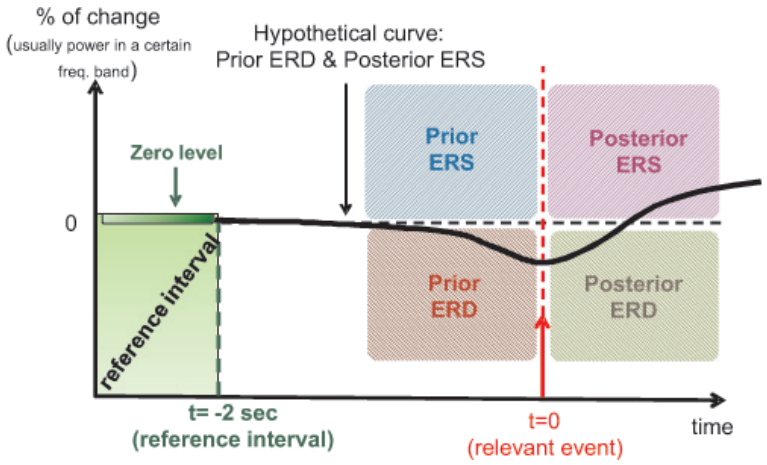

Figure 3.13: Reference period in green for a ERS/ERD calculation.

3.3.5 Artifact rejection

Once the trials are extracted from the RAW_EEG signals, the next point is removing the artifacts, by analyzing, detecting and rejecting this data that produces various types of interference waveforms (artifacts) that have added to the EEG signal during the recording sessions. As explained in the previous chapter, these artifacts are originated from many sources, eye movements, eye blinks, muscular artifacts. Our purpose is to remove them in a suitable way in order to use only accepted trials for training (explained in the previous section) and the test sequence. Nevertheless, we can already mention the impossibility to detect all the possible artifacts, even more by automatic methods[3]. For this reason, the trial selection of the train data is made manually, even though the algorithm is applied to all data signals without using the manual rejection. In this way, no corrupted trials are used to calibrate the system, and an automatic artifact detection is necessary for the process, in order to reject all the usual artifacts that exist in a RAW_EEG signal. On the other hand, since a very rigorous artifact rejection technique takes out too many trials, and leaves insufficient trials for the analysis, we design a simply detector.

Artifacts can be caused by facial muscle activity represented by the electro-myogram component (EMG), generating high frequencies waves in the gamma range [18]. Another type of artifacts is created for eye movement, called elecro-oculogram (EOG), described in [35]. Ex-

[3]Even with the intervention of professional EEG technicians is not possible to make a perfect detection.

tracting information from the subject recorded signals is easy to prove that the EOG have a much large amplitude than the mean eeg, the normal brain activity, see figure 3.14. This type of artifacts is emplaced in the frontal part of the skull. Low frequency distortions and noise are added for the recording system (amplifiers and wires), and also amplitude artifacts are created if the sensor position is moved.

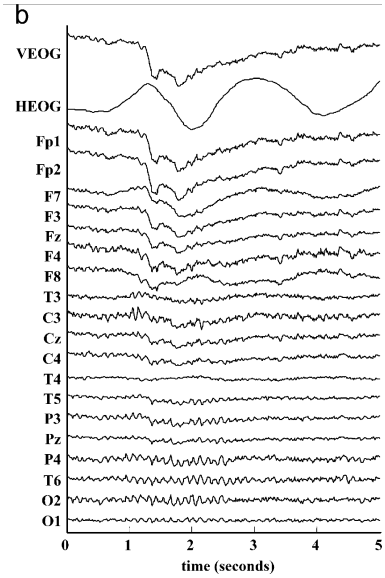

Figure 3.14: EOG components produce wide amplitude patterns in the RAW EEG, especially in the forehead channels.

To accomplish a correct rejection and detection of the artifact we need to use two classes of filters. Frequency domain artifacts can easily be rejected using a High-pass filter centered on 4 Hz and a Low-pass filter that erase all the components with a higher frequency of 25 Hz as the study is focused in alpha and beta bands.

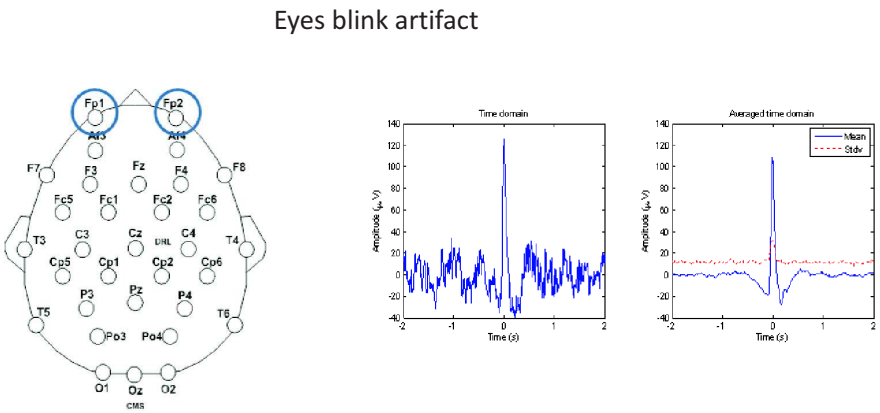

Figure 3.15: Eye blink and amplitude in Fp sensors

In the other, the rejection of OEG or sensor/cap movement artifacts is more complicated, but easy to detect, because it has a larger amplitude compared with the normal activity of the brain.

An amplitude detector is designed to reject this kind of corrupted data. The mean energy of the signal is calculated from the training data, obtaining a level of brain activity for each subject. A moving window is used to filter the signal. The energy of the signal is obtained online and a threshold comparator rejects all the data that has a specific level time (usually 5 times more) with more energy that the normal brain activity of the subject, figure 3.16. This simple artifact detector doesn't reject all artifacts, but it prevents the processing of trials containing large artifacts.

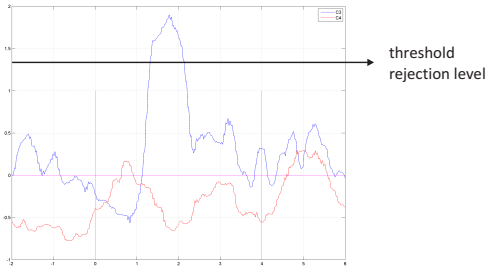

Figure 3.16: Threshold level with amplitude artifact.

3.4 ERS/ERD quantification

The algorithm designed is a learning process that takes a small training group of trials. Then, this algorithm extracts the most important features personalized for each subject and use this learned characteristics for the rest of the data, that never has been studied for the system. The idea is that a real BCI need some time to learn about the subject that is using the machine to obtain better results. This learning phase involves extracting those features of the training signal that display certain characteristic properties of EEG signal that are unique but suitable for the classification of the future data. To achieve this, the ERD/ERS characteristics are used to difference between right and left hand movement. Theory exposes that in the contralateral brain cortex to the movement, the energy in alpha bands decrease, this effect is called de-synchronization, [36] [37] [22].

The trials that satisfy this de-synchronization are the data that is not corrupted by artifacts, external noise, blinks, or other states that corrupt the signal and the features extraction. It makes very important that the trials used for training are not contaminated and, at the same time, are from the brain states that we are trying to detect in future data [38]. If the training data is not good or, in the worse case, has the features from an opposite brain state, it cause several errors. One of the worse ones is that the algorithm will attempt to maximize and look for a characteristic that does not correspond to a target market in the objectives of the BCI.

For this reason each part is carried by visual inspection for a human expert in EEG processing, although exist many techniques to detect ERS/ERD characteristics in EEG signals, but they are not infallible. For each subject the RAW_EEG_class 1 and 2 are filtered using several bands, low1-alpha, low2-alpha, high alpha, among others bands. A moving window that run across the data is used for calculating the energy of each signal in the sensor C3 and C4. The most important sensors are placed in the moving cortex to detect the ERS/ERD, [28]. A display

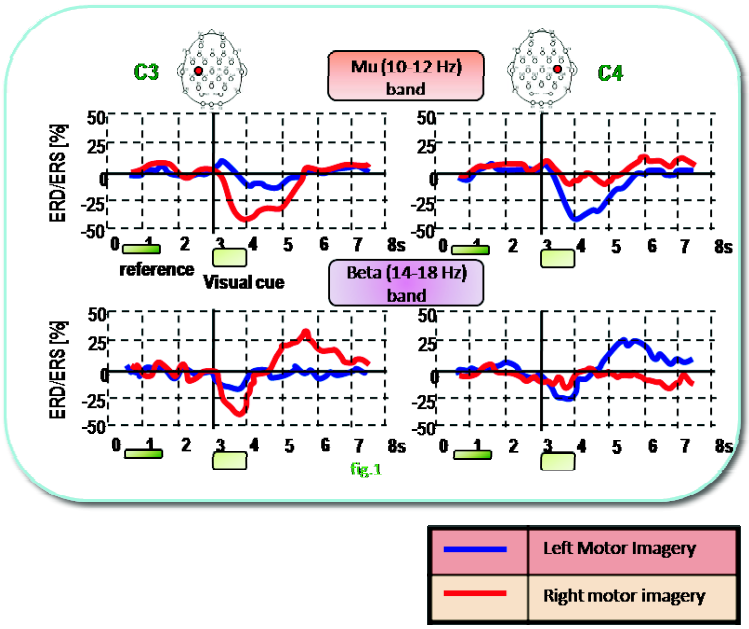

Figure 3.17: ERD/ERS characteristics using C3 and C4 sensors.

system permits the expert to select the trial or to reject it and, at the same time, allows to mark the trial as an artifact influence.

The trials used in the training sequence can be random or selected trials, is in the processing part that the algorithm has the possibility to use the training trials or randomize. Then, in the figure 3.20 the difference of a selection system and a random system are show. It is possible to appreciate that the selected system is more accurate to the theory and the ERD are more pronounced and, thus, more easy to detect. The differences between these selections are shown in the training data stage, see chapter 5 and 6.

Knowing the main reactive frequency bands for each subject, low 1 & 2 alpha and high alpha, the ERD/ERS process can be now quantified. ERD/ERS calculation displays the EEG power filter for a concrete band, relative to the power of the EEG recorded during the reference period, described in 3.3.4.

The calculation method used has the following steps:

- Band-pass filtering in subject personalized reactive bands (see Section 3.3.2)
- Squaring the amplitude samples and calculate the signal energy
- Averaging over trials

Once the decomposition into personal bands (see appendix C) and subbands has been performed, the following step consists of finding a technique to compute the evolution of the average power of these bands and subbands across time. An averaging with time-sliding rectangular windows of 1 second running on the squared signal is used, and at the same time the ERS/ERD

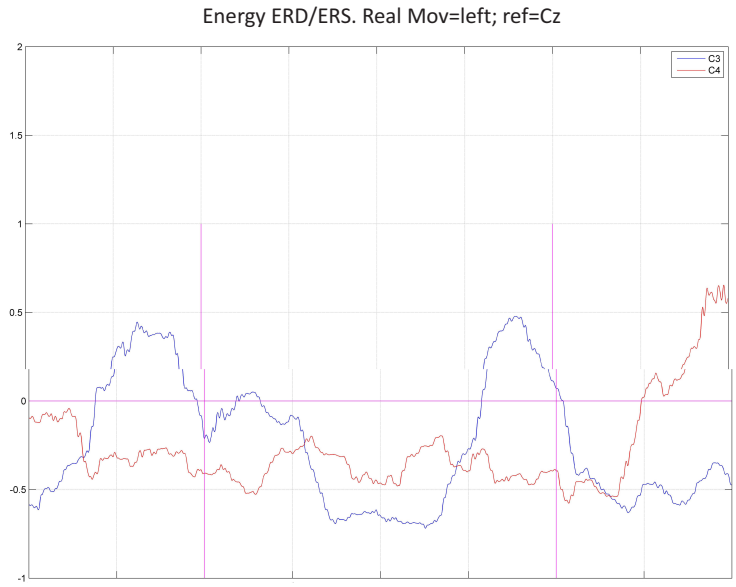

Figure 3.18: Screen shot of the manual ERS/ERD trial selection.

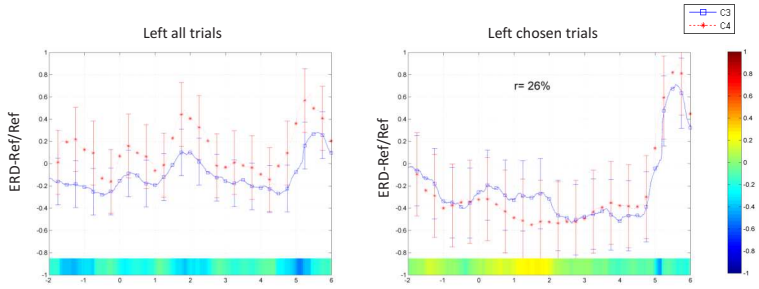

Figure 3.19: Event-Related Desynchronization (ERD) of subject 1 during real left movement referenced to all scalp sensors using a auditory clue. Finger movement.

signal is being smoothed [27].

The equation used is:

$$ERD(ch,j) = \frac{EEG\_Power[ch,n] - Ref(ch)}{Ref(ch)} \tag{3.8}$$

where

$$\text{EEG\_Power[ch, n]} = \frac{1}{\text{Ntrials}} \sum_{T=1}^{Ntrials} EEG\_enrg[ch,n,T] \tag{3.9}$$

$$EEG\_enrg[ch,n,T] = \frac{1}{long\_wind} \sum_{w=1}^{long\_wind} eeg\_Class[ch,n+w,T]^2 \forall n, \forall T, \forall ch \tag{3.10}$$

$$n \in 1...Nsamples$$

The ERD is calculated for every channel in a mean of all trials (Ntrials). Nsamples is the number of samples in every trial and long_wind is the longitude of the sliding windows used.

The reference is calculated with:

$$Ref[ch] = \frac{1}{Train\_T} \sum_{T=1}^{Train\_T} \left(\frac{1}{ref\_duration} \sum_{j=n_0}^{n_0+ref\_duration} EEG\_Class[ch, j, T] \right) \tag{3.11}$$

Train_T is the number of trials used in the train sequence and the ref_duration is the time of the reference period, usually 1 second.

Results of this process are show in the figure 3.20, were a negative ERD percentage value indicates a power decrease and a positive ERD percentage value a power increase (ERS).

3.5 Processing

This part englobes all techniques and mathematics used for the main part of the algorithm, and at the same time the explication of the equations.

3.5.1 Principal component analysis

The first step on the processing process is the PCA, Principal Component Analysis. This mathematical procedure transforms a number of possibly correlated variables into a smaller number of uncorrelated variables called principal components. The first principal component accounts for as much of the variability in the data as possible, and each succeeding component account for tries to represent the maximum quantity of the the remaining variability. In other words, PCA defines an orthogonal linear transformation that transforms the data to a new coordinate system such that the greatest variance of any projection of the data lies on the first coordinate (like figure 3.22), the second greatest variance on the second coordinate, and so on. PCA is theoretically the optimum transform for a given data in least square terms.

PCA is the optimal linear scheme, in terms of least mean square error, for compressing a set of high dimensional vectors into a set of lower dimensional vectors and then reconstructing the original set. It is a non-parametric analysis and the answer is unique and independent of any hypothesis about data probability distribution. However, the latter two properties are regarded as weakness as well as strength, as it is non-parametric, no prior knowledge can be incorporated and PCA compressions often incur in loss of information.

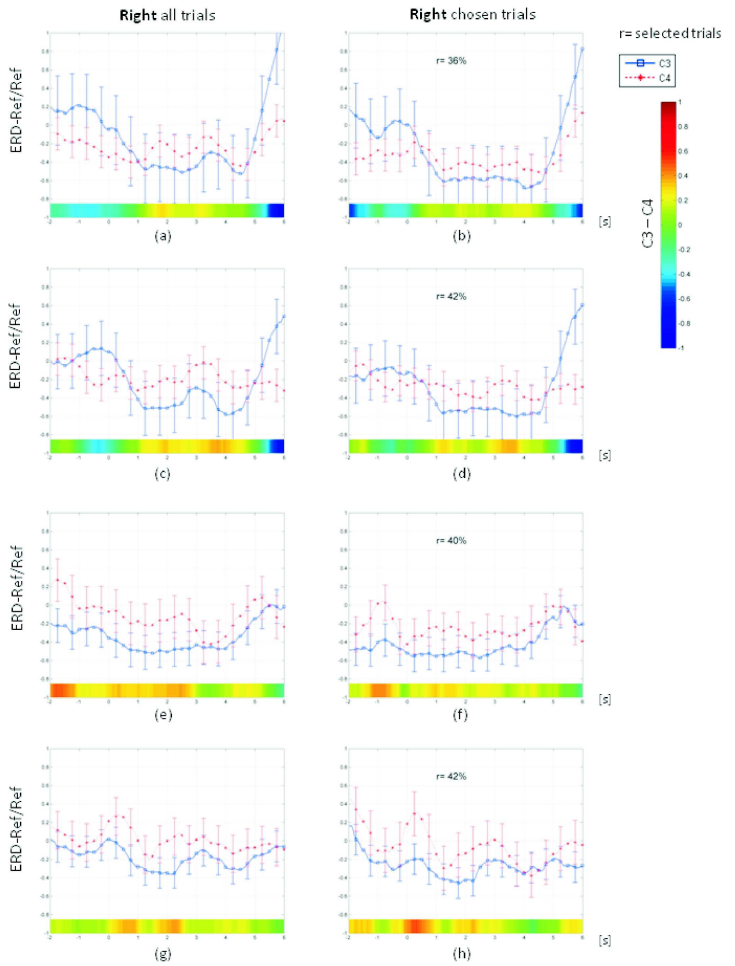

Figure 3.20: Event-Related Desynchronization (ERD) of subject 1 during real right movement referenced to all scalp sensors using a visual clue. (a)/(b) Open & close movement. (c)/(d) Up & down movement. (e)/(f) Finger movement. (g)/(h) Strong movement.

The applicability of PCA is limited to some assumptions [39] that we have to take into account. These assumptions are:

- Assumption on Linearity
- Assumption on the statistical importance of mean and covariance
- Assumption that large variances have important dynamics
- The principal components are orthogonal

PCA is used to identify meaningful underlying patterns in the EEG signals and are performed to eliminate the common components [40]. Principal components are found by extracting the eigenvectors and eigenvalues of the covariance matrix of the data, and are calculated efficiently via singular value decomposition (SVD). These eigenvectors describe an orthogonal basis that is effectively a rotation of the original cartesian basis figure 3.22.

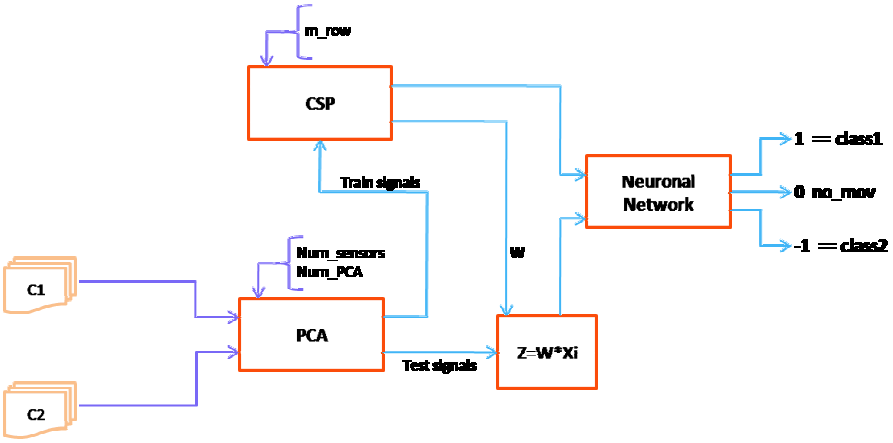

Figure 3.21: Scheme of the main processing part of the algorithm.

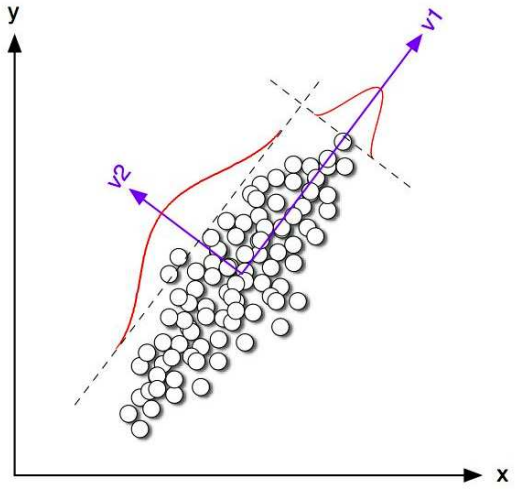

Figure 3.22: Graphical representation of a PCA transformation in only two dimensions. The variance of the data in the original cartesian space (x, y) is best captured by the basis vectors v1 and v2 in a rotated space.

3.5.2 Common spatial filters

The common spatial pattern (CSP) algorithm [41] is highly successful in calculating spatial filters for detecting ERD/ERS effects and for ERD-based BCIs (see [7]). Given two distributions in a high-dimensional space, the CSP algorithm finds directions (spatial filters) that maximize the variance for one class and that at the same time minimize the variance for the other classes. Using this method, after having band pass filtered the EEG signals in the frequency domain of interest, high (low) signal variance reflects a strong (an attenuated) rhythmic activity of the brain. At the same time this method allows to determine the best linear electrode combination to analyze the cortex activation during motor tasks.

Using this technique, the system discriminate left hand against right hand real or imagery movement. According to [28], after the preprocessing filtering to focus the signal EEG data in the reactive frequency band, a spatial filter focuses on the right hand area characterized by a strong motor rhythm during the imagination of left hand movements (right hand is in idle state),

and by an attenuated motor rhythm if movement of the right hand is imagined, see figure 3.23.

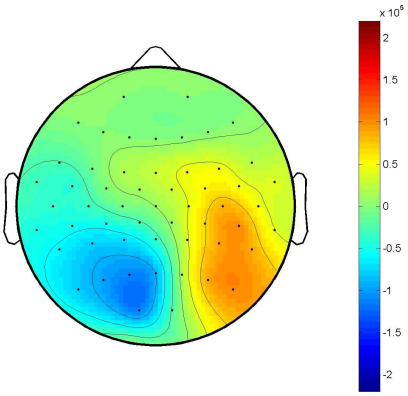

Figure 3.23: Motor cortex rhythm during left hand imagery movement of subject 3. Signal filter in the alpha band.

Maximizing variance for the EEG class1 (right hand trials) and at the same time minimizing variance for EEG class2 (left hand trials) is possible to determine the difference between both brain states, obtaining a brain activity selector. In the figure 3.24 a maximization of variance class1 (and minimization class2) is shown. Additionally, the CSP algorithm calculates the dual filter that will focus on the spatial area of the right hand in the sensor space. Moreover a series of orthogonal filters of both types can be determined. For the technical details the reader is referred to [41], [7], [26], as others.

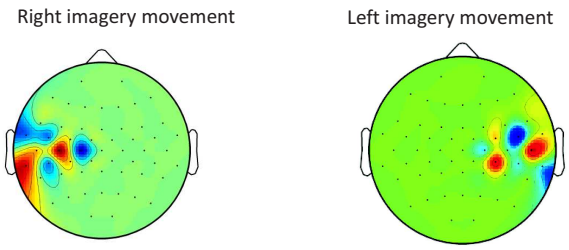

Figure 3.24: The graph shows a band-pass filter EEG signal after applying the CSP filters, maximizing a variance class an minimizing the other.

Denote average referenced multiple channel evoked responses under two conditions as spatio-temporal signal matrices X_L and X_R. Each matrices are artifact free, have dimension of ch (channels) by Nt (samples) and suppose $Nt > ch$. The normalized covariance matrices for each trial are:

$$C_L[ch, ch, Ti] = \frac{X_L[ch, Nt] \cdot X_L^T[ch, Nt]}{trace(X_L X_L^T)} \quad , \forall Ti$$

$$C_R[ch, ch, Ti] = \frac{X_R[ch, Nt] \cdot X_R^T[ch, Nt]}{trace(X_R X_R^T)} \quad , \forall Ti \tag{3.12}$$

The averaged normalized covariances over trials $\overline{C_L}$ and $\overline{C_F}$ are calculated.

$$\overline{C_L}[ch, ch] = mean(C_L[ch, ch, Ti]) \qquad over \quad Ti$$

$$\overline{C_R}[ch, ch] = mean(C_R[ch, ch, Ti]) \qquad over \quad Ti \tag{3.13}$$

$\overline{C_L}$ and $\overline{C_R}$ are symmetric positive definite matrices, thus their sum is also a symmetric positive definite matrix [4], and for this reason, all eigenvalues λ_i of $\overline{C_L}$ and $\overline{C_R}$ are positive. Therefore $\overline{C_L}$ and $\overline{C_R}$ are diagonalizable [5] hence factorize the sum covariance matrix of $\overline{C_L}$ and $\overline{C_R}$ into the product of eigenvectors and eigenvalues by:

$$\overline{C} = \overline{C_L} + \overline{C_R} = U \cdot D \cdot U^T \tag{3.14}$$

where U is the matrix of eigenvectors (since U is an orthogonal matrix [6], then $U^{-1} = U^T$) and D is the diagonal matrix of the eigenvalues, that are always positive. In subsequent steps we take only the components with non zero singular values into consideration. The whitening transformation matrix is then formed as:

$$P = D^{-1/2} \cdot U^T \tag{3.15}$$

The whitening transformation matrix P forms the equation 3.14, as we show:

$$\overline{\mathrm{C}} = UDU^T$$

$$\begin{aligned} \left(D^{-1/2}U^T\right) C \left(UD^{-1/2}\right) &= \underbrace{\left(D^{-1/2}U^T\right)}_{P} UDU^T \underbrace{\left(UD^{-1/2}\right)}_{P^T} \\ &= \underset{where: UU^T = I}{D^{-1/2}D} D^{-1/2} = I \end{aligned} \tag{3.16}$$

Now $\overline{C_L}$ and $\overline{C_R}$ are individually transformed using 3.16 as:

$$P\left(\overline{C_L} + \overline{C_R}\right) P^T = I \tag{3.17}$$

[4] A real symmetric n*n matrix A, which entries are real numbers, is positive definite if $x^T Ax > 0$ for all non-zero vectors x in R^n.

[5] An n*n matrix A is said to be diagonalizable if it can be written as $A = P \cdot D \cdot P^{-1}$, where D is a diagonal n*n matrix with the eigenvalues of A as its entries and P is an invertible n*n matrix consisting of the eigenvectors corresponding to the eigenvalues in D.

[6] An n*n matrix A is an orthogonal matrix if $AA^T = I$, where A^T is the transpose of A and I is the identity matrix. In particular, an orthogonal matrix is always invertible, and $A^{-1} = A^T$.

$$\underbrace{P\overline{C_L}P^T}_{S_L} + \underbrace{P\overline{C_R}P^T}_{S_R} = I \tag{3.18}$$

and we obtain the $\overline{C_L}$ and $\overline{C_R}$ individually transformation S_L and S_F defined:

$$\begin{aligned} S_L &= P\overline{C_L}P^T \\ S_R &= P\overline{C_R}P^T \end{aligned} \tag{3.19}$$

S_L and S_F are diagonalizable and exhibit the following two important properties:

1. They share common eigenvectors, i.e.

$$S_L = U_0 D_L U_0^T \qquad , \qquad S_R = U_0 D_R U_0^T \tag{3.20}$$

2. The sum of the corresponding eigenvalues for the two matrices will always be I, i.e.

$$S_L + S_R = I \tag{3.21}$$

(Mathematical demonstration of these axioms are in the Appendix B.)

Assume that the diagonal elements in S_L are in descending order, then the variance accounted for by the first several spatial factors are maximal for condition L, and minimal for condition R. Hence, this transformation is optimal for separating the variance in two signal matrices because the eigenvectors with the largest eigenvalues of S_L have the smallest eigenvalues of S_R and vice-versa.

Finally, equalizing $S_L = P\overline{C_L}P^T$ with $S_L = U_0 D_L U_0^T$, the projection W matrix is obtained:

$$P\overline{C_L}P^T = U_0 D_L U_0^T \tag{3.22}$$

$$\underbrace{U_0^T P}_{W}\,\overline{C_L}\,\underbrace{P^T U_0}_{W^T} = D_L \tag{3.23}$$

$$W = U_0^T P \tag{3.24}$$

The rows of W represent the **common spatial filters**. Taking the first rows of W, associated to the most important eigenvalue of class L, the equation 3.25 maximize the variance of class L

and, therefore, minimize the variance of class R.

Using this decomposition matrix, the entire EEG signal X can be projected as:

$$Z = WX \tag{3.25}$$

And the original signal can be reconstructed by equation 3.26, where the columns of W^{-1} are the **common spatial patterns**:

$$X = W^{-1}Z \tag{3.26}$$

Details of the described algorithm are from [42] and[40].

3.6 Neural network

Since brain data is non-stationary, characterized by significant trial-to-trial and subject-to-subject variability, highly dimensionated with only relatively few samples available for fitting models to the data and with highly unfavorable signal-to-noise ratio, Machine learning techniques are required. Due to this variability, machine learning methods have become the tool of choice for the online analysis of single-trial brain data [43].

The Brain-Computer Interfacing has pushed single trial EEG analysis to an extreme, as the methods applied in this field need to be performed in real-time without significant processing delays. In the following the basic machine learning methods for single trial EEG analysis are introduced: feature extraction - an approach using spatial filters is presented - and classification, which is discussed with the example of a framework of regularized Single-Layer networks, eventhough Linear Discriminant Analysis (LDA) can be used too, like in [44].

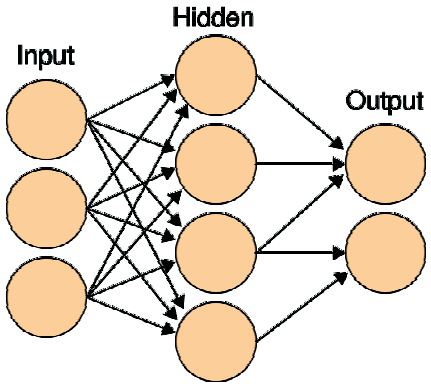

Figure 3.25: A neural network as an interconnected group of nodes.

Furthermore when analyzing high dimensional data it is not only important to visualize, predict or classify the data with low error, but it is essential that the exploratory data analysis tools allow to explain the underlying structure in order to contribute to a better understanding of the data.

3.6.1 Single-Layer networks

Also called Perceptron, is a type of Artificial Neural Network invented in 1957 at the Cornell Aeronautical Laboratory by Frank Rosenblatt. Single layer networks implement the well known statistical techniques of linear regression and generalized linear models (GLMs), these models consist of a linear combination of the input variables, in which the coefficients are the parameters of the model, followed by an activation function adjusted to the type of data being modeled.

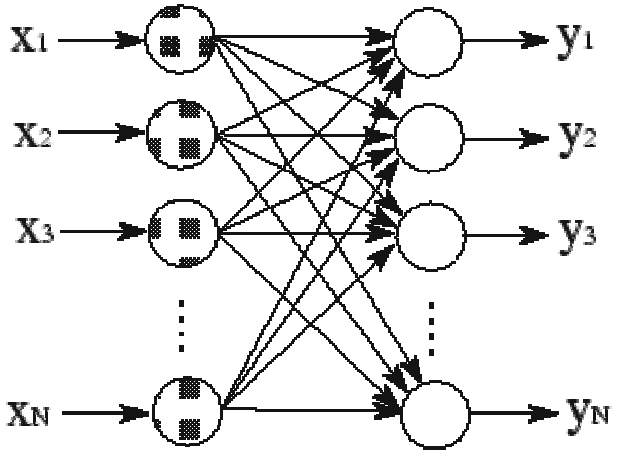

Figure 3.26: Single Layer Neural Network.

This kind of network can be created using any values for the activated and deactivated states as long as the threshold value lies between the two. Most perceptrons have outputs of 1 or -1 with a threshold of 0 and there is some evidence that such networks can be trained more quickly than networks created from nodes with different activation and deactivation values.

Perceptrons can be trained by a simple learning algorithm that is usually called the delta rule. It calculates the errors between calculated output and sample output data, and uses this to create an adjustment to the weights, thus implementing a form of descent gradient.

3.6.2 Implementation

Netlab three-class codes from [45] (ie., figure 3.27) are use to design our neuronal network, using the free-artifacts train trials for the learning process of the network. After this, on line trial can be processed obtaining an output signal between 1, 0 or -1 for each case.

- 1: for class 1 movement

- 0: for no movement
- -1: for class 2 movement

Fast transitions have to be removed, smoothing the signal, based on the assumption that a brain state has to take some time to change to the opposite state.

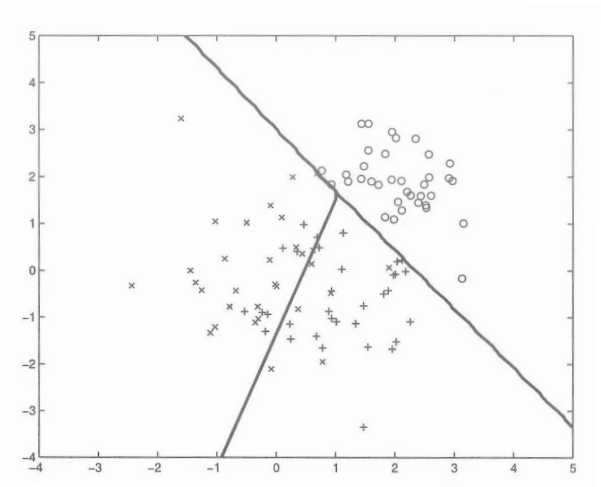

Figure 3.27: Data belonging to class 1 (circles), class 2 (crosses) or class 3 (plus signs). Decision boundaries (solid line) shown where two posterior classes probabilities are equal.

For more information see [46] and [43].

Section 4

Experiment and protocol

IN PREVIOUS SECTIONS, the architecture and the inner mechanisms of the brain are explained and also the algorithm designed to detect the kind of movement recorded in the EEG signals. In this chapter, the experiments realized with the protocols are shown, giving a set of rules and procedures commands that act on a computer -rendered environment. These procedures are set experimentally, and depend on the realization, changing for every different test that we have done.

In this study we apply the recording procedure, the preprocessing, feature extraction, and the algorithms presented in the previous chapter, to analyze the four subjects that participated in the motor real and imagery brain computer interface experiment. At the same time, the recorded EEG signals from the "BCI competition IV 2008", *motor imagery, uncued classifier application* were used to test the algorithms and extract the first conclusions and ideas to design our's experiments.

Figure 4.1: Emblem of the BCI competition IV.

The data sets used in the experiment were recorded using a BioSemi system from healthy subjects. In the whole session, motor real and imaginary brain activity was performed without feedback. For each subject two classes of real and imaginary movements, left hand and right hand were recorded. The data recorded for the competition consisted, for each subject, of two classes of motor imagery selected from the three classes *left hand, right hand*, and *foot* (the side was chosen by the subject; optionally also both feet).

4.1 Experiment setup

Four male subjects (denoted S1 to S4 respectively) aged 26, 29, 23, 29, respectively, participated in the recording seasons distributed over 3 months. These seasons were carried out in a quiet and good illuminated laboratory room where the subjects were comfortably sitting in an armchair, with his arms in stand, and placed about one meter from the table that contained all the recording

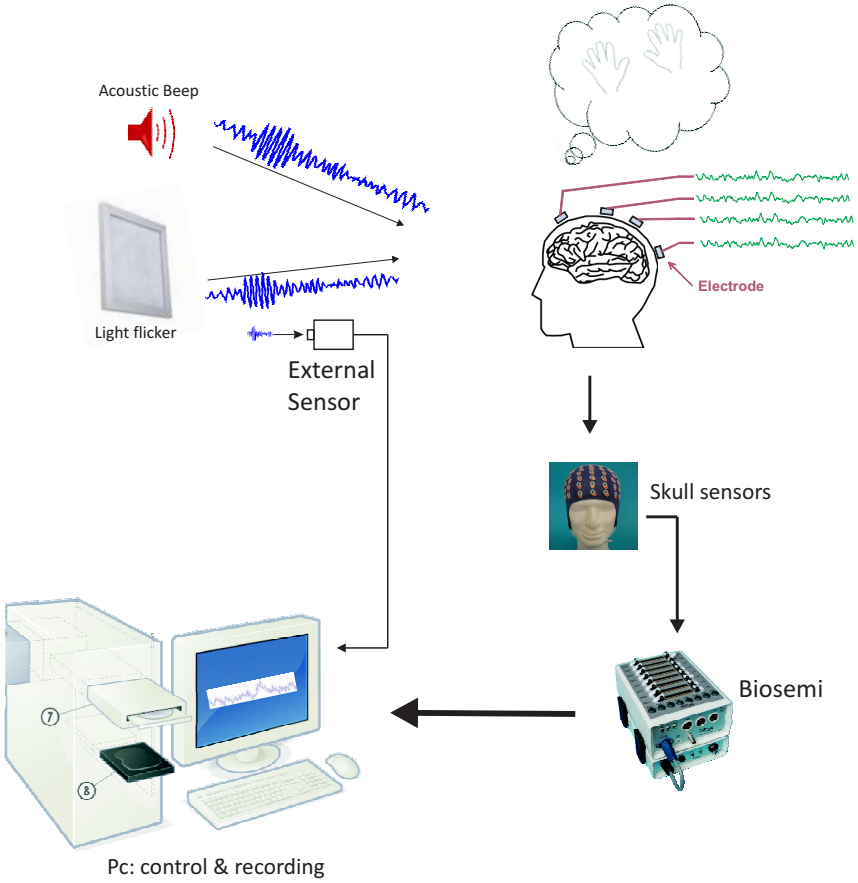

Figure 4.2: Schematic connections in the experiments.

system and the PC that controled the whole system.

The subjects were instructed to avoid eye movements and to keep their arms and hands relaxed during the experiment. The blinks are impossible to avoid, for this reason the subjects were forced to try to blink in the relaxing or waiting time, never during the recorded brain activity. Four kind of voluntary and imaginary hand movements were performed for every hand and subject, obtaining 48 files to analyze.

These kinds of movements are:

- Open and close the hands
- Up and down the hands (moving the wrist)
- Index finger movement
- Muscular fixation in closing movement of the hand

Every recording season took around one hour, within this time two movements of each hand were recorded, with fifty repetitions of movement for each file. Voluntary or imaginary movements were performed, approximately every 9 seconds, and the trigger signal was recorded in

Figure 4.3: The complete setup including the cap with the 32 electrodes, the AD-box, USB2 converter and PC used for recording the EEG signals of the subject S1.

the same file by an external sensor in a additional channel. It is known that a external signal, like the trigger, effects in the brain activity (evoked potentials). With the goal of study differences between different external effect signals, two different trigger signals are used, one visual, with a flicker of light, and one acoustic, with a beep, both less than 400 milliseconds of duration.

An external stimuli (light or beep) was displayed to show the beginning and the ending of a period of 4 seconds in which the subject was instructed to perform the cued brain task. These periods were interleaved with 2 seconds of relax and 3 seconds of preparation, and repeated 50 times for each file. Between these repetitions, we introduced a random waiting time, which range between 0 and 2 seconds. These data sets are provided with complete marker information.

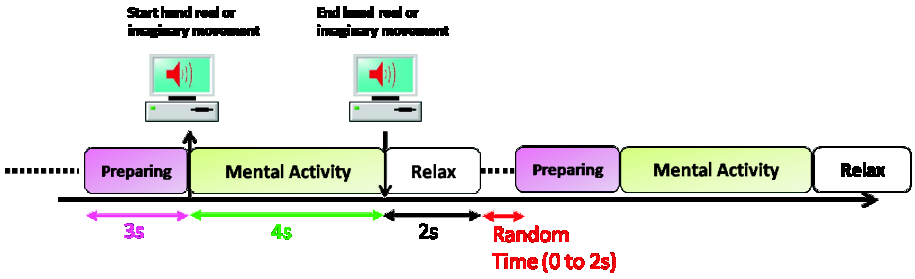

Figure 4.4: Scheme of each repetition

At time -3 seconds, time = 0 is defined as the moment of beginning the brain activity of the subject that corresponds with the marker. There is a preparation period of 3 seconds that allows the subject to blink and relax in order to obtain a normal normal background activity in his brain, so it is ready for the next interaction.

At time = 0, an external marker (a light or a beep) indicates at the subject to start the corresponding movement (real or imaginary), and in the same way, a maker indicates the end of the

activity, after 4 seconds.

A relax time of 2 seconds after the activity period is introduced to permit the brain relaxation and allow the ERD study that appears after the mental activity. A random period is used after it to block the subject to make his repetitions in a mechanical way, the random time forces to pay attention.

The intention of using a type of marker is to study the effect of Evoked Potential inside the brain on the subject, because an external stimulus can affect the inner brain activity. For this reason, two different marks are used: one visual with a flicker of light, and one acoustic, with a beep, and the conclusions of this selection are explained at the end of this chapter.

A Matlab code has been designed to control all the trigger marks, and the corresponding time. This program records the times of the marker signal for a posteriori use in the program.

Skull helmets with 32 pin sensors are used to obtain the data brain activity. The electrodes were placed on the scalp at positions defined by the 10-20 International System: electrodes FP1, FP2, F7, F3, Fz, F4, F8, C3, Cz, C4, P7, P3, Pz, P4, P8, T7, T8, O1,Oz, and O2. The remaining electrodes were from a 10-10 system: electrodes AF3, AF4, FC1, FC2, CP1, CP2, PO3, PO4, FC5, FC6, CP5, and CP6. BioSemi systems are used to pre-filter and record the signal, to obtain files with the extension .bdf.

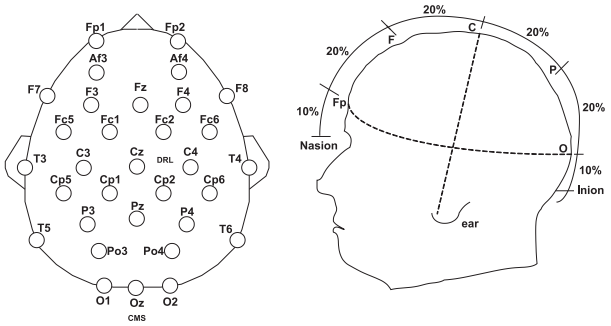

Figure 4.5: The 10-20 International System.

Data collected was stored in a 2D matrix having in the columns the 32 channels and in the rows the number of samples (see figure 4.6), changing the format to .mat to make possible the analysis. In order to simplify the processing of this matrix, the values from each channel are segmented in trials. A trial last 9 seconds. The new EEG data is collected into a 3D matrix where the 3rd dimension indicates the number of trials. Before segmentation, the EEG signals were preprocessed (see Section 3.3, preprocessing) and resampled at 256Hz. This transformation is schematized in figure 4.6.

(See chapter 2.3.1, for an extend explanation of the recording system)

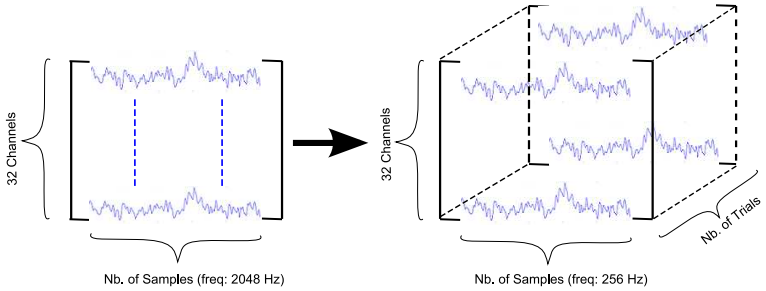

Figure 4.6: Transforming data to 3D matrix, to ease the calculations.

4.2 Applied stimuli

When an external stimulus takes place, some specific pathways are involved in the conduction of the information. This shows the existence of phase-locked responses that provide indications about the electrical activity during the physical relay of information. If the same stimulus is repeated, the same pathways will be activated again. These responses called Evoked Potentials (4.7) and although they mainly come from deeper structures, they are perceived on the scalp.

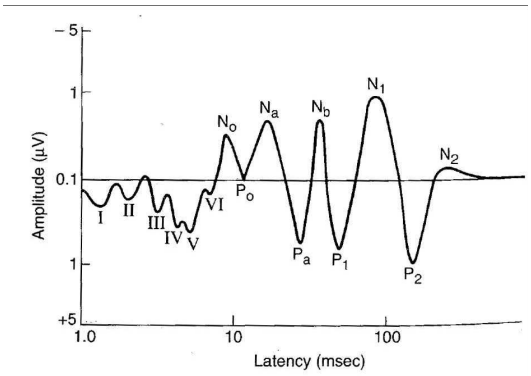

Figure 4.7: The auditory evoked potential shows of some peaks which correspond to the presence of electrical activity during the relay of information from the sensory neurons to the cortex, from [2].

External stimuli is applied over the subjects to mark the precise time in which the activity period has to start and end. Light and acoustic stimuli are used and the reason of this stimuli selection and its consequences are explained in this part.

4.2.1 Threshold

In order to interpret correctly the position of the mark in time, an arbitrary threshold is used, and recalculated for each file. The final value is defined by equation 4.1 and implemented in the preprocessing to extract the trials of the data files using a trigger, as defined in equation 4.2. The threshold is recalculated for each data file because the background activity changes with the time, even in the same experiment season. Therefore the threshold value is not fixed.

$$threshold = \frac{(\max(Energy\_threshold\_signal) + \min(Energy\_threshold\_signal))}{2} \tag{4.1}$$

$$trigger = \begin{cases} 1 \leftarrow mark\_signal > threshold \\ 0 \leftarrow mark\_signal < threshold \end{cases} \tag{4.2}$$

4.2.2 Visual stimulation

A visual evoked potential (VEP) is an evoked potential caused by a visual stimulus such as an alternating checkerboard pattern on a computer screen. In our experiment a light flick of 100 milliseconds approximately is used as a type of marker.

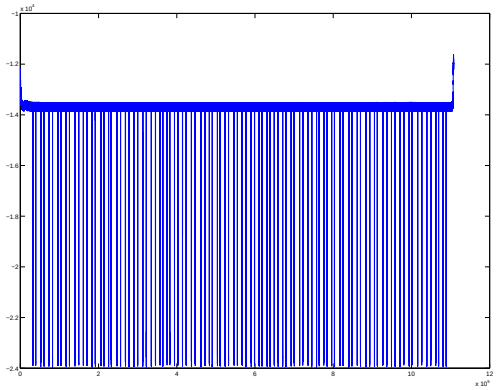

Figure 4.8: Light sensor signal. Every peak is a mark.

[2] define the existence of phase-locked responses which provide indications about the electrical activity during the physical relay of information. These responses are Evoked Potentials and generate an inner signal on the back of the head, usually in the occipital cortex, the area of the brain involved in receiving and interpreting visual signals.

This induced potential has a frequency behavior (or in the harmonics) equal to the original stimuli, 40 Hz in this experiment. The algorithm focuses on the frequency bands between 5 and 30 Hz, specifically the alpha band (8-12Hz), as is the one used by EVP's filters block. Using this visual stimulation appears an event-related potential (ERP). It is any measured brain response that is directly the result of a thought or perception like in the figure 4.10. More formally, it is any stereotyped electrophysiological response to an external stimulus.

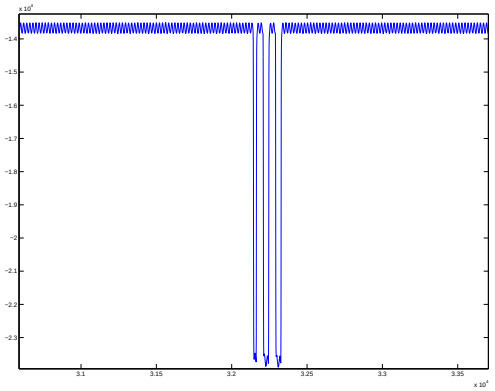

Figure 4.9: Trigger of light mark. Duration 95 milliseconds aprox.

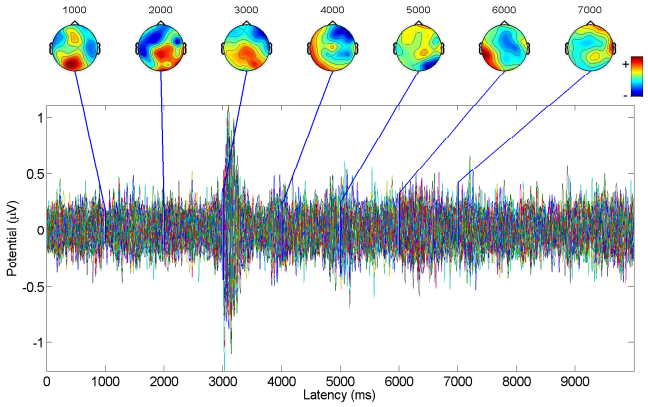

Figure 4.10: Event-related potential and the brain activity of the subject S1. A average of trials is show.

4.2.3 Audio stimulation

The stimulation of hearing receptors with acoustic stimulus and the analysis of evoked response of the brain is a well known method widely used in clinical examinations. This method allows to investigate the mechanism of the human acoustic-neural system. Brainstem auditory evoked potentials (BAEP) is the brain response for acoustic stimulation. Usually tone or click stimuli are used (figure 4.12), in our experiment an acoustic beep of 400 milliseconds is the second marker type, with an acoustic frequency of 250 Hz.

Similarly to the visual stimulus case, the acoustic one has no appearance of evoked potentials in the relevant frequency bands of the study, only an event-related potential. In figure 4.13 it is possible to see that the acoustic potential is not focused in the auditory zone of the brain.

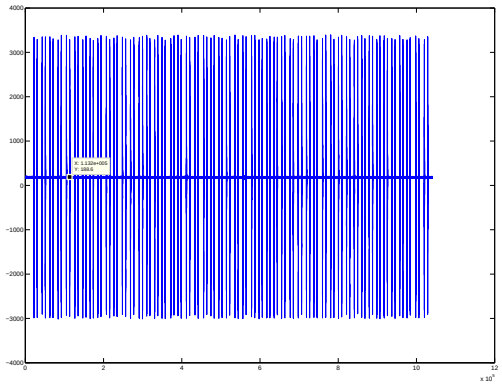

Figure 4.11: Acoustic sensor signal. Every peak is a mark.

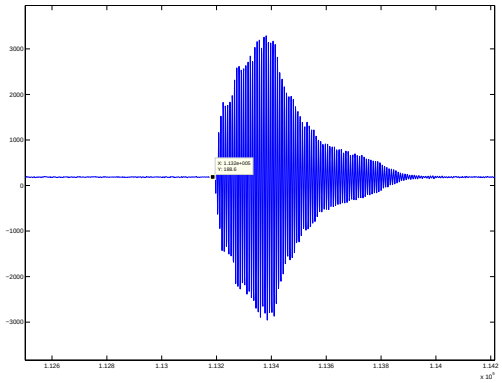

Figure 4.12: Trigger of acoustic mark. Duration 375 milliseconds aprox.

4.2.4 Conclusion

Each external stimuli, even the markers, generate a response inside the brain of the subject, an evoked potential (EV) and an event-related potential (ERP). The Evoked potential is easily dismissed because appear in a different frequency band than the studied one by the algorithm. Therefore, only appear an event-related potential (ERP) (see figure 4.10 and 4.13). These Event related potentials are transient signals which appear as voltage deviations in the electroencephalogram (EEG) and are caused by external stimuli or cognitive processes triggered by external events. ERPs, like most other real life signals, are nonstationary and have characteristics that vary across stimulus trials during the course of an experiment. Such variations may be associated with fluctuating attention levels, adoption to stimuli, fatigue, or other unknown factors, [47].

Consequently, a trigger mark induces an ERP, but does not affect in the algorithm results because is present in both class signals and the algorithm is focused in the signal patterns that difference both mental states. If the mental activity is the same in all classes, the common spatial patterns (CSP) minimize the effect.

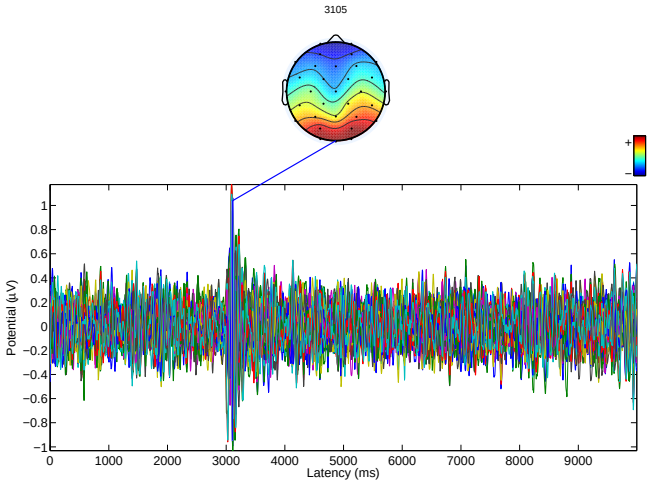

Figure 4.13: Event-related potential and the brain activity of the subject S1 to an acoustic stimuli. An average of trials is shown.

4.3 Alpha experiment

As we described in the chapter 3.3.2 , the alpha peak changes for every person, is not constant, and it is necessary to take and analyze it individually. With this goal a short alpha experiment has been realized for every subject. Using an acoustic beep to mark the beginning and the ending, the subjects are asked to close and open their eyes 20 times.

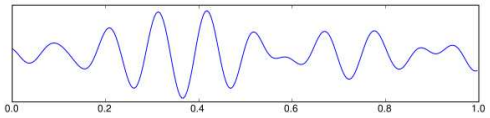

Figure 4.14: Alpha waves.

Alpha is the frequency range from 8 Hz to 12 Hz. This is the activity seen in the 8-12 Hz range in the posterior regions of the head on both sides, being higher in amplitude on the dominant side. It is brought out by closing the eyes and by relaxation. It was noted to attenuate due to eye opening or mental exertion.

Several methods for the exact alpha band calculation have been studied in the realization, using autocorrelation analysis [29], Fourier transforms (FT), Fast Fourier Transforms [30], Auto Adaptive Auto-Regressive (AAR), among others. We could prove that every subject is not stable in a peak of alpha frequency. Therefore, the frequency alpha peak changes for each person, and also the peak is not stable between different trials separated in time.

(See chapter 3 and Annex C to see different values of alpha peak for different subjects)

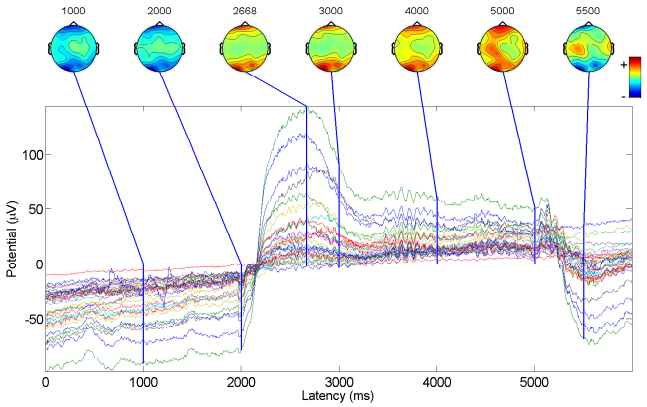

Figure 4.15: Brain activity of different trials in the *alpha experiment*. Is possible to see the difference between the close eyes period (values under zero) and the eyes open period (values over zero).

4.4 Preliminary experiment

The recorded EEG signals from the "BCI competition IV 2008", *motor imagery, uncued classifier application* was used to test the algorithms and to extract the first conclusions and ideas for designing our experiments. Following there is a description of this data and its structure.

4.4.1 Data from Brain Computer Interface Competition IV

(From http://ida.first.fraunhofer.de/projects/bci/competition_iv/)

In the first part of this study, data from BCI competition IV was used. After some recording experiments our recorded data was used. In this part the description of the data used at the beginning of the study is shown, like its structure and characteristics.

Data sets were recorded from healthy subjects. In the whole session motor imagery was performed without feedback. For each subject two classes of motor imagery were selected from the three classes *left hand, right hand* and *foot* (side chosen by the subject; optionally also both feet).

Calibration data: In the first two runs, arrows pointing left, right or down were presented as visual cues on a computer screen. Cues were displayed for a period of 4 seconds during which the subject was instructed to perform the cued motor imagery task. These periods were interleaved with 2 seconds of blank screen and 2 seconds with a fixation cross shown in the center of the screen. The fixation cross was superimposed on the cues, i.e. it was shown for 6 seconds. These data sets are provided with complete marker information.

Evaluation data: Is composed of 4 runs followed which are used to evaluate the submissions to the competitions. The motor imagery tasks were cued by soft acoustic stimuli (words *left, right* and *foot*) for periods of varying length between 1.5 and 8 seconds. The end of the mo-

tor imagery period was indicated by the word stop. The intermitting periods had also a varying duration of 1.5 to 8 seconds. Note that in the evaluation data, there are not necessarily equal trials from each condition.

Special Feature: Some of the data sets were *artificially generated*. The idea is to have a means for generating artificial EEG signals with specified properties that is so realistic that it can be used to evaluate and compare analysis techniques. The outcome of the competition will show whether the applied methods perform comparably on artificial and real data. The only information we provide is that there is at least one real and at least one artificial data set, while the true distribution remains undisclosed until the submission deadline. For the competition purposes, only results for the real data set(s) are considered. The functions for generating artificial data were provided by Guido Nolte and Carmen Vidaurre.

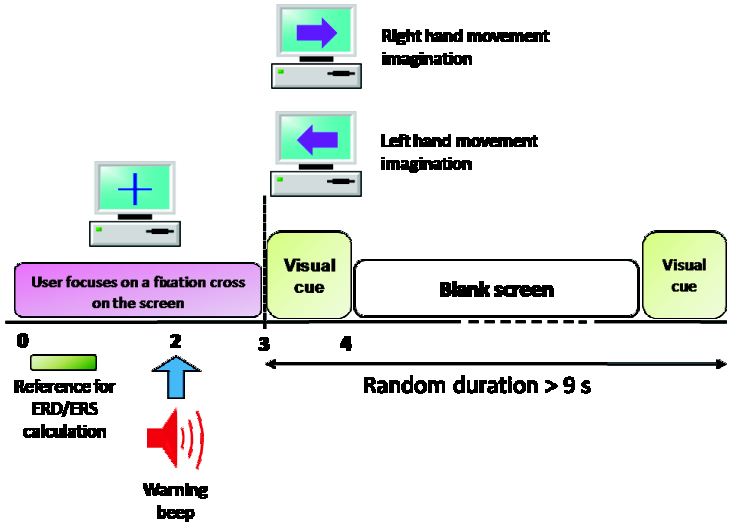

Figure 4.16: BCI competition IV's experiment.

4.4.2 Requirements and Evaluation

Information data and requirements for apply the obtained results to the Brain Computer Interface Competition IV (extracted from http://ida.first.fraunhofer.de/projects/bci/competition_iv/):

Please provide an ASC II file (named 'Result_BCIC_IV_ds1.txt') containing classifier outputs (real number between -1 and 1) for each sample point of the evaluation signals, one value per line. The submissions are evaluated in view of one dimensional cursor control application ranged from -1 to 1. The mental state of class one is used to position the cursor at -1, and the mental state of class two is used to position the cursor near 1. In the absence of those mental states (intermitting intervals) the cursor should be at position 0. Note that it is unknown to the competitors at what intervals the subject is in a defined mental state. Competitors submit classifier outputs for all time points. The evaluation function calculates the squared error for the target vector that is -1 for class one, 1 for class two, and 0 otherwise, averaged across time points. In the averaging we will ignore time points during transient periods (1 second starting from each cue). For the competition purpose, only results for the real data set(s) are considered,

but results for artificial data are also reported for comparison.

Optionally, please report which of the data sets you think to be artificially generated. You also have to provide a description of the used algorithm (ASC II, HTML or PDF format) for publication at the results web page.

4.4.3 Technical Information

The recording was made using BrainAmp MR plus amplifiers and an Ag/AgCl electrode cap. Signals from 59 EEG positions were measured that were most densely distributed over sensorimotor areas. Signals were band-pass filtered between 0.05 and 200 Hz and then digitized at 1000 Hz with 16 bit (0.1 uV) accuracy. We provide also a version of the data that is down sampled at 100 Hz (first low-pass filtering the original data [1] and then calculating the mean of blocks of 10 samples).

[1] Chebyshev Type II filter of order 10 with stop band ripple 50dB down and stop band edge frequency 49Hz.

Section 5

Real & imaginary movement results

THROUGH THIS CHAPTER, we have been performed some advanced time-frequency digital signal processing techniques and statistics in order to extract information about the functional activity in the brain. This information, called features, is quantified by the ERS/ERD curves, computed in different frequency bands and subands over different regions of the cerebral cortex for each subject. This requires to pay special attention to the evolution of the zones of relevance for different frequency bands or subands, and to identify, there, the nature of the differences between the two populations. From these results, an analysis of the importance of specific bands or channels is performed. The feature extraction allows to use the algorithm focus in time and frequency, cerebral region, among others.

Through this chapter, we have made rational choices to get sharp but generalized signals from each subject, to compute meaningful ERS/ERD curves, and apply features to extract common spatial patterns from the data. To make more relevant comments about the system performances, new data is tested using the features extracted before. The main purpose of the chapter is to detect and quantify where significant differences appear between these features in order to make the distinction between mental activities related to motor cortex activity and to create a classifier able to perform a decision, between different mental states, in new data from the subjects.

Finally, statistics tests of the results system are achieved to compare the population means using variance analysis techniques. The outputs returned by the algorithm are analyzed using one-way variance analysis (ANOVA), used to find differences between two independent groups, and Student's t-test technique, that advice us if the variation between the two distributions is "significant", determine whether the means are distinct, returning a parameter of significance, p-value. If the calculated p-value is below the threshold chosen for statistical significance (usually the 0.10, the 0.05, or 0.01 level), then the null hypothesis which usually states that the two groups do not differ is rejected in favor of an alternative hypothesis, which typically states that the groups really differ. All these steps are discussed below.

5.1 Spatiotemporal pattern localization

In this section, the plotting of relevance functions of the different channels according to their interpolated head positions as a function of time is explained. These functions provide mappings

of specific band patterns for subjects and show the evolution of the patterns found in the classical band ERS/ERD curves.

5.1.1 Classical frequency bands

One of the most critical issue in multichannel ERD/ERS analysis methods involving diverse frequency bands, such as the method described here, is the adequate selection of the frequency bands.

As seen in the section 3.3.2 we use several bands to obtain the most significant results of the algorithm, however, we focus in the alpha and beta bands, therefore it is necessary to know in which frequencies operates every subject and focus the filters in consequence. Several methods for the exact alpha band calculation have been studied in the realization, using autocorrelation analysis [29], Fourier transforms (FT), Fast Fourier Transforms [30], Adaptive Auto-Regressive (AAR)[30], among others. We could prove that every subject is not stable in a peak of alpha frequency, therefore, the frequency alpha peak changes for each person, therefore, the peak is not stable between different trials separated in time. In figure 5.1 the alpha peak for subject 1 between different sensor is show. It is possible to see that the alpha peak is more intensive in the back part of the brain, in the optical cortex zone.

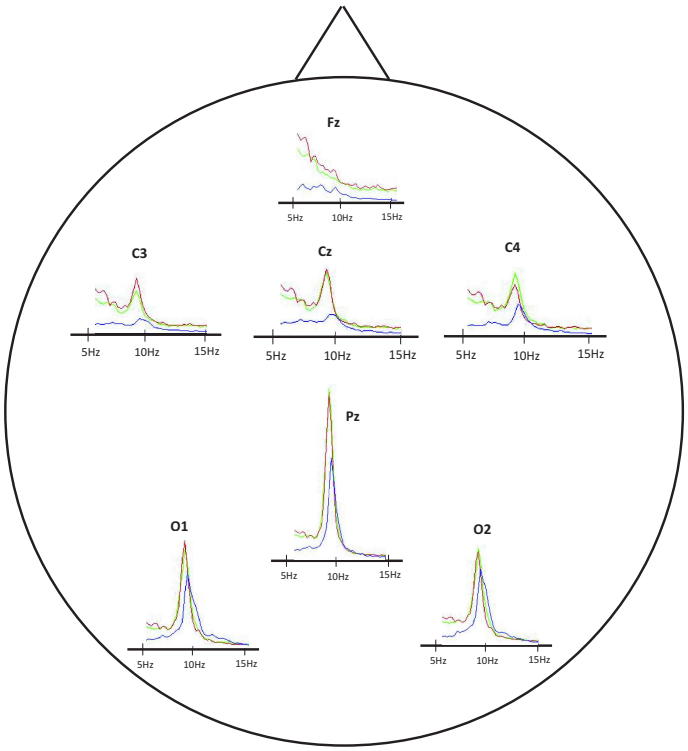

Figure 5.1: Power spectral density of different sensors in the scull for subject 1, right Up & down hand movement.

In table 5.1 we can see the different mean alpha frequencies for each subject of the experiment.

Table 5.1: Subject Alpha frequencies

Subject	Alpha dominant Pitch	Std between trials	Std between sensors
S1	10.94 Hz	0.33	0.33
S2	11.01 Hz	0.688	0.477
S3	12.24 Hz	0.759	0.814
S4	9.29 Hz	0.95	0.77

A different topographical plot of brain frequencies is shown in figure 5.2 for the subject S1. Several comments can be made from this figure. First, although brain frequencies have not the same importance, each classical band is involved in the extraction features, but the most relevant are alpha and beta bands. Secondly, relevant differences appear in some regions after the trigger onset. This is the case of the α and β bands, where the ERD are completely visible, and demonstrate that, like in the theory, each cerebral hemisphere controls the movements of the opposite side of the body, but it appears around 1 second after the start of the movement. In figure 5.2 the mental activity of right movement is shown. It is possible to see in the left side of the brain that the mental activity decrease considerably.

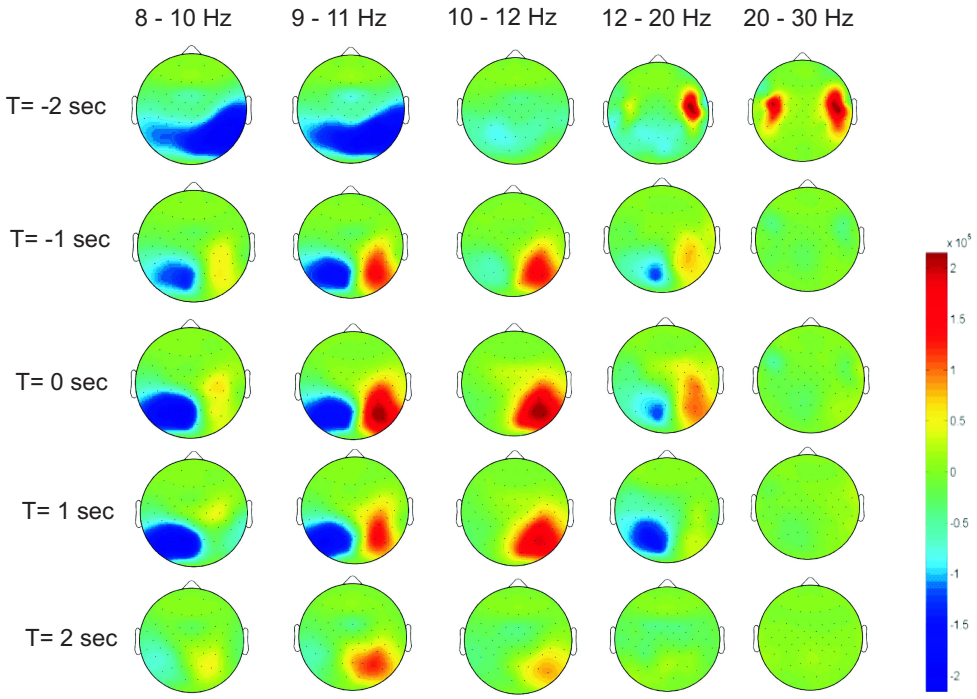

Figure 5.2: Topographical plot of the mental activity in the subject S1 using differences reactive frequency bands. Right movent.

5.1.2 ERS/ERD inter-trial standard deviation

In chapter 3, ERS/ERD curves of a given subject were computed from the average scalogram computed to calculate the training trials, extract features and apply them in the test trials. From this training trials, curves representing the percentage of deviation arising between the ERS/ERD curves over time were also expressed according to a reference period. These curves act as indicators of a given subject trial synchronization spreadings which could maybe act as indicators if we repeat the pattern recognition techniques on test trials.

The ERD quantification explained in section 2.5 is extracted from continuous recorded and transformed EEG data (resampled at 256Hz). From this data movement, synchronous epochs were extracted, band pass filtered in the reactive frequency bands found in table 5.1 for each subject, squared and averaged over trials. This procedure results in an average band power time course as:

$$Ps(j) = \frac{1}{NbTrials} \sum_{i=1}^{NbTrials} x(i,j)^2 \tag{5.1}$$

The moving average technique is applied to the time signal, where each sample is the sum of the 256 post samples as follows:

$$P_{sMA}(j) = \frac{1}{256} \sum_{k=0}^{255} Ps(j-k) \tag{5.2}$$

The number of 256 samples was chosen since ERD is meant to compare all the epochs having a length of 256 samples (1 second) with a reference period defined as the mean of all 256 samples taken in the interval between -3 and -2 seconds before the movement onset. Finally the ERD is calculated as:

$$ERD(j) = \frac{P_{sMA}(j) - R}{R} \tag{5.3}$$

where R is the averaged reference period:

$$R = \frac{1}{NbTrials} \sum_{i=1}^{NbTrials} R(i) \tag{5.4}$$

with

$$R(i) = \frac{1}{256} \sum_{j=n_0}^{n_0+255} P_{sMA}(j,i) \tag{5.5}$$

The quantification of EEG desynchronization and synchronization is shown in figure 5.3. A decrease of band power indicates ERD and an increase of band power ERS. Figures 5.4 and 5.5 represent the EEG signal from electrode C3 and C4 which was band pass filtered in the frequency range of interest (i.e. for subject 1: 10.94-12.94 Hz (high alpha band) and subject 3: 12.24-14.24 Hz (high alpha band)), squared and averaged over trials. It can also be seen that due to the moving average algorithm, the ERD and ERS curves are shifted forward in the time

axis by 0.5 seconds. This usually occurs as for calculating the relative power, one-second long windows with an overlap of $\frac{255}{256} = 996ms$ is used.

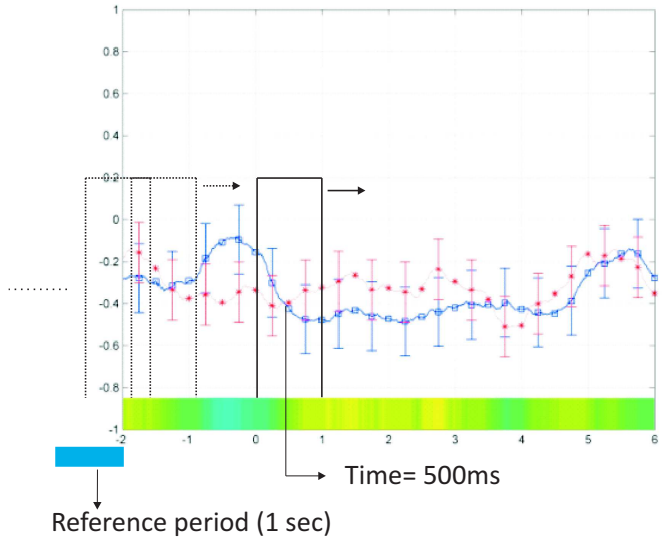

Figure 5.3: Event-Related Desynchronization (ERD) of subject 1 during real right movement referenced to all scalp sensors using an auditory clue. Reference period and energy window are shown.

To emphasize the principle that contra lateral cerebral hemisphere controls the movements of the opposite side of the body, a topographical plot is calculated and displayed in figure 5.4. It is focus in the reactive bands of subject S1 for the left and right movements.

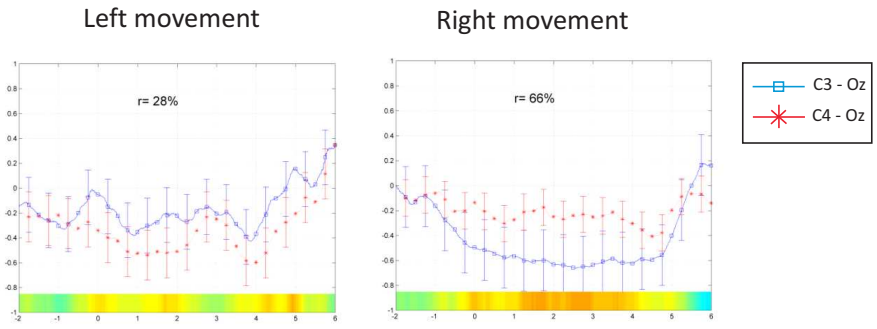

Figure 5.4: Event-Related Desynchronization (ERD) and Synchronization (ERS) of subject 1 during real Open & close movement, referenced to Cz scalp sensors using a auditory clue. High alpha band.

The graph accentuates the fact that the left side of the body is wired to the right side of the brain and vice versa. However, this effect is more or less remarked depending on the subject. Thus for subject 1, performing right or left hand movement has an effect on both hemispheres, even though the right movement seems to activate the left part of the brain more than the left one, and vice versa. Furthermore, the right hemisphere is more relevant, the decreasing are higher. However, for subject 3 (figure 5.5), moving the left hand results in an activation of the right hemisphere more relevant that moving the right hand. This is due to the fact that the left and right hemispheres of the brain process information in different ways. Hence, each subject tends

to process information using the dominant side.

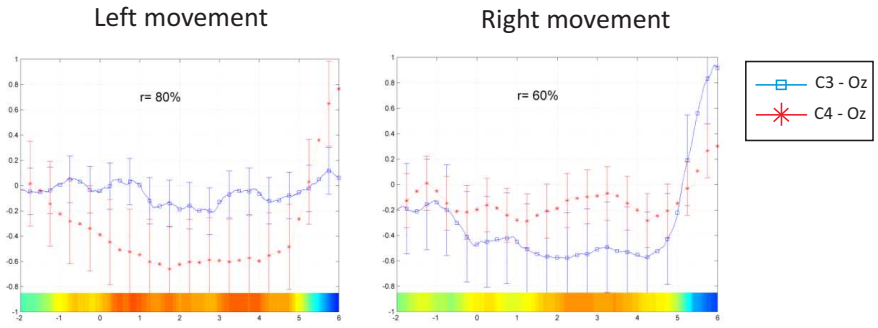

Figure 5.5: Event-Related Desynchronization (ERD) and Synchronization (ERS) of subject 3 during real Open & close movement, referenced to Cz scalp sensors using a auditory clue. High alpha band.

Another observation that can be made is that ERD and ERS are slightly larger for the left movement than for the right one. Consequently, those results confirm that the left hand movement produce more relevant patterns than the right one. Furthermore, the activation of the contra lateral side of the brain takes place 1 seconds before execution of the movement. The figures in Appendix D also show that the ERD starts between 2 and 1 seconds before the movement, even 5.5 (subject 3), and recovers within 1-2 seconds after the movement. Note that the power curves are shifted forward by 1 seconds, thus, we extract that mu desynchronization is more widespread that the synchronization.

5.1.3 ERD/ERS in motor imagery

In [24], [28] and [48] , where subjects were required to perform and to imagine a brisk movement of the left or right hand, is shown similar cortical activity over the contralateral hand area during execution and imagination of movement. Accordingly, both real and mental movements should elicit similar patterns of cortical activation in relevant brain regions. The activation of hand area neurons either by the preparation for a real hand movement or by imagination of a hand movement is accompanied by a circumscribed ERD over the hand area.

It was observed that the prominent changes in the EEG were localized in the hand area sensorimotor cortex. A similar ERD has been found on the contralateral side during the motor imagery as it is usually found during the preparation of the real movement. An example of ERD distribution during motor imagery, mapped on the reconstructed cortical surface of one subject is shown in figure 5.6.

Despite the theory, there are some differences between real movement and imaginary movement in the mental activity. First of all, in motor imagery we need to realize a selection of the trials for the ERS/ERD, the imaginary action is more unstable, the mean of all trials extracted from the subjects do not show the same patterns that in real movement activity. It is possible to see in figure 5.7 that the mean of all trial does not corroborate the theory. The right movement does not to activate the left part of the brain more than the left one, and vice versa. Anyway, a selection of the trials that we extract from each subject, allows to found the ERS/ERD, and extract

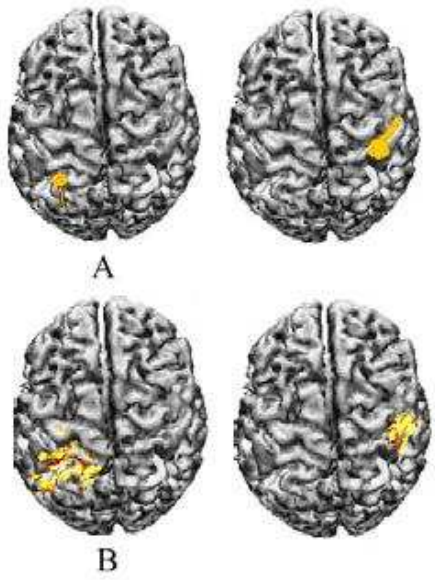

Figure 5.6: The alpha band cortical current source analysis from a human subject during the movement imagination (A) and (B) for both left and right hand movement imagination. Note the clear separation of neural sources during different tasks contributes classification of motor imagery tasks.

the patterns for the algorithm. Note that the correct trials that follow the theory are around 25%, this prove that the imaginary state are more unstable and variable, and, for this reason, the results of the algorithm for imaginary actions are worse that the results for real movement analysis.

When performing the imaginary movement, subjects are trained to use pathways. One is imaging a visual image of his moving hand, the other is imaging the muscle of the corresponding moving hand. Some differences appear between subjects, Subject 3 is good in both systems, presenting a ERD after selecting the trials similar to the real movement, so subject 2 present better results in the imaginary muscular system opposite to subject 1, that are better for visual motor imagery.

In the appendix D, the pictures of the ERS/ERD for all subjects are placed.

5.2 Diagnostic support

First, in this section, we study the responses of this system in different configurations for the training trials. However, to take conclusions about its ability to generalize and test the algorithm, response to new data trials are also evaluated to detect a specific mental activity from new data.

5.2.1 Training data

Through this chapter, we have seen that some channels are more important in the differentiation between subjects. Also, it was mentioned that using a combination of the classical frequency

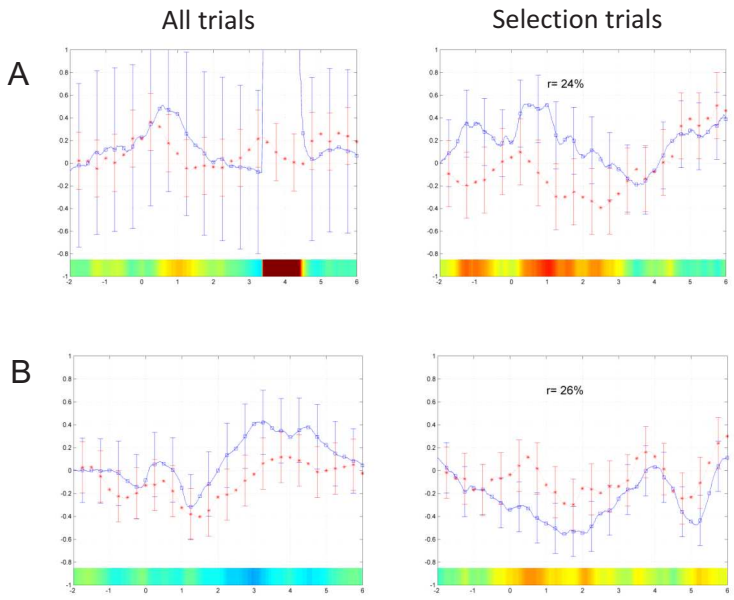

Figure 5.7: ERD in imaginary motor activity. A.- ERS of subject 1 during real left imaginary visual movement, referenced to Cz. B.- ERS of subject 2 during imaginary right muscle movement, referenced to Cz.

bands as well as the theta-alpha suband decompositions may improve the trade-off between accuracy and robustness. These different configurations of the decision system will be evaluated below on different types of subjects.

It is assumed that the active state can be found in more cortical areas. To investigate whether or not multiple channels are involved in the execution of the voluntary movement, the method of common spatial patterns was applied to the EEG data. The method is based on the decomposition of the raw EEG signals into spatial patterns which are extracted from two populations, and different active periods.

The signals were preprocessed in the same way as for the quantification of ERD and ERS i.e. band pass filtered in the reactive frequency bands and resampling at 256Hz. The projection matrix W for all three active periods was obtained, and the firsts three rows of W representing the most important common spatial filters, along with the firsts three columns of the inverse matrix describing the most important common spatial patterns were applied to the signals and tested. Applying the spatial filter in the form of the matrix W, to the test signal, the energy of the two different mental states was computed using the same method as before. The signals obtained are plotted (see figure 5.8). It is possible to see that in the 4 seconds of the mental activity of one movement, after the algorithm has been applied, energy of one class are bigger that the other.

Each subject has a different response, and do not have the same reaction to the CSP (see figure 5.9). For this reason, a three frequency band is calculated for each subject, all the EEG data of the two populations (class 1: left hand movement; class 2 right hand movement) of real and imaginary states are tested for different sensors selection, CSP without PCA and CSP with PCA of different orders of decreasing data.

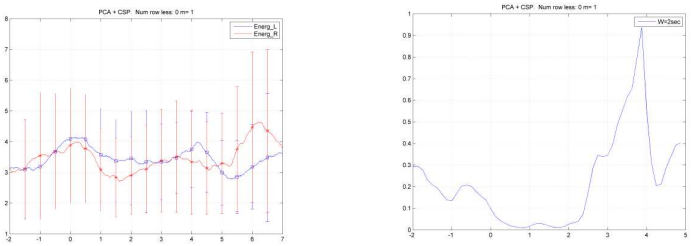

Figure 5.8: Maximization of EEG data from left hand real movement of subject 1(blue) over right (red) , using the second alpha band and motor cortex sensors. Referenced to Cz. The evolution of p-value is plotted in blue, and shows the great significance of the results.

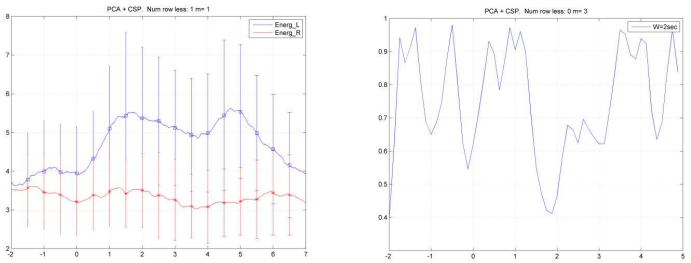

Figure 5.9: Maximization of EEG data from left hand real up & down movement of subject 2(blue) over right (red), using the high alpha band and motor cortex sensors. Referenced to Cz. The evolution of p-value is plotted in blue, and shows that the significance of the results is not as good as the others, it cause that the analysis of the results has to be supervised.

In the figure 5.10 the subject 3 shows a result of the algorithm to the motor imagery activity in the motor cortex area of right and left hand movement and the significance of the result. The significance verifies that it is possible to differentiate the two populations.

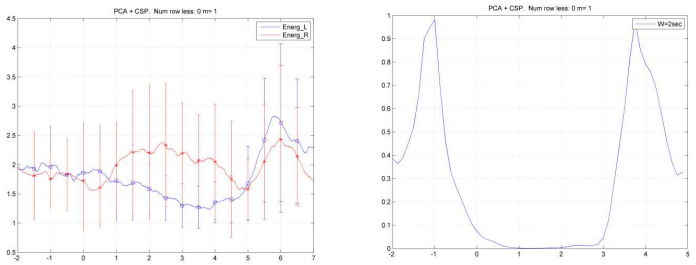

Figure 5.10: Maximization of EEG data from right hand imaginary movement of subject 3(red) over left (blue) , using the high alpha band and motor cortex sensors. Referenced to Cz. The evolution of p-value is plotted in blue, and shows the great significance of the results.

The other subjects do not present the same reaction in this interaction of the algorithm, due to the fact that the analysis of the results and its significance has to be implemented for each subject, extracting the most relevant interactions for future application in the test data.

The discussion has been based on the results provided by the algorithm when is was tested

with the data used during the learning process. However, to study its ability to generalize to new cases, it has been tested with a new set of subjects.

5.2.2 Test data

To make a detailed study of the algorithm responses, a set of new cases has been created. It contains new data from the experiment subjects different of the training trials, so new trials are applied to the algorithm, using the settings extracted from the training data having different characteristics. This should help to take better conclusions about the performance and robustness of the system.

Figure 5.11 shows the output of the algorithm to new data of real movement and certificate that it is possible to use the algorithm for new data, obtaining good results. In some zones, where the CSP method has been used, the significance is lower than 0.01. It probe that it is possible to differentiate the two class of mental activity..

Figure 5.12 presents a result of the algorithm to the motor imagery activity in the motor cortex area of right and left hand movement and his significance for the subject 3. It certificates that it is possible to differentiate between the two populations, although if we see the results of the real movement, the accuracy has decreased and the significance of the imaginary state is worse that the real state. This is due to the fact that the population of motor imagery is more unstable that the real motor population.

5.2.3 Analysis of variance ANOVA

Statistical tests of the results system are performed to compare the population means using variance analysis techniques. The outputs returned by the algorithm are analyzed using an analysis of variance (ANOVA) of one-way, used to test for differences among two independent groups. Also a Student's t-test technique, that tells us if the variation between the two distributions is "significant", determine whether the means are distinct, returning a parameter of significance, p-value.

As we are testing differences among only two population groups, Student t-test is enough. This technique is applied when the population is assumed to be normally distributed but the sample sizes are small enough that the statistic on which inference is based is not normally distributed because it relies on an uncertain estimate of standard deviation rather than on a precisely known value. Assumptions of the analysis are:

- Independence of cases - this is a requirement of the design.
- Normality - the distributions in each of the groups are normal.
- Equality (or "homogeneity") of variances, called homoscedasticity - the variance of data in groups should be the same.

The analysis is applied to outputs obtained from the algorithm, taken the population of the two classes of outputs (class1 with maximization of variance and class 2 with minimization of

variance) using a slider windows of 2 seconds. In figure 5.13 it is possible to see the evolution of the p-value among the time. If the calculated p-value is below the threshold chosen for statistical significance (usually the 0.10, 0.05, or 0.01 level), then the null hypothesis which usually states that the two groups do not differ is rejected in favor of an alternative hypothesis, which typically states that the groups do differ. Then, in the zone where the CSP algorithm is applied, the p-value decreases down to significant values to discriminate both classes.

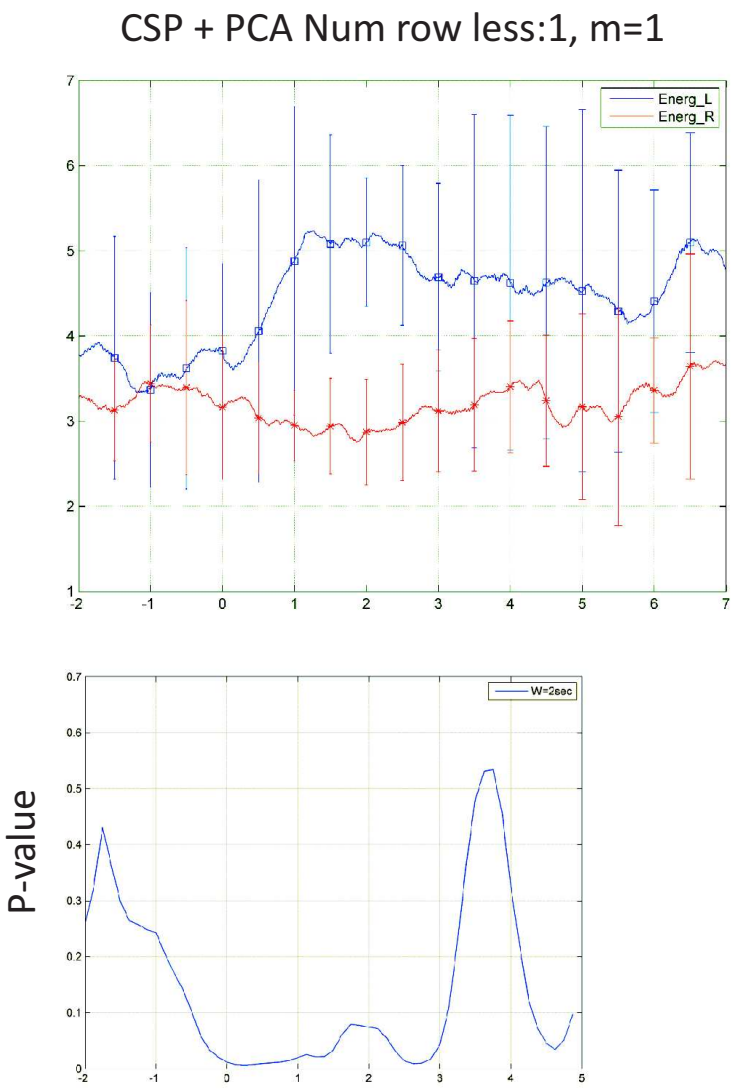

Figure 5.11: Maximization of EEG data from left hand real Up & down movement of subject 2(blue) over right movement (red), using the high alpha band and motor cortex sensors and PCA level 1. Referenced to Cz. The evolution of p-value is plotted in blue, and shows the great significance of the results, below 0.01 in some zones.

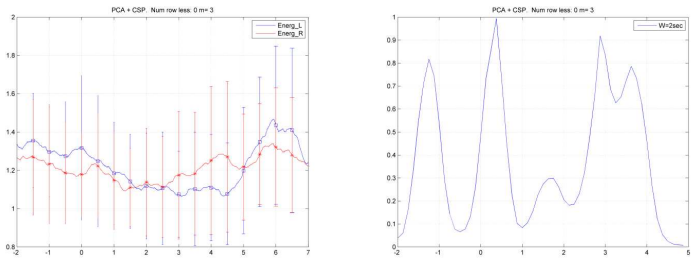

Figure 5.12: Maximization of EEG data from right hand imaginary movement of subject 3(red) over left imaginary movement (blue), using the high alpha band and motor cortex sensors ans PCA level 1. Referenced to Cz. The evolution of p-value are ploted in blue, this is worse in motor imagery signals.

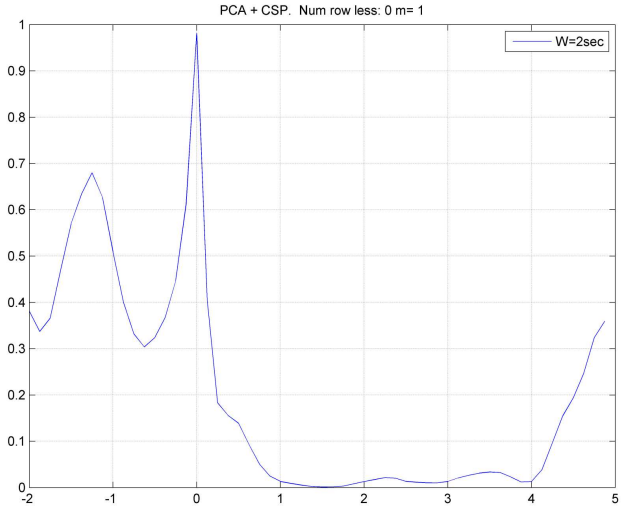

Figure 5.13: Evolution of P-value in the ANOVA analysis, among time, between the outputs of the algorithm. Slice windows of 2 seconds are used. Note that the p-valued decrease in the zone where the CSP has been applied. Subject 3, Up & down real movement, filtered in high alpha and focus in the motor cortex sensors zone.

Section 6

Conclusions

In the previous chapter, the application of several methods to the analysis of EEG signals recorded during performance of real and imaginary movement is showed. The long term goal of this research is to build an intuitive and reliable brain-computer interface that can be simply operated by everybody, even by people with severe motor disabilities.

After reading the previous chapters, different conclusions can be extracted. First, through interpreting the location in time, space and frequency of the differences in synchronization between subjects and settings, conclusions about the possible underlying causes of this trouble can be given and discussed. Also, study the responses of the algorithm in different configurations, allows to obtain new knowledge about the system behavior which becomes useful to refine the final conclusions.

Finally, this chapter reviews the most important contributions and the possible future work. The objectives of this thesis were:

- Study of the EEG characteristics and their pertinent information which can be used in order to discriminate between a mental activity and a resting period.
- Investigate on and implementation of different existing feature extraction methods in the brain area for controlling hand movement area.
- Identification of the key features characterizing the EEG signals while performing a hand movement.
- Focus the study in the brain activity created by real movement action and motor imagery. Extract the most relevant and common (between different subjects) patterns and characteristics.
- Designing of a Neuronal Network able to differentiate the kinds of features extracted from different EEG signals and show the results. Make the system capable of develop an online analysis and learn from data analyzed previously.

The final conclusion of this project is that the suggested techniques have shown great potential, and further research on this topic is recommended.

6.1 Summary of achievements

The important aspect of the work presented in this thesis was the evaluation of different signal analysis techniques and algorithms on the EEG recorded during voluntary and imaginary hand movements.

From the analysis of the results, the following conclusions are obtained:

- Movement reactive frequency components were detected by a Fourier analysis of the alpha peak, extracted in response (closing eyes) from visual cortex, for each subject. The observation is that the reactive frequency bands are not constant during time and differ from subject to subject. Frequency bands, showing significant differences between the reference interval and the activity interval, were chosen for ERD/ERS computations. Topographical plots of the mental activity in the motor cortex zone also show that each cerebral hemisphere controls the movements of the opposite side of the body. Probing the theory. Motor imagery ERS/ERD follow the theory and are similar to real movement, but more unstable. ERD and ERS are slightly larger for the left movement than for the right one. Consequently, those results confirm what was explained in Section 5.1.2, the left movement produces more relevant patterns than the right one.

- Hand movements result in a desynchronization of mu and central beta rhythms close to the hand area in every subject. The ERD/ERS are highly frequency band specific, whereby either the same or different locations on the scalp can display ERD and ERS simultaneously. ERD starts 1 second before the movement and recovers within 1-2 seconds after the movement. A contralateral beta ERS was observed. This is due to the fact that motor area neurons shift from an activated state during preparation and execution of movement to resting state after finishing the movement. During those idling states the oscillations in the lower beta bands display large amplitudes (synchronization). ERS is shorter and less widespread than the ERD, this is not surprising knowing that when performing a movement there are always more cortical areas in a processing mode than in a resting mode.

- The CSP method was used for spatial analysis of EEG signals given their multivariate nature, and more specifically to find spatial structures of ERD and ERS in a BCI context. The CSP analysis for a two class problem (1st class: right real or imagery movement, 2nd class: left real or imagery movement) provided a linear combinations of channels for which the variance of the signal for one class was maximized while the variance of the other was minimized. A spatial filter in the form of a matrix resulted from the analysis leading to new signals that are linear combinations or weighted averages of the recordings from all the electrodes. Calculating the ERD of the new signals, the power variation showed a greater decrease. Hence, the spatial filters designed in accordance with common spatial patterns for the reactive frequency bands found represent a great ability to deal with multi channel EEG signals and give promising key features characterizing the ERD that can be extracted with this method. However, the CSP feature is quite sensitive to the frequency range of the band pass filtered and it is subject specific.

- Principal Component Analysis transforms a number of possibly correlated variables into smaller number of uncorrelated variables called principal components. This partitioning allows us to easily differentiate mental activity classes using CSP, which has two primary benefits: the remaining signals are less correlated, and it has lower dimensionality. Using PCA the accuracy and reliability of the classification system increases.

- Analyzing high dimensional data it is not only important to visualize, predict or classify the data with low error, but it is essential that the exploratory data analysis tools allow to explain the underlying structure in order to contribute to a better understanding of the data, a single layer Neural Network allows to make an optimal extraction of information. One of the main advantages of the neural network is that they provide an adaptive system that changes its structure based on external information that flows through the network during the learning phase, then the algorithm learns from its results, also, if the neural model, cost function and learning algorithm are selected appropriately, the resulting network can be extremely robust. The neural network can also be used in an online system, giving the possibility of a future design of a BCI online application.

- Variance analysis applied to outputs, taken the population of the two classes of outputs (class1 with maximization of variance and class 2 with minimization of variance), using a slider windows of 2 seconds, shows that in the zone where the algorithm is applied the significance decreases to levels around 0.1, and sometimes below 0.01, making viable a differentiation of mental states classes. Anyway, these results are not always stables, and in some interactions, the application of the algorithm increases the p-value (significance). For this reason, a variance analysis allows to find the interactions that are more significant and apply to the test data only these interactions of the algorithm.

- Although during performance of the voluntary movement a great intersubject variability existed, these results give a valuable contribution in understanding the brain dynamics. The EEG is one of the main tools to access one of the most unknown and complex systems in nature, and one of the still elusive treasures of science. In this context, the development of a great variety of methods is required as well as their improvements up to the limits of their abilities in order to learn more about the behavior of the brain. And this is what makes the study of the brain, including this one, so fascinating.

6.2 Future research

This section is devoted to suggestions for follow up research.

- Single trial assessment is necessary in order to design an operational BCI system. The methods and results described in this report should be tested on a single trial data.

- All the subjects tested in this project were right handed males with a mean age of 23 - 29 years. Hence left handed subjects must also be tested, as well as women and people with different ages.

- All the results shown in the report are subject specific, in other words, need a period of training for each subject and have to be readjusted after some time. A line for improvement is to incorporate strategies for a continuous adaptation of the algorithms to account for the non-stationary characteristics of the EEG as for example the development of an adaptive version of the CSP algorithm.
- Characterizing the non-stationarity properties of the mental activity signal with strategies or methods of signal processing, i.e. the AAR model [49] or[50], for its implementation in the algorithm.
- Design a most perfect system to detect, and erase the artifacts, for example using Independent Component Analysis (ICA) algorithms, like [51] or [52].
- Design and test an extension of the algorithm to improve on the extraction of data from the scalp sensors, using for example Laplacian models, [53], [20], [54], [55] or [19].
- Investigation and implementation of different classifiers to find the optimal combination with the best feature extractors studied in the project.

Appendix A

Appendix: figures of EEG theory

Distortions and artifacts figures

Pictures from [21].

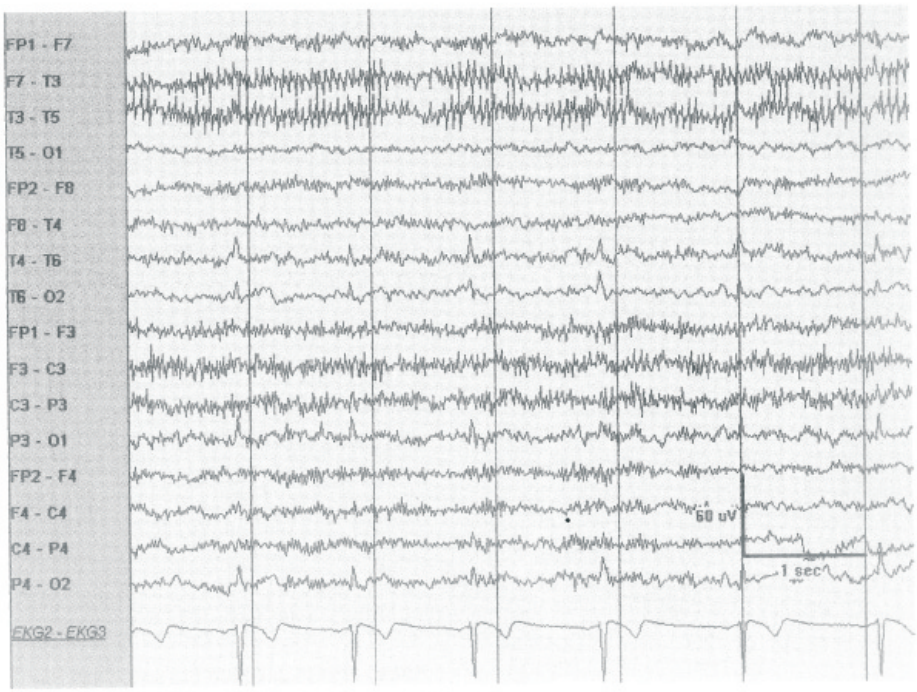

Figure A.1: Muscle(EMG) and EKG artifact. Muscle is seen as high-amplitude, very fast (>50Hz), and variable frequency discharges, which are more prominent on the left in this sample. EKG is easily identified in several channels as clearly simultaneous to the EKG channel.

Brain rhythms figures

Pictures from [21].

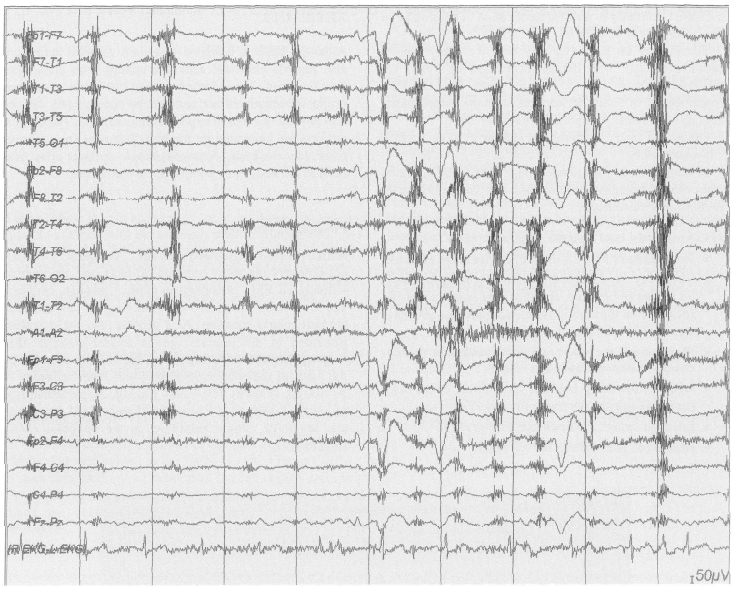

Figure A.2: Chewing artifact. This EMG artifact occurs in rhythmic bursts of muscle maximum in the temporal chains.

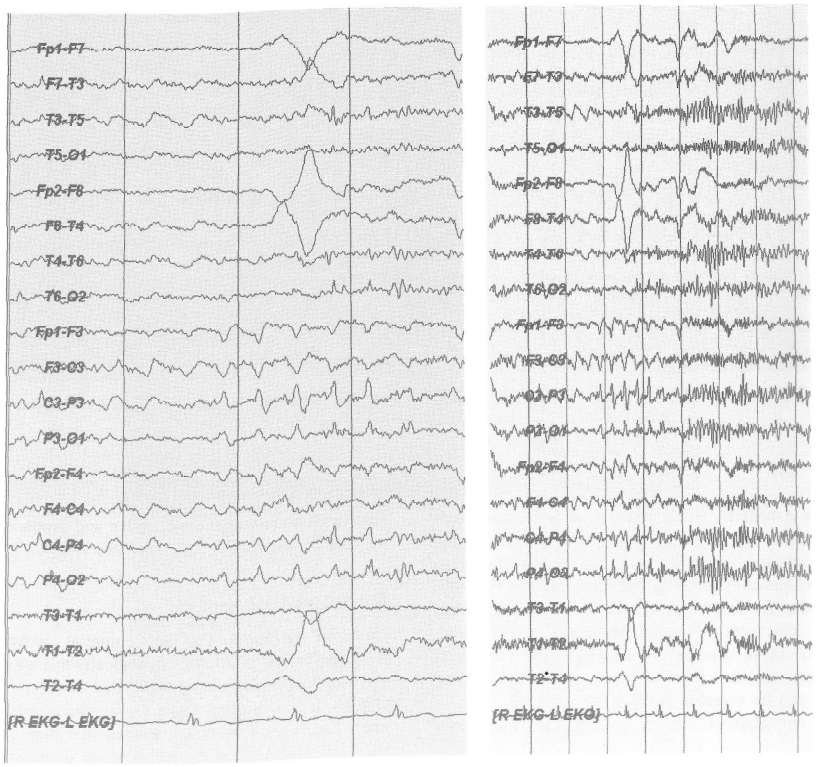

Figure A.3: Eye movements and sawtooth waves in REM sleep. During this rapid lateral eye movement to the left, there is a maximum positivity in electrode F7 and maximum negativity simultaneously in electrode F8. In the vicinity of the rapid eye movement, there are typical sawtooth waves in the central region.

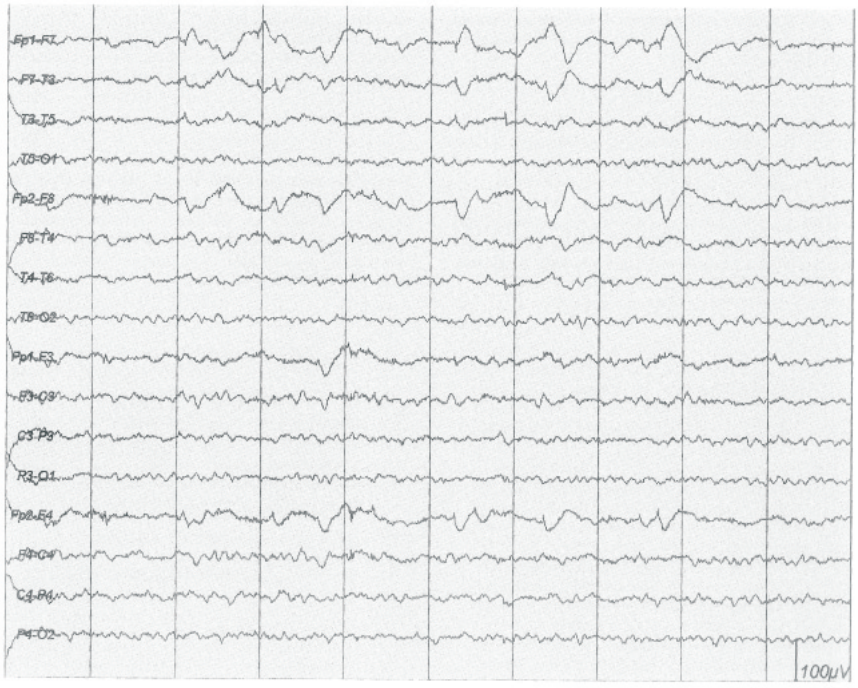

Figure A.4: Rapid eyes movement and lateral rectus spikes. With the eye movements to the left, lateral rectus spikes are seen in electrode F7.

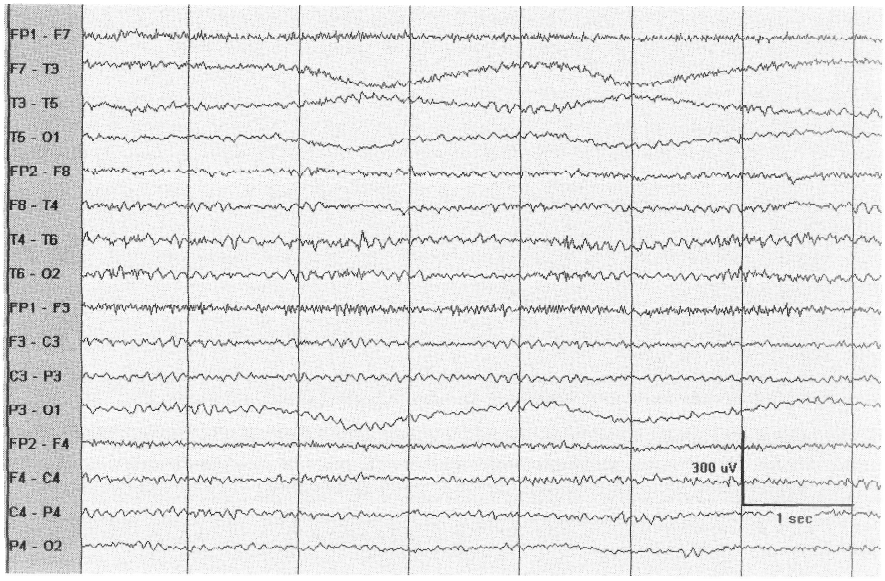

Figure A.5: Sweat artifact. Note the very slow(0.5 Hz) sways. The slow frequency is similar to slow rolling eye movements, but the distribution is not (in this case it affects electrodes on the left side of the head).

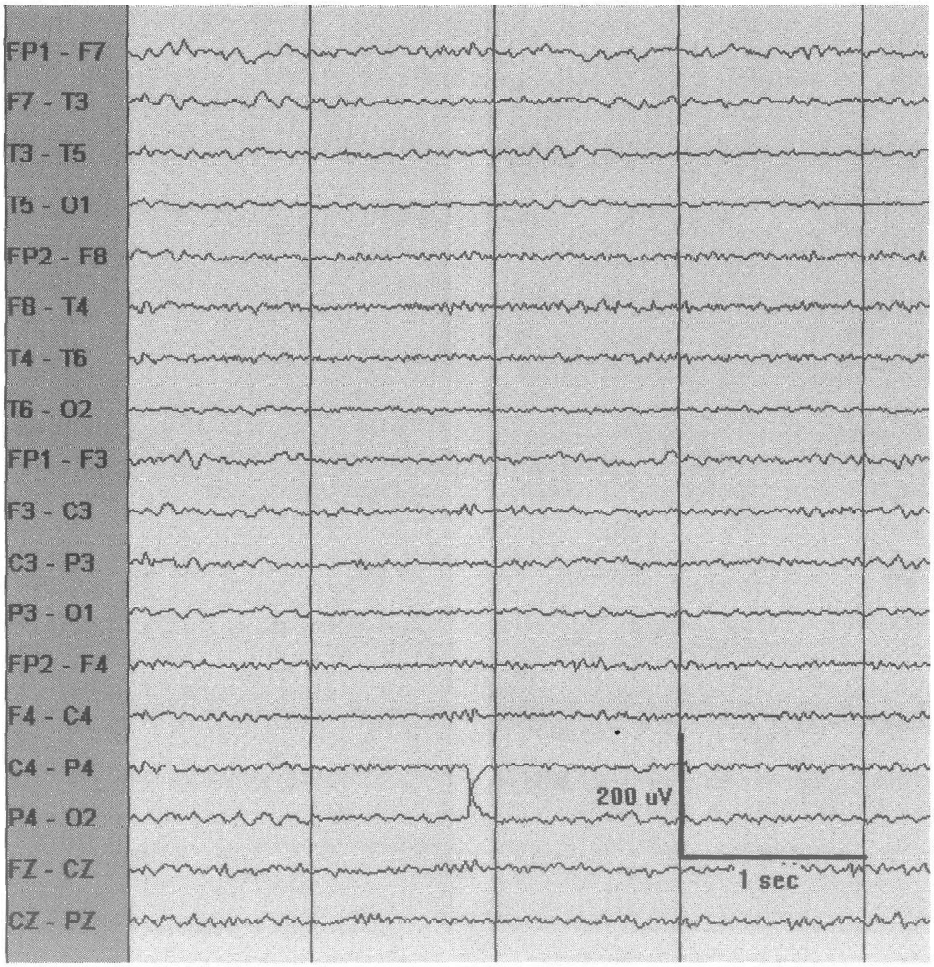

Figure A.6: Electrode artifact. This typical artifact is the electrode "pop". Note the single sharp waveform with abrupt vertical transient that does not modify the background activity, and its distribution is limited to a single electrode (P4).

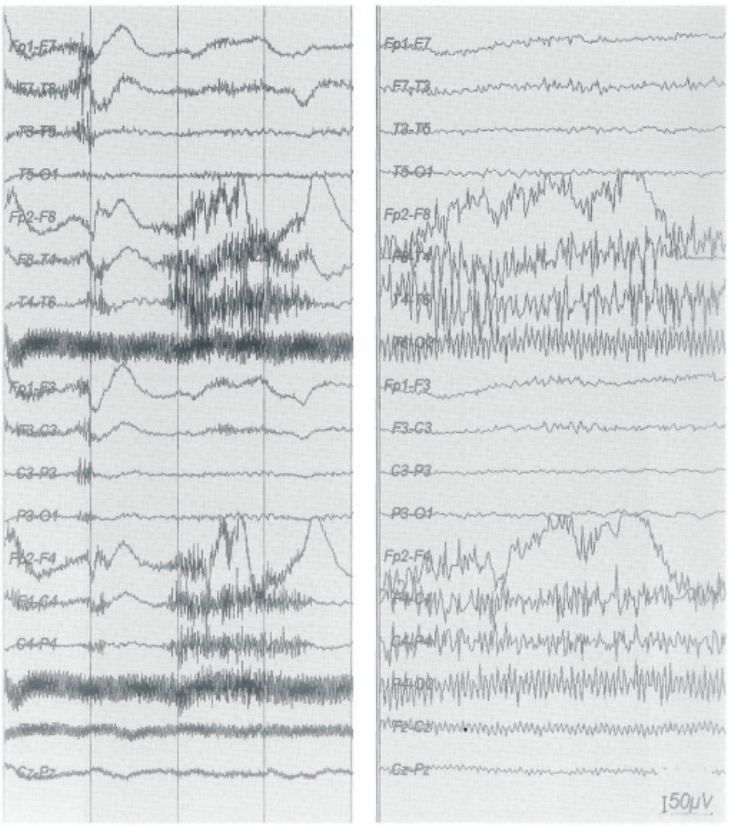

Figure A.7: The 50 Hz and muscle (EMG) artifact. The 50 Hz artifact is at electrode O2 (thus seen in channels T6-O2 and P4-02). Note that its amplitude is perfectly regular and exactly and steadily at 50 Hz. EMG (muscle) artifact, by contrast, is of comparable frequency but affects several electrodes, is variable in amplitude, and variable in frequency (not always nor exactly at 50 Hz).

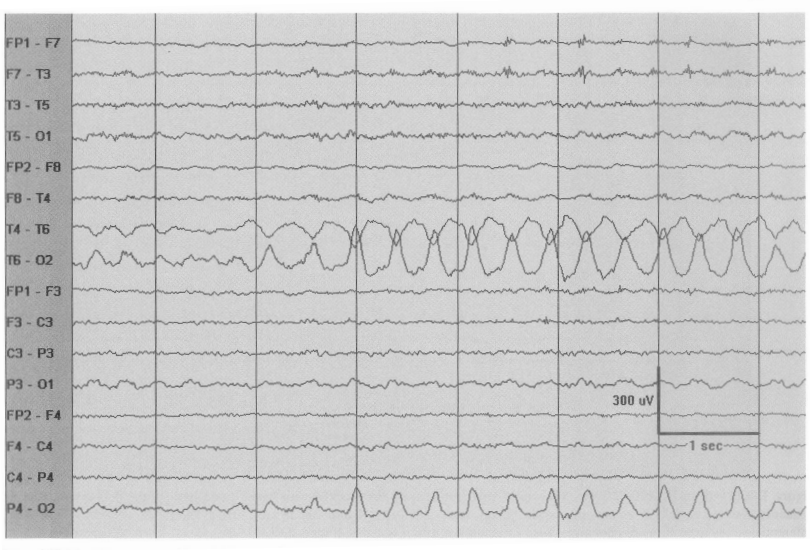

Figure A.8: Movement artifact. This is an example of rhythmic artifact generated by respective movements (shaking the head on the pillow hitting the right posterior electrodes T6 and O2). This should not be mistaken for local seizure. Note the "phase reversal" at T6, even though this an artifact.

Figure A.9: Normal alpha rhythm. This sample depicts well-formed sinusoidal rhythmic activity at 9 Hz in the occipital regions.

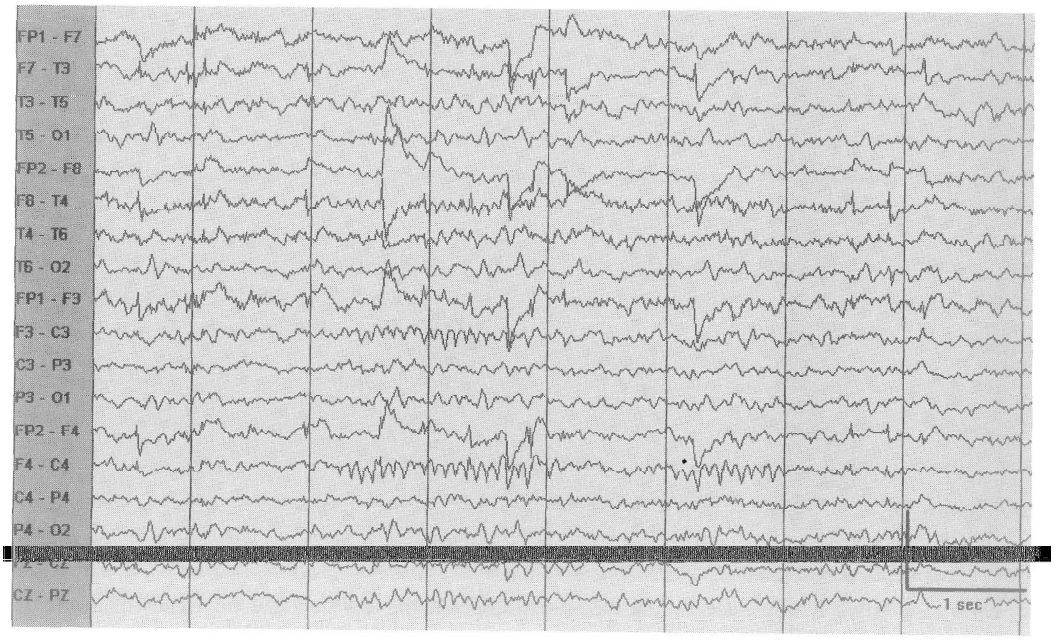

Figure A.10: Mu rhythm. This sample depicts the typical m-shaped bicentral bursts at a frequency of 8-12 Hz. If tested, this would react (attenuate) to contralateral movement.

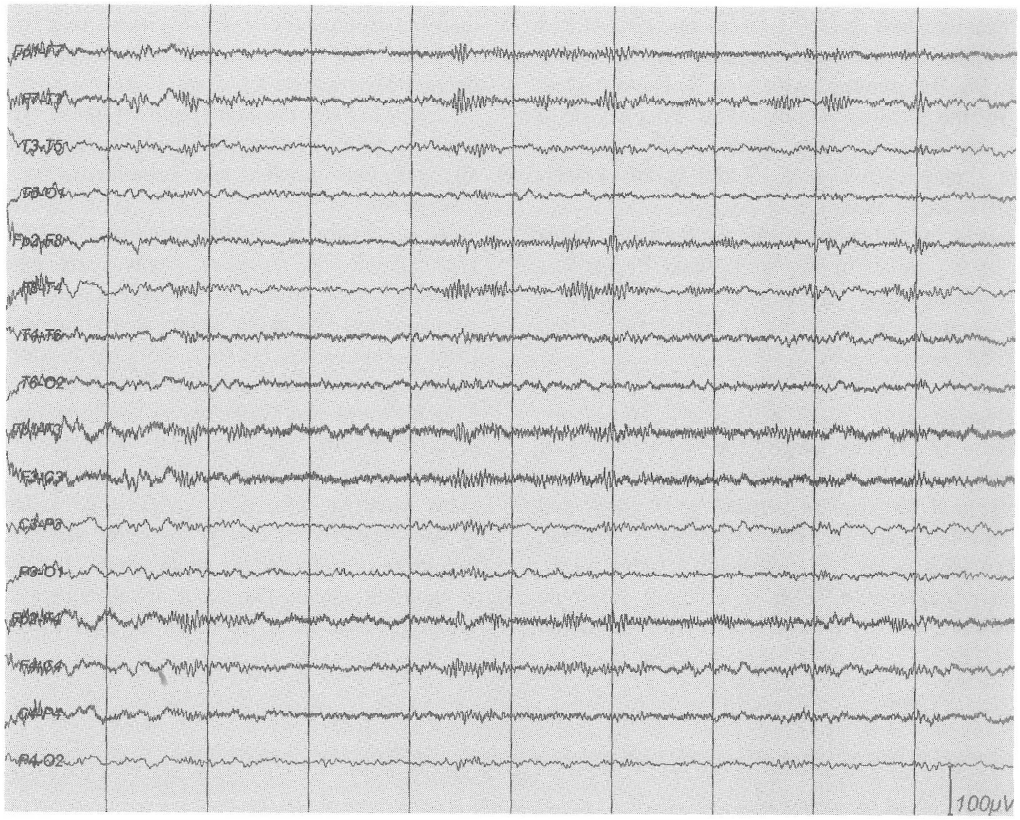

Figure A.11: Normal beta activity. This sample depicts the typical ($\sim$ 18-25 Hz) low-amplitude activity in both frontal regions. As shown here, normal amounts of beta activity are moderate and tend to wax and wane.

Appendix B

Mathematics of Common Spatial Patterns

B.1 Demonstration of S_L and S_R proprieties

1. They share common eigenvectors, i.e.

$$S_L = U_0 D_L U_0^T \quad , \quad S_R = U_0 D_R U_0^T \tag{B.1}$$

Demo:

If S_L are diagonalizable then, is possible to decompose it like

$$S_L = U_0 D_L U_0^T \tag{B.2}$$

and from equation 3.18 we know:

$$S_L + S_R = I \tag{B.3}$$

then:

$$S_R = I - S_L = I - U_0 D_L U_0^T = U_0 \left(I - D_L\right) U_0^T \tag{B.4}$$

2. The sum of the corresponding eigenvalues for the two matrices will always be I, are easily demonstrable, using the last equation, that the equation B.1 is obtained from:

$$S_R = U_0 \underbrace{(I - D_L)}_{D_R} U_0^T \tag{B.5}$$

Where we know that:

$$D_R = I - D_L \tag{B.6}$$

$$S_L + S_R = I \tag{B.7}$$

Appendix C

Alpha peak for each experiment subject

Automatic VS manual peak selection

With these tables we could prove that every subject has not a stable peak for alpha frequency. Alpha frequency peak changes for each person, also the peak is not stable between different trials separate in time or between sensors located in difference positions of the scalp.

Also we can see the existence of difference between the manual selection of the alpha peak and the automatic selection for the subject 3.

Automatic peak calculation for subject1

Manual selection peak for Subject 1

Manual selection peak for Subject 2

Manual selection peak for Subject 3

Manual selection peak for Subject 4

Table C.1: Automatic peak calculation for subject 3

Trial num	1	2	3	4	5	6	7	8	9	10	Mean
FP1	8,26	9,47	10,32	10,25	9,73	9,67	9,85	8,59	10,05	9,68	9,59
FP2	7,90	9,27	9,68	10,26	9,22	9,41	9,65	8,85	9,57	9,25	9,31
AF3	9,86	9,80	10,39	10,44	9,67	10,25	9,92	9,78	10,24	10,20	10,06
AF4	9,13	10,28	10,17	10,35	10,01	9,84	9,80	9,70	10,14	9,78	9,92
F7	10,04	10,17	10,75	10,30	9,58	9,90	10,17	9,46	9,37	10,07	9,98
F3	10,30	10,26	10,65	10,62	9,91	10,36	9,86	9,64	10,46	10,22	10,23
Fz	10,53	10,36	10,44	10,54	9,92	10,05	9,53	10,05	10,89	10,09	10,24
F4	10,19	10,17	10,17	10,38	10,18	9,99	9,82	10,30	9,84	10,24	10,13
F8	9,70	10,35	9,77	9,88	9,13	9,40	9,80	9,63	8,75	9,97	9,64
FC5	10,18	10,39	10,67	9,50	9,04	9,93	9,96	10,71	9,95	9,95	10,03
FC1	10,30	9,81	10,12	10,39	9,53	9,80	9,69	10,36	10,69	8,85	9,95
FC2	10,60	9,80	10,35	10,24	10,00	9,17	9,72	10,25	10,04	9,78	10,00
FC6	9,22	9,55	9,62	9,32	9,97	9,37	9,41	9,50	9,51	10,11	9,56
T7	9,08	8,89	10,58	9,72	8,56	9,07	9,90	9,45	8,62	9,44	9,33
C3	9,74	10,11	9,34	10,19	9,41	10,01	9,63	9,90	10,04	9,93	9,83
Cz	9,73	9,69	10,10	10,06	9,49	9,62	9,75	10,19	10,35	9,82	9,88
C4	10,69	11,05	11,24	11,30	10,02	10,65	11,21	11,03	10,91	10,76	10,89
T8	9,96	9,90	10,24	10,10	9,39	9,82	9,59	9,66	9,70	9,61	9,80
CP5	10,78	10,51	11,19	10,92	9,76	10,34	10,62	10,84	10,30	10,11	10,54
CP1	10,67	10,40	11,06	11,06	9,67	10,86	10,96	11,23	10,95	10,08	10,69
CP2	10,83	11,25	11,83	11,52	10,66	11,20	11,74	11,87	11,07	11,32	11,33
CP6	9,63	10,53	10,98	11,03	9,96	10,35	10,38	10,86	11,15	10,41	10,53
P7	9,93	9,78	10,13	9,87	9,84	9,56	9,74	10,01	10,00	9,98	9,88
P3	10,66	11,12	10,72	11,32	10,93	10,43	10,93	11,02	10,85	9,38	10,73
Pz	10,83	10,97	11,17	11,32	9,68	10,55	10,74	11,24	10,78	10,83	10,81
P4	10,98	10,81	11,26	10,98	10,43	10,79	10,73	11,31	11,36	11,00	10,96
P8	9,96	9,89	10,04	9,78	9,65	9,92	9,40	9,44	10,58	10,03	9,87
PO3	10,68	9,10	9,01	9,74	10,71	9,36	9,66	9,05	8,99	8,50	9,48
P04	10,68	10,54	10,51	10,34	10,21	10,40	10,11	10,48	10,78	10,84	10,49
O1	10,69	10,57	10,38	10,38	10,60	10,32	10,26	10,24	10,82	10,82	10,51
Oz	10,68	10,35	10,39	10,30	10,22	10,21	10,07	10,30	10,62	10,79	10,39
O2	10,71	10,51	10,42	10,23	10,14	10,29	9,93	10,35	10,73	10,75	10,41
Mean	10,10	10,18	10,43	10,40	9,85	10,03	10,08	10,17	10,25	10,08	10,16

Table C.2: Manual Alpha Peak: Subject 1

Trial num	1	2	3	4	5	6	7	8	9	10	Mean	Std
FP1	11.12	10.75	10.86	10.63	10.87	10.87	10.50	10.75	11.38	10.75	**10.85**	0.25
FP2	11.12	10.75	10.76	10.63	10.87	10.87	10.50	10.75	11.37	10.75	**10.84**	0.25
AF3	11.01	10.75	10.86	10.63	10.88	10.87	10.50	10.75	11.38	10.75	**10.84**	0.24
AF4	11.12	10.75	10.86	10.63	10.87	10.87	10.50	10.75	11.38	10.74	**10.85**	0.25
F7	8.88	10.76	10.87	10.63	11.00	10.75	10.50	10.75	11.26	11.63	**10.70**	0.72
F3	11.01	10.76	10.87	10.63	10.87	10.87	10.50	10.75	11.12	10.75	**10.81**	0.18
Fz	11.00	10.75	10.87	10.63	10.87	10.87	10.50	10.75	11.00	10.75	**10.80**	0.16
F4	11.01	10.75	10.87	10.63	10.87	10.87	10.50	10.88	11.38	10.74	**10.85**	0.24
F8	11.01	10.75	10.87	11.26	10.87	10.87	10.50	11.00	11.38	11.50	**11.00**	0.30
FC5	12.88	10.76	10.87	10.63	11.00	10.75	11.50	10.74	11.12	10.87	**11.11**	0.67
FC1	11.00	10.75	10.87	10.63	10.87	10.87	10.50	10.74	11.00	10.75	**10.80**	0.16
FC2	11.00	10.75	10.87	10.63	10.87	10.87	10.50	10.63	11.00	10.75	**10.79**	0.17
FC6	11.01	10.75	11.50	11.26	10.87	10.87	10.50	11.00	11.26	11.50	**11.05**	0.32
T7	10.25	10.87	10.99	10.49	11.76	11.49	11.49	11.12	11.26	10.87	**11.06**	0.47
C3	12.87	10.76	10.87	10.75	10.87	10.87	10.50	10.50	11.12	10.75	**10.99**	0.69
Cz	11.00	10.75	10.86	10.75	10.87	10.87	10.50	10.50	11.00	10.75	**10.79**	0.18
C4	11.00	10.74	10.88	10.51	10.76	10.87	10.50	10.99	10.87	10.64	**10.78**	0.18
T8	12.88	11.13	11.50	11.26	11.50	11.38	11.24	11.11	12.00	10.64	**11.46**	0.61
CP5	10.25	12.37	10.87	10.39	11.75	10.87	11.38	11.00	12.00	10.87	**11.18**	0.69
CP1	12.00	11.00	11.50	11.26	10.87	11.38	11.12	11.12	11.00	10.75	**11.20**	0.36
CP2	11.00	11.00	11.39	10.63	10.87	11.50	11.88	11.26	10.88	10.64	**11.10**	0.40
CP6	12.63	11.00	10.75	10.63	11.00	10.25	11.50	10.63	10.51	10.87	**10.98**	0.67
P7	11.01	10.75	10.87	10.63	10.75	10.87	10.50	10.76	10.87	10.75	**10.78**	0.14
P3	11.01	10.75	10.87	11.38	10.75	10.87	10.50	11.00	11.38	10.63	**10.91**	0.29
Pz	11.13	11.12	11.50	11.26	10.87	11.38	11.26	11.11	11.88	11.65	**11.32**	0.29
P4	11.37	10.87	10.87	10.63	11.00	11.50	11.50	10.75	11.00	10.87	**11.04**	0.31
P8	11.00	10.75	10.84	10.74	10.94	11.11	11.41	10.60	10.94	10.79	**10.91**	0.23
PO3	11.00	10.77	10.84	10.68	10.81	10.85	10.50	10.91	11.38	10.65	**10.84**	0.24
PO4	11.26	10.77	10.85	10.63	10.99	11.44	11.44	10.93	11.08	10.81	**11.02**	0.28
O1	11.00	10.73	10.94	10.67	10.83	10.89	10.51	10.79	11.17	10.66	**10.82**	0.19
OZ	11.00	10.79	10.89	10.67	10.87	10.85	10.56	10.79	11.16	10.72	**10.83**	0.17
O2	11.00	10.79	10.88	10.67	10.91	10.89	10.51	10.71	11.16	10.76	**10.83**	0.18
Mean	**11.18**	**10.86**	**10.96**	**10.75**	**10.96**	**10.98**	**10.82**	**10.84**	**11.21**	**10.85**	**10.94**	0.15
Std	0.78	0.30	0.23	0.27	0.24	0.28	0.46	0.19	0.32	0.28		
											10.94	

Table C.3: Manual Alpha Peak: Subject 2

Trial num	1	2	3	4	5	6	7	8	9	10	Mean	Std
FP1	11.00	10.87	10.50	10.51	10.75	11.98	10.38	10.50	10.99	11.00	**10.85**	0.46
FP2	11.00	10.87	10.50	10.51	10.75	10.64	10.38	10.51	10.99	11.00	**10.72**	0.24
AF3	11.00	10.75	10.50	10.51	10.75	10.63	10.39	10.50	11.00	11.00	**10.70**	0.24
AF4	11.00	10.87	10.50	10.51	10.75	10.63	10.38	10.50	11.00	11.00	**10.71**	0.24
F7	11.00	10.75	10.39	10.50	10.75	11.12	10.38	10.50	11.00	11.00	**10.74**	0.28
F3	11.01	10.75	10.50	10.50	10.75	10.63	10.38	10.50	11.00	11.00	**10.70**	0.24
Fz	11.01	10.75	10.50	10.75	10.01	10.63	10.50	10.51	11.00	10.87	**10.65**	0.30
F4	11.01	10.87	10.50	10.76	10.14	10.63	10.38	10.50	11.00	10.87	**10.67**	0.29
F8	11.01	10.87	10.50	10.75	**Nan**	10.75	10.38	10.63	10.87	10.87	**10.74**	0.20
FC5	11.00	10.75	10.51	10.50	10.63	10.62	10.50	10.50	11.00	10.87	**10.69**	0.21
FC1	11.01	10.75	10.51	10.63	10.12	10.63	10.50	10.51	11.00	10.75	**10.64**	0.26
FC2	11.00	10.76	10.50	10.75	10.12	10.63	10.50	10.50	11.00	10.99	**10.68**	0.29
FC6	10.87	10.87	10.50	10.75	**Nan**	10.75	10.38	10.63	10.87	10.88	**10.72**	0.18
T7	11.00	10.67	12.37	10.50	10.64	10.62	10.39	10.50	11.38	11.00	**10.91**	0.60
C3	11.00	10.75	11.12	10.53	10.74	10.63	10.50	10.50	11.00	10.88	**10.77**	0.23
Cz	11.12	10.75	11.00	10.76	10.12	10.63	10.50	10.50	11.00	10.87	**10.73**	0.30
C4	11.75	11.00	12.51	11.12	12.35	11.38	10.49	10.63	10.87	11.12	**11.32**	0.68
T8	**Nan**	10.63	10.49	13.25	10.63	11.01	10.38	12.37	10.87	11.88	**11.28**	1.00
CP5	13.00	**Nan**	12.51	13.38	10.90	10.63	**Nan**	14.25	12.25	10.87	**12.22**	1.32
CP1	13.00	13.25	11.75	13.37	10.87	11.88	13.89	12.37	11.99	11.88	**12.43**	0.92
CP2	13.50	12.75	12.37	11.12	12.51	11.13	12.88	12.75	12.12	12.51	**12.36**	0.75
CP6	**Nan**	**Nan**	10.65	12.75	10.75	11.37	10.50	12.88	11.63	11.88	**11.55**	0.92
P7	11.12	10.76	10.50	11.00	10.50	11.00	10.50	10.50	11.01	12.12	**10.90**	0.50
P3	13.76	10.75	11.75	12.51	11.00	11.88	10.38	10.50	12.87	12.01	**11.74**	1.10
Pz	11.00	10.85	12.37	12.52	12.63	11.12	10.38	12.37	12.00	11.00	**11.63**	0.83
P4	11.00	10.87	12.37	10.50	10.75	10.63	10.38	12.87	11.63	10.88	**11.19**	0.84
P8	11.00	10.75	11.11	10.51	10.75	10.63	10.50	10.50	11.00	10.88	**10.76**	0.23
PO3	11.00	10.75	10.50	10.63	10.63	11.88	10.44	10.50	11.00	10.88	**10.82**	0.42
PO4	11.00	10.88	10.50	10.63	10.75	10.63	10.39	10.50	11.00	10.88	**10.72**	0.22
O1	11.12	10.75	10.50	10.75	10.63	10.63	10.38	10.51	11.05	11.00	**10.73**	0.25
OZ	11.00	10.75	10.50	10.75	10.63	10.63	10.42	10.52	11.00	11.00	**10.72**	0.22
O2	11.00	11.38	10.50	10.75	10.75	10.63	10.44	10.55	11.00	11.00	**10.80**	0.29
Mean	**11.35**	**10.96**	**10.99**	**11.10**	**10.80**	**10.91**	**10.62**	**11.03**	**11.23**	**11.15**	**11.01**	0.21
Std	0.81	0.57	0.77	0.94	0.63	0.44	0.75	1.02	0.49	0.46		
											11.01	

Table C.4: Manual Alpha Peak: Subject 3

Trial num	1	2	3	4	5	6	7	8	9	10	Mean	Std
FP1	11.00	10.87	10.50	10.51	10.75	11.98	10.38	10.50	10.99	11.00	**10.85**	0.46
FP2	11.00	10.87	10.50	10.51	10.75	10.64	10.38	10.51	10.99	11.00	**10.72**	0.24
AF3	11.00	10.75	10.50	10.51	10.75	10.63	10.39	10.50	11.00	11.00	**10.70**	0.24
AF4	11.00	10.87	10.50	10.51	10.75	10.63	10.38	10.50	11.00	11.00	**10.71**	0.24
F7	11.00	10.75	10.39	10.50	10.75	11.12	10.38	10.50	11.00	11.00	**10.74**	0.28
F3	11.01	10.75	10.50	10.50	10.75	10.63	10.38	10.50	11.00	11.00	**10.70**	0.24
Fz	11.01	10.75	10.50	10.75	10.01	10.63	10.50	10.51	11.00	10.87	**10.65**	0.30
F4	11.01	10.87	10.50	10.76	10.14	10.63	10.38	10.50	11.00	10.87	**10.67**	0.29
F8	11.01	10.87	10.50	10.75	**Nan**	10.75	10.38	10.63	10.87	10.87	**10.74**	0.20
FC5	11.00	10.75	10.51	10.50	10.63	10.62	10.50	10.50	11.00	10.87	**10.69**	0.21
FC1	11.01	10.75	10.51	10.63	10.12	10.63	10.50	10.51	11.00	10.75	**10.64**	0.26
FC2	11.00	10.76	10.50	10.75	10.12	10.63	10.50	10.50	11.00	10.99	**10.68**	0.29
FC6	10.87	10.87	10.50	10.75	**Nan**	10.75	10.38	10.63	10.87	10.88	**10.72**	0.18
T7	11.00	10.67	12.37	10.50	10.64	10.62	10.39	10.50	11.38	11.00	**10.91**	0.60
C3	11.00	10.75	11.12	10.53	10.74	10.63	10.50	10.50	11.00	10.88	**10.77**	0.23
Cz	11.12	10.75	11.00	10.76	10.12	10.63	10.50	10.50	11.00	10.87	**10.73**	0.30
C4	11.75	11.00	12.51	11.12	12.35	11.38	10.49	10.63	10.87	11.12	**11.32**	0.68
T8	**Nan**	10.63	10.49	13.25	10.63	11.01	10.38	12.37	10.87	11.88	**11.28**	1.00
CP5	13.00	**Nan**	12.51	13.38	10.90	10.63	**Nan**	14.25	12.25	10.87	**12.22**	1.32
CP1	13.00	13.25	11.75	13.37	10.87	11.88	13.89	12.37	11.99	11.88	**12.43**	0.92
CP2	13.50	12.75	12.37	11.12	12.51	11.13	12.88	12.75	12.12	12.51	**12.36**	0.75
CP6	**Nan**	**Nan**	10.65	12.75	10.75	11.37	10.50	12.88	11.63	11.88	**11.55**	0.92
P7	11.12	10.76	10.50	11.00	10.50	11.00	10.50	10.50	11.01	12.12	**10.90**	0.50
P3	13.76	10.75	11.75	12.51	11.00	11.88	10.38	10.50	12.87	12.01	**11.74**	1.10
Pz	11.00	10.85	12.37	12.52	12.63	11.12	10.38	12.37	12.00	11.00	**11.63**	0.83
P4	11.00	10.87	12.37	10.50	10.75	10.63	10.38	12.87	11.63	10.88	**11.19**	0.84
P8	11.00	10.75	11.11	10.51	10.75	10.63	10.50	10.50	11.00	10.88	**10.76**	0.23
PO3	11.00	10.75	10.50	10.63	10.63	11.88	10.44	10.50	11.00	10.88	**10.82**	0.42
PO4	11.00	10.88	10.50	10.63	10.75	10.63	10.39	10.50	11.00	10.88	**10.72**	0.22
O1	11.12	10.75	10.50	10.75	10.63	10.63	10.38	10.51	11.05	11.00	**10.73**	0.25
OZ	11.00	10.75	10.50	10.75	10.63	10.63	10.42	10.52	11.00	11.00	**10.72**	0.22
O2	11.00	11.38	10.50	10.75	10.75	10.63	10.44	10.55	11.00	11.00	**10.80**	0.29
Mean	**11.35**	**10.96**	**10.99**	**11.10**	**10.80**	**10.91**	**10.62**	**11.03**	**11.23**	**11.15**	**11.01**	0.21
Std	0.81	0.57	0.77	0.94	0.63	0.44	0.75	1.02	0.49	0.46		
											11.01	

Table C.5: Manual Alpha Peak: Subject 4

Trial num	1	2	3	4	5	6	7	8	9	10	Mean	Std
FP1	10.24	10.01	6.88	9.75	9.62	9.75	9.00	9.88	10.01	9.50	**9.46**	0.97
FP2	10.25	10.01	6.88	9.75	9.63	9.75	8.99	10.01	10.01	9.50	**9.48**	0.98
AF3	10.25	10.01	6.87	9.75	9.62	9.75	9.00	9.86	9.87	9.50	**9.45**	0.96
AF4	10.25	10.01	6.88	9.75	9.62	9.75	8.99	10.01	10.01	9.50	**9.48**	0.98
F7	**Nan**	9.25	9.50	9.75	9.48	9.75	8.86	9.00	9.75	9.40	**9.42**	0.33
F3	10.24	9.87	9.46	9.75	9.62	9.75	9.00	10.02	9.87	9.49	**9.71**	0.34
Fz	10.24	9.88	9.50	9.63	9.62	9.75	9.00	10.02	9.87	9.50	**9.70**	0.34
F4	10.26	9.87	9.50	9.74	9.63	9.75	9.00	9.99	10.01	9.50	**9.73**	0.35
F8	**Nan**	10.02	7.25	9.62	6.75	9.75	9.50	7.37	5.75	6.89	**8.10**	1.61
FC5	6.11	9.87	9.26	9.75	9.51	9.75	8.88	9.75	9.87	9.38	**9.21**	1.13
FC1	10.27	9.87	9.86	9.75	9.62	9.75	9.25	9.88	9.87	9.50	**9.76**	0.27
FC2	6.50	9.88	9.50	9.75	9.62	9.75	9.00	10.01	9.87	9.49	**9.34**	1.04
FC6	10.63	9.88	**Nan**	9.75	6.63	9.75	7.00	9.51	**Nan**	9.00	**9.02**	1.44
T7	6.11	9.87	6.88	9.00	**Nan**	7.51	6.50	9.00	7.63	**Nan**	**7.81**	1.35
C3	**Nan**	9.14	9.62	9.63	9.50	9.62	9.25	9.83	9.87	9.38	**9.54**	0.25
Cz	9.50	9.87	9.99	9.86	9.76	9.74	9.25	9.76	9.87	9.39	**9.70**	0.24
C4	**Nan**	9.87	**Nan**	9.87	**Nan**	8.76	**Nan**	**Nan**	9.88	10.38	**9.75**	0.60
T8	9.87	8.62	10.38	9.00	8.86	9.12	10.14	7.37	9.99	7.00	**9.04**	1.14
CP5	10.12	9.01	**Nan**	9.01	9.50	**Nan**	8.50	7.75	5.74	8.76	**8.55**	1.33
CP1	**Nan**	9.00	9.61	8.36	8.88	8.00	9.25	6.51	9.90	6.88	**8.49**	1.17
CP2	**Nan**	9.88	9.62	**Nan**	9.13	7.00	9.88	6.50	10.12	6.88	**8.63**	1.55
CP6	9.86	8.51	10.06	9.75	9.62	9.75	8.89	10.12	9.75	9.48	**9.58**	0.51
P7	10.26	10.01	10.63	9.86	9.75	9.75	8.37	10.13	10.01	10.25	**9.90**	0.60
P3	6.12	8.63	7.25	8.36	6.75	8.13	9.00	7.25	7.25	9.50	**7.83**	1.07
Pz	6.12	8.50	7.25	9.74	9.61	9.75	6.89	9.25	7.38	9.50	**8.40**	1.37
P4	7.51	8.62	9.50	9.62	9.62	9.75	8.99	9.62	9.87	9.00	**9.21**	0.72
P8	9.87	9.87	10.03	9.75	9.62	9.75	9.26	10.01	9.87	9.38	**9.74**	0.25
PO3	10.27	9.87	9.48	9.76	9.62	9.76	9.50	9.99	9.87	9.50	**9.76**	0.25
PO4	10.38	9.87	9.50	9.75	9.62	9.74	9.25	10.01	9.87	9.38	**9.74**	0.33
O1	10.37	9.87	9.50	9.75	9.62	9.75	9.50	10.01	9.88	9.50	**9.78**	0.27
OZ	10.26	9.87	9.50	9.75	9.62	9.75	9.50	10.01	9.87	9.38	**9.75**	0.26
O2	10.38	9.87	9.50	9.75	9.62	9.75	9.25	10.01	9.88	9.38	**9.74**	0.33
Mean	**9.32**	**9.60**	**8.95**	**9.58**	**9.26**	**9.43**	**8.92**	**9.30**	**9.40**	**9.13**	**9.29**	0.23
Std	1.65	0.53	1.25	0.40	0.89	0.74	0.79	1.14	1.23	0.91		
											9.29	

Appendix D

Appendix: ERS/ERD figures

Subject 1: different types of movements

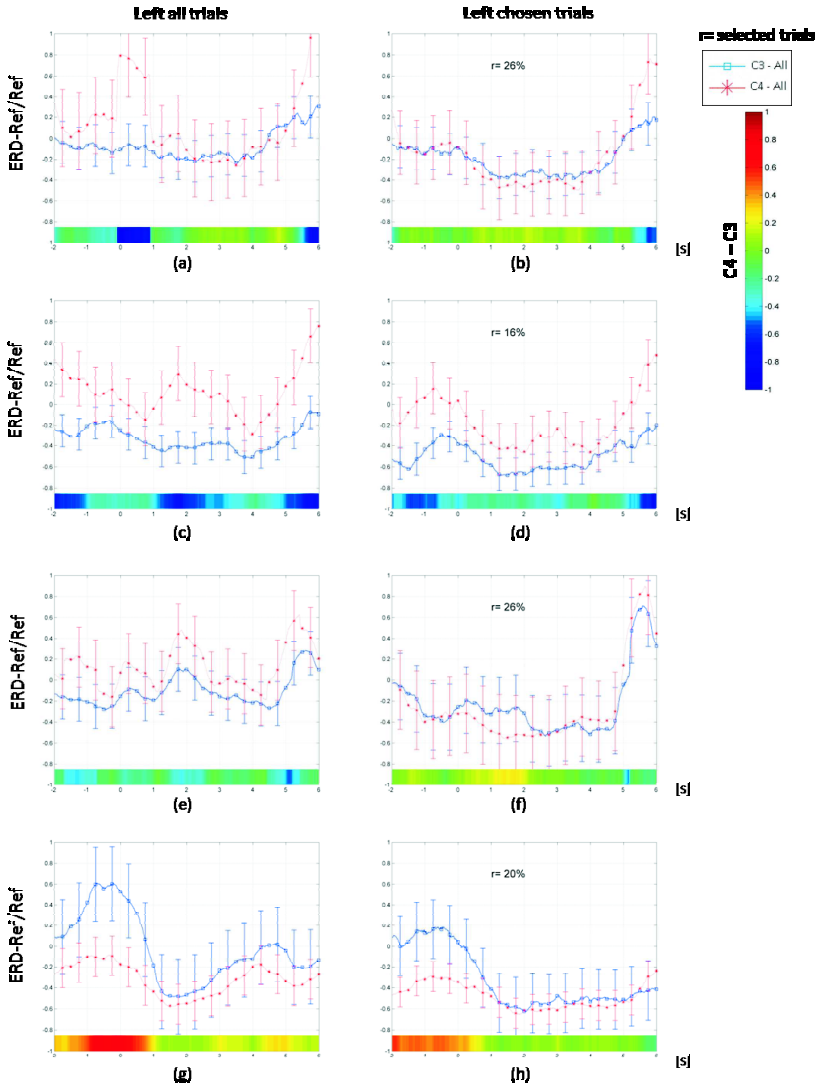

Figure D.1: Event-Related Desynchronization (ERD) of subject 1 during real left movement referenced to all scalp sensors using an auditory clue. (a)/(b) Open & close movement. (c)/(d) Up & down movement. (e)/(f) Finger movement. (g)/(h) Strong movement.

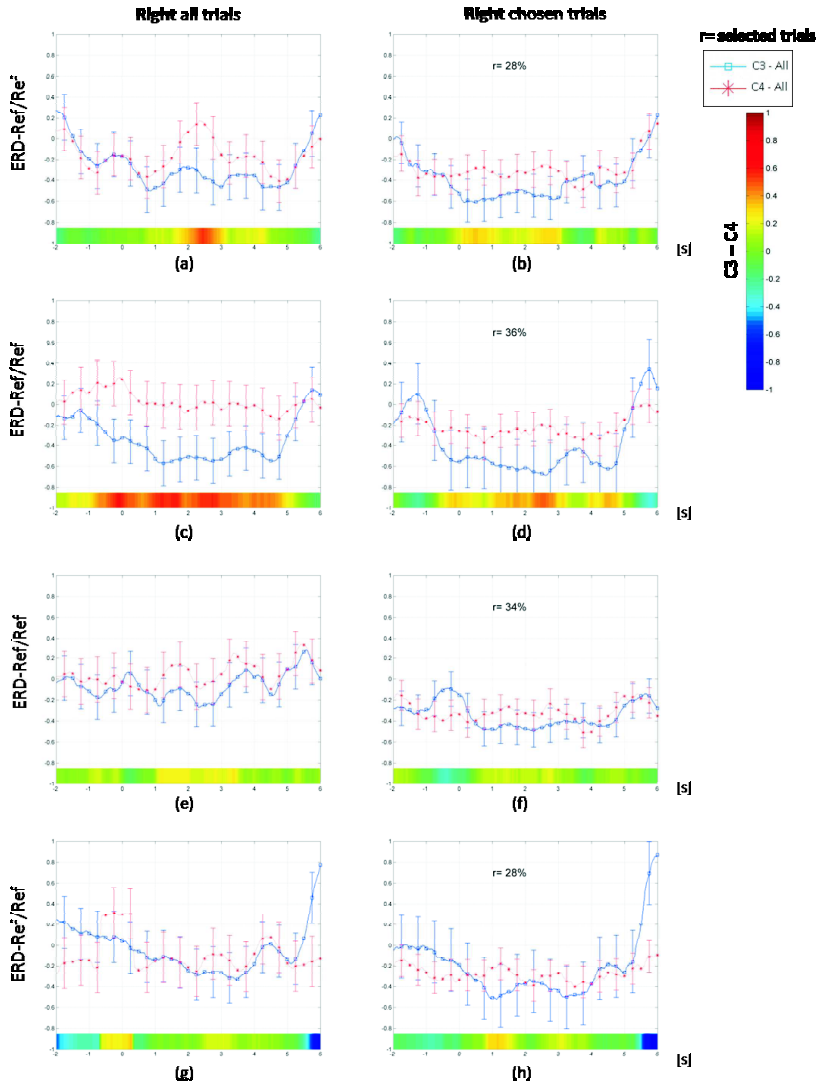

Figure D.2: Event-Related Desynchronization (ERD) of subject 1 during real right movement referenced to all scalp sensors using an auditory clue. (a)/(b) Open & close movement. (c)/(d) Up & down movement. (e)/(f) Finger movement. (g)/(h) Strong movement.

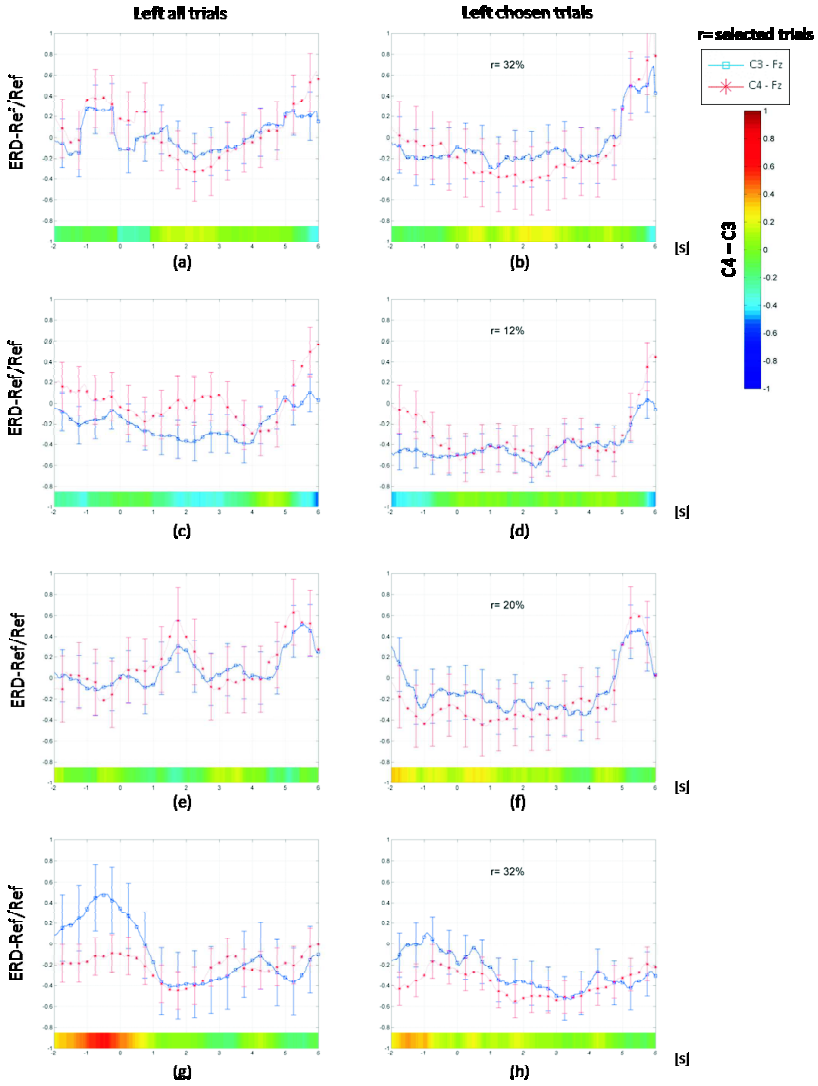

Figure D.3: Event-Related Desynchronization (ERD) of subject 1 during real left movement referenced to Fz sensor using an auditory clue. (a)/(b) Open & close movement. (c)/(d) Up & down movement. (e)/(f) Finger movement. (g)/(h) Strong movement.

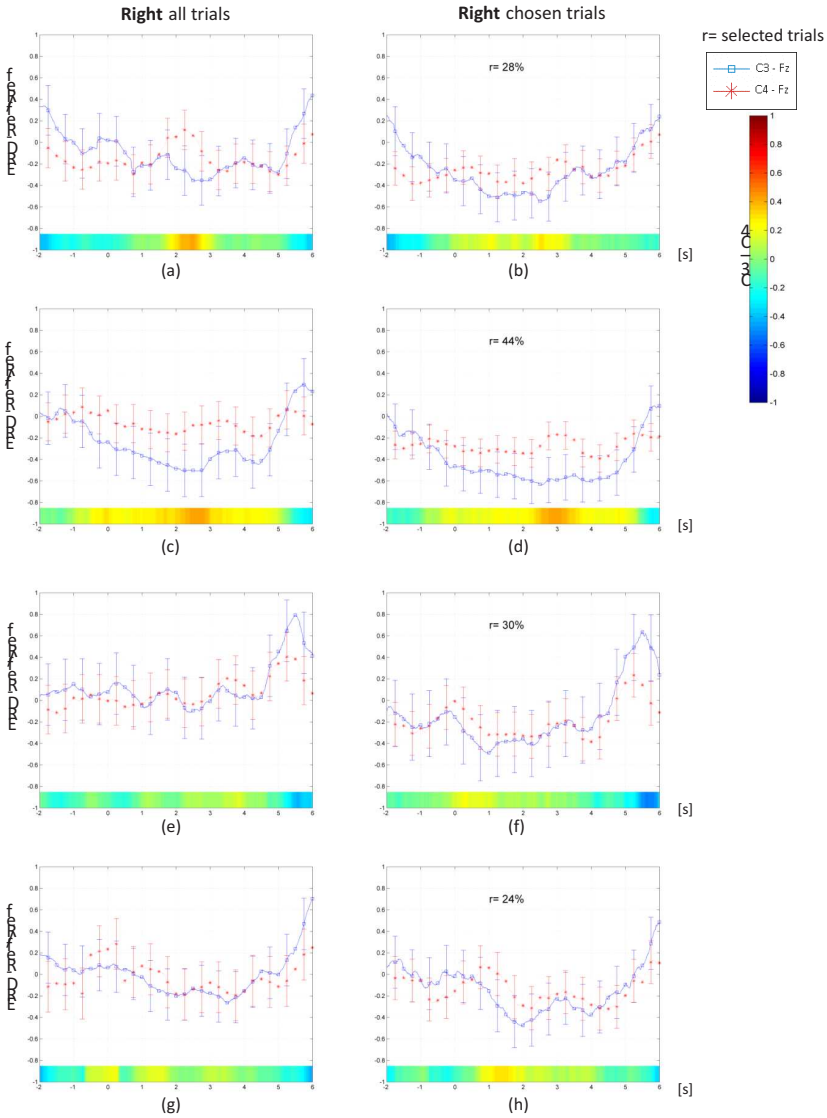

Figure D.4: Event-Related Desynchronization (ERD) of subject 1 during real right movement referenced to Fz sensor using an auditory clue. (a)/(b) Open & close movement. (c)/(d) Up & down movement. (e)/(f) Finger movement. (g)/(h) Strong movement.

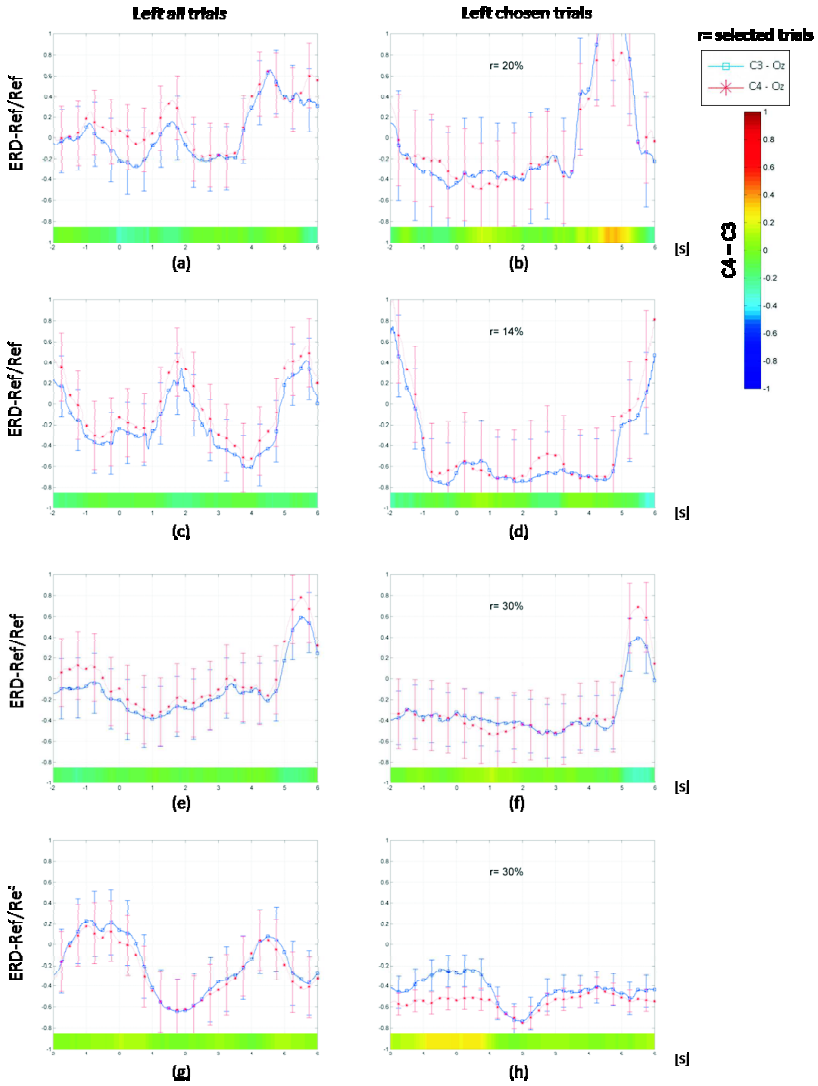

Figure D.5: Event-Related Desynchronization (ERD) of subject 1 during real left movement referenced to Oz sensor using an auditory clue. (a)/(b) Open & close movement. (c)/(d) Up & down movement. (e)/(f) Finger movement. (g)/(h) Strong movement.

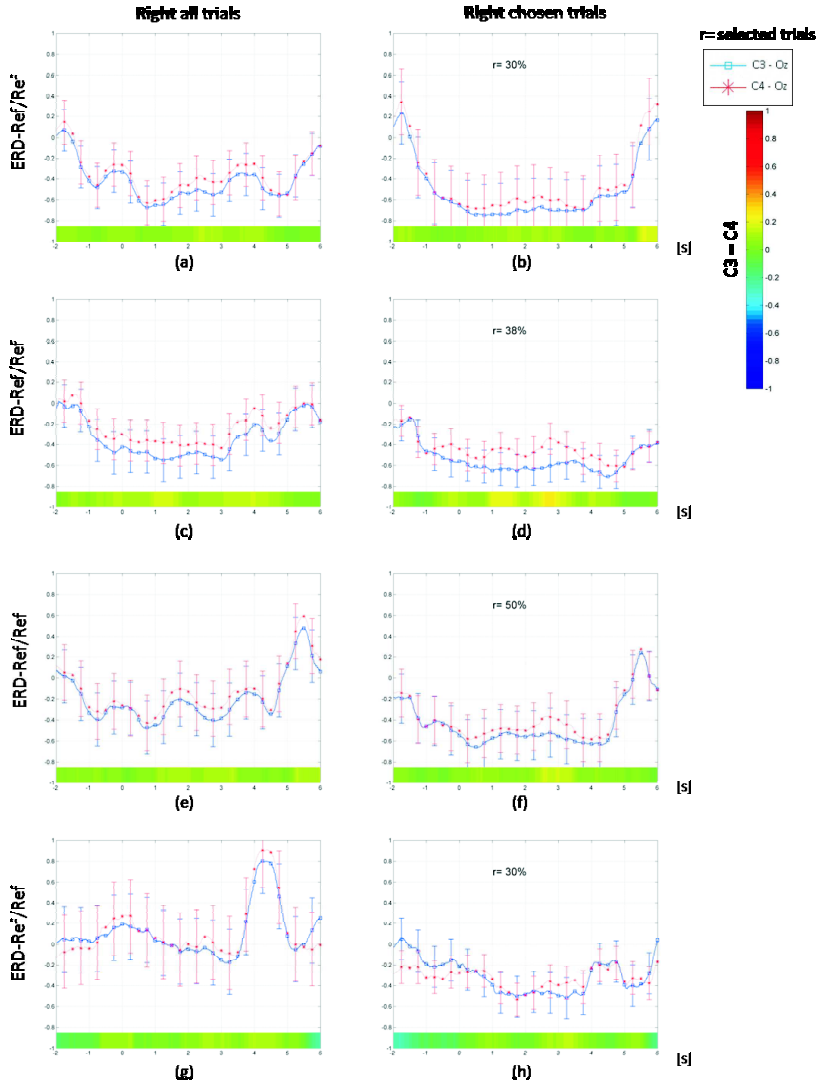

Figure D.6: Event-Related Desynchronization (ERD) of subject 1 during real right movement referenced to Oz sensor using an auditory clue. (a)/(b) Open & close movement. (c)/(d) Up & down movement. (e)/(f) Finger movement. (g)/(h) Strong movement.

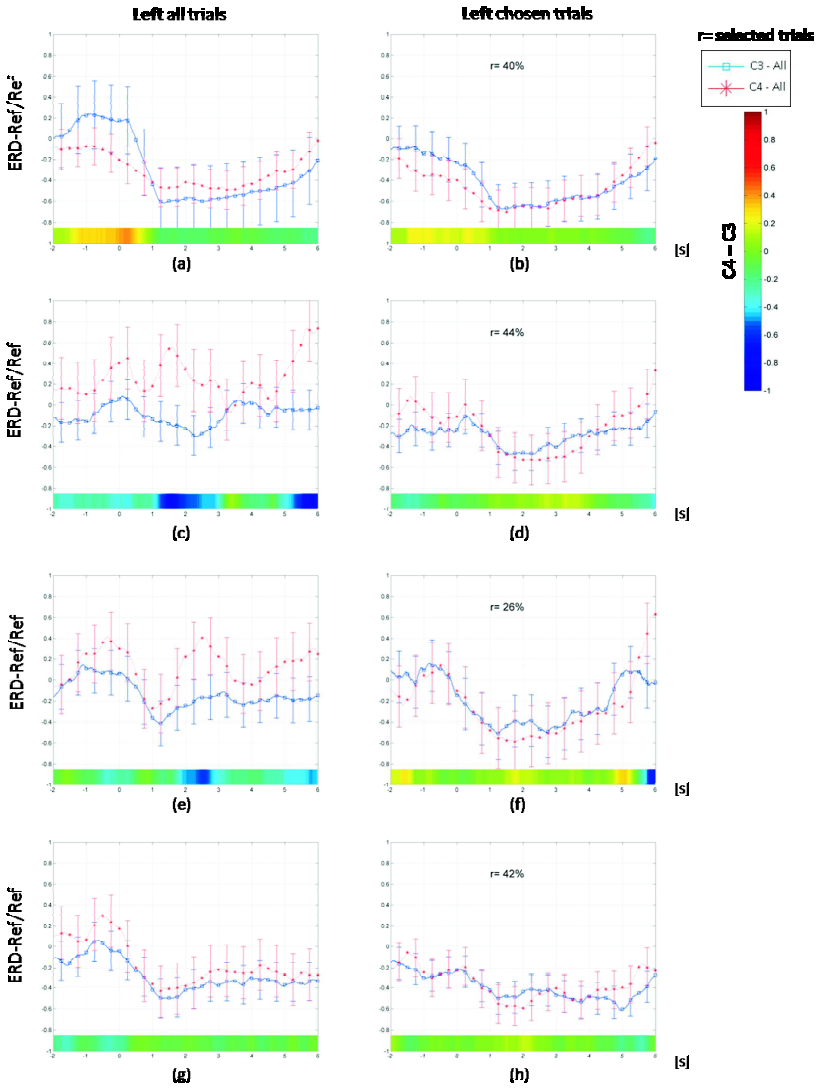

Figure D.7: Event-Related Desynchronization (ERD) of subject 1 during real left movement referenced to all scalp sensors using a visual clue. (a)/(b) Open & close movement. (c)/(d) Up & down movement. (e)/(f) Finger movement. (g)/(h) Strong movement.

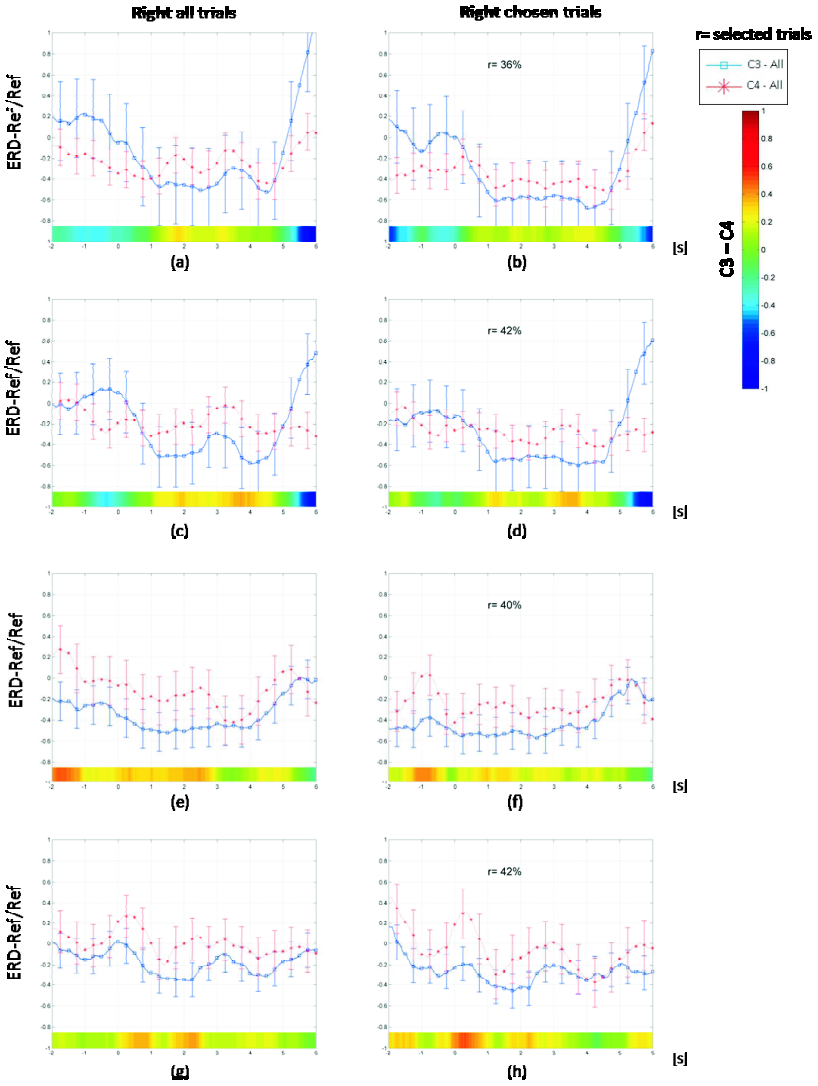

Figure D.8: Event-Related Desynchronization (ERD) of subject 1 during real right movement referenced to all scalp sensors using a visual clue. (a)/(b) Open & close movement. (c)/(d) Up & down movement. (e)/(f) Finger movement. (g)/(h) Strong movement.

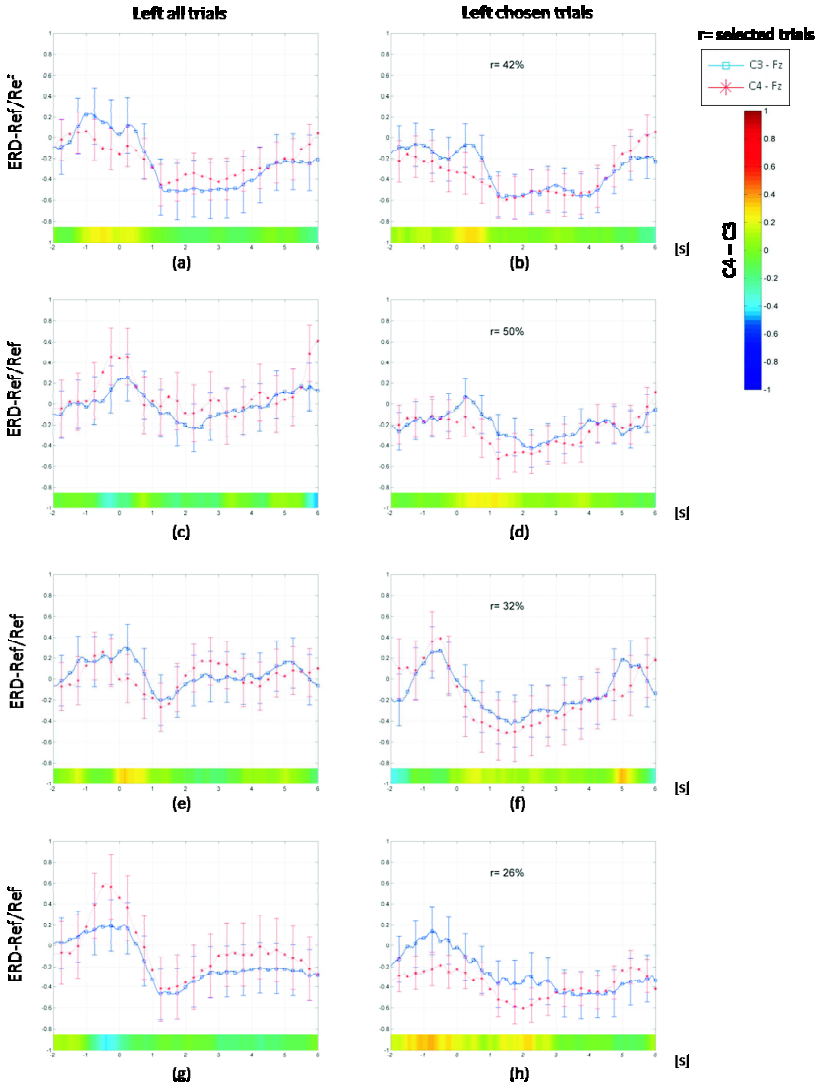

Figure D.9: Event-Related Desynchronization (ERD) of subject 1 during real left movement referenced to Fz sensor using a visual clue. (a)/(b) Open & close movement. (c)/(d) Up & down movement. (e)/(f) Finger movement. (g)/(h) Strong movement.

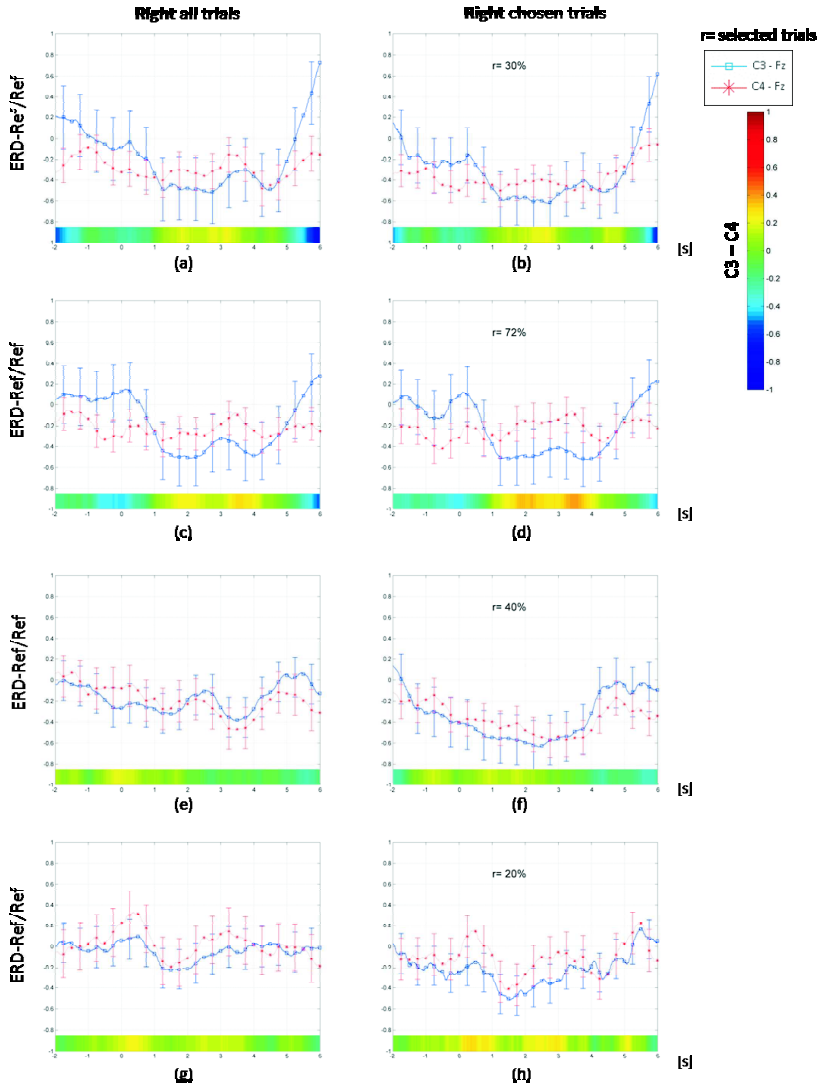

Figure D.10: Event-Related Desynchronization (ERD) of subject 1 during real right movement referenced to Fz sensor using a visual clue. (a)/(b) Open & close movement. (c)/(d) Up & down movement. (e)/(f) Finger movement. (g)/(h) Strong movement.

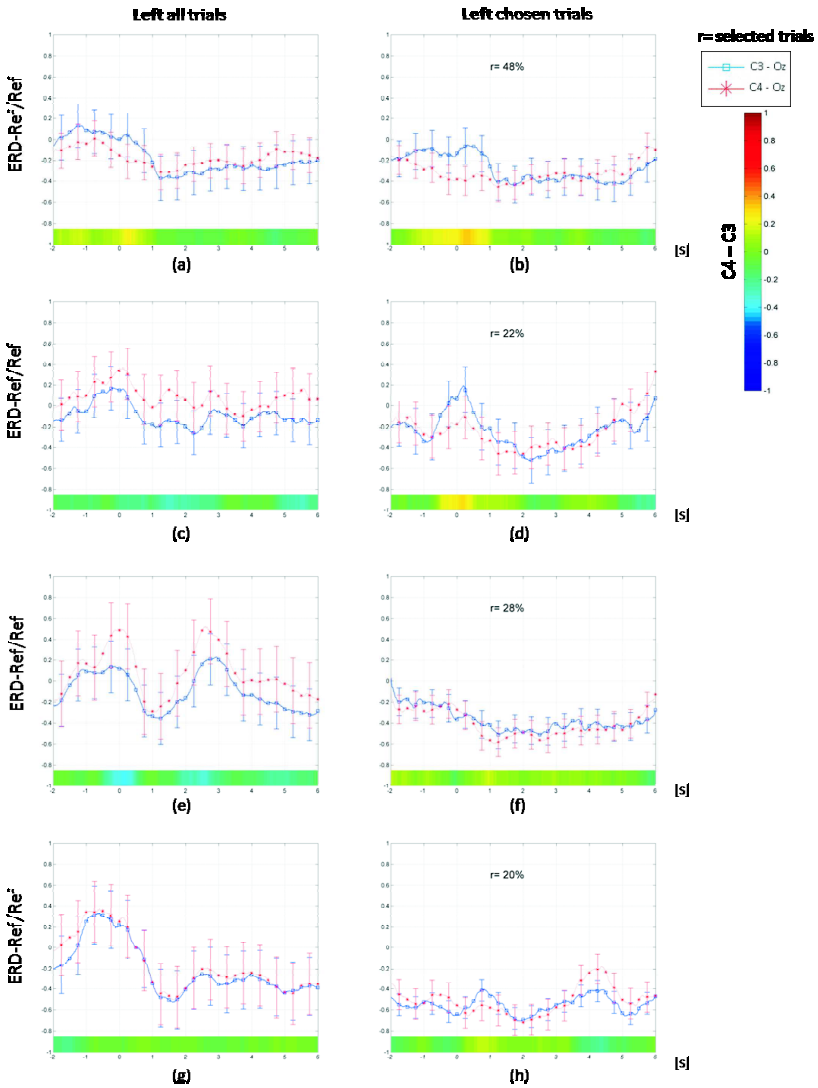

Figure D.11: Event-Related Desynchronization (ERD) of subject 1 during real left movement referenced to Oz sensor using a visual clue. (a)/(b) Open & close movement. (c)/(d) Up & down movement. (e)/(f) Finger movement. (g)/(h) Strong movement.

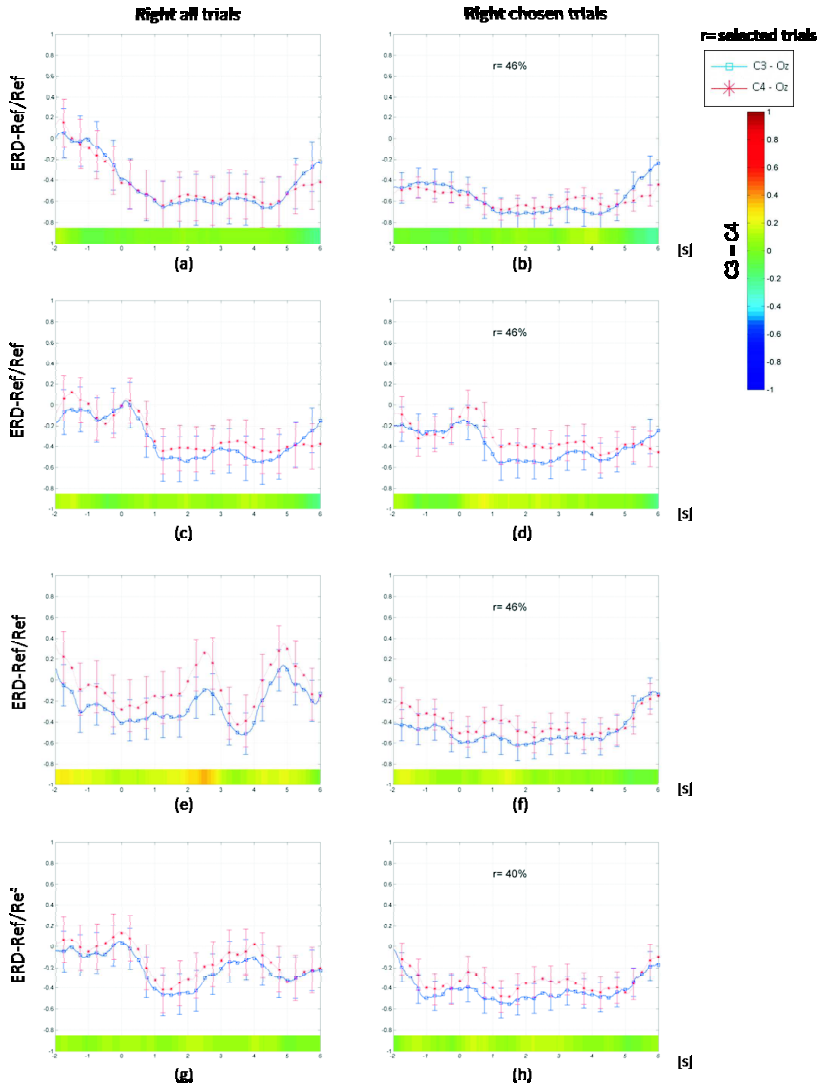

Figure D.12: Event-Related Desynchronization (ERD) of subject 1 during real right movement referenced to Oz sensor using a visual clue. (a)/(b) Open & close movement. (c)/(d) Up & down movement. (e)/(f) Finger movement. (g)/(h) Strong movement.

Subject 1: ERS/ERD in frequency bands

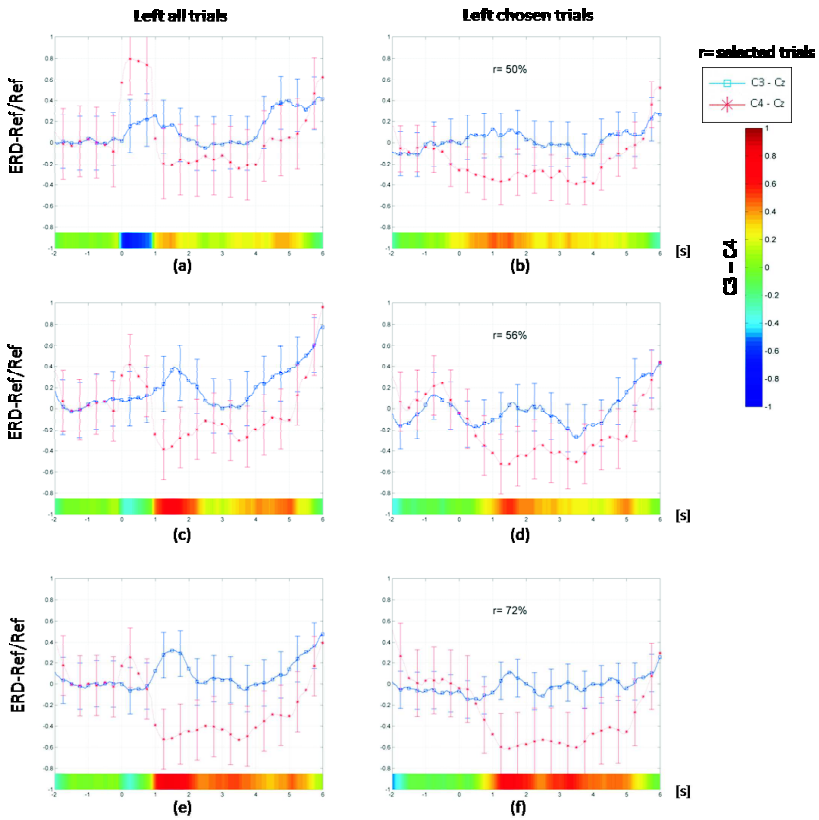

Figure D.13: Event-Related Desynchronization (ERD) and Synchronization (ERS) of subject 1 during real left Open & Close movement, referenced to Cz scalp sensors using an auditory clue. (a)/(b) First Alpha. (c)/(d) Second Alpha. (e)/(f) High Alpha.

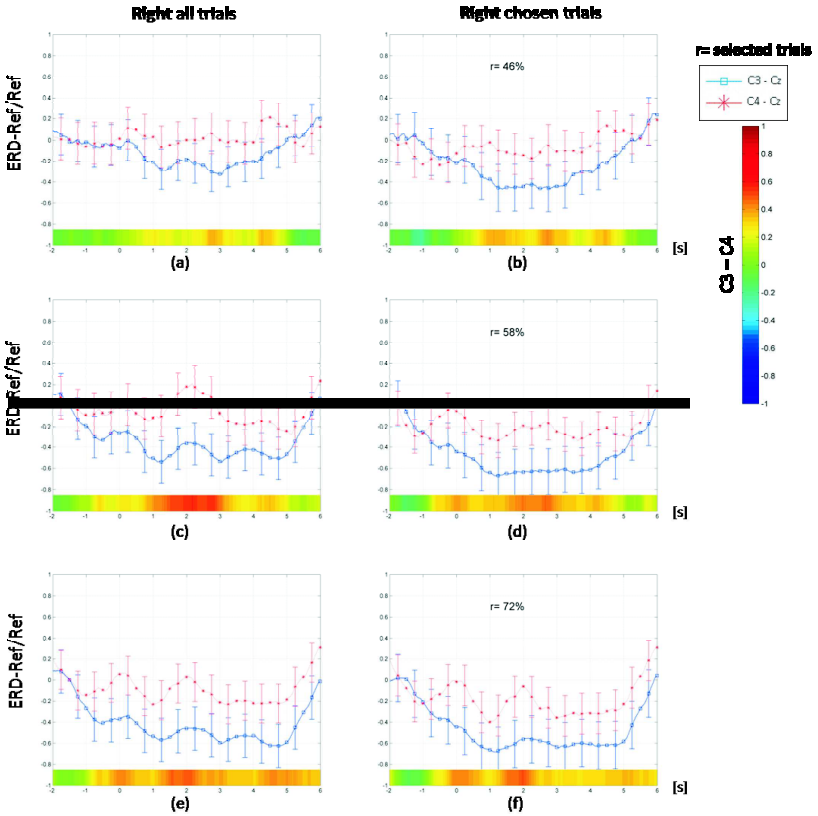

Figure D.14: Event-Related Desynchronization (ERD) and Synchronization (ERS) of subject 1 during real right Open & close movement, referenced to Cz scalp sensors using an auditory clue. (a)/(b) First Alpha. (c)/(d) Second Alpha. (e)/(f) High Alpha.

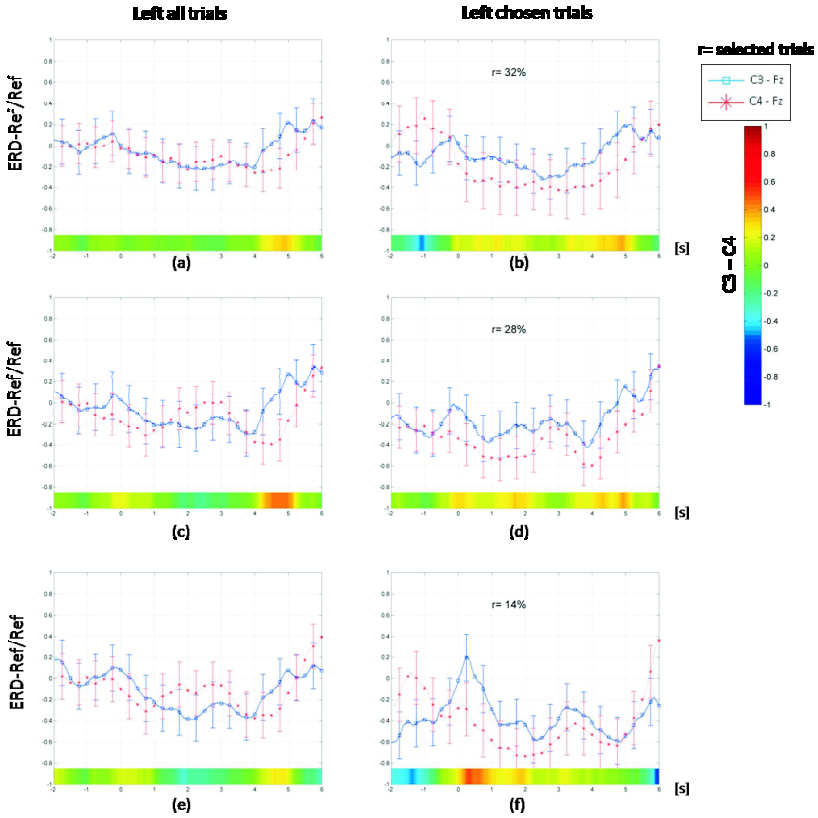

Figure D.15: Event-Related Desynchronization (ERD) and Synchronization (ERS) of subject 1 during real left Up & down movement, referenced to Fz scalp sensors using an auditory clue. (a)/(b) First Alpha. (c)/(d) Second Alpha. (e)/(f) High Alpha.

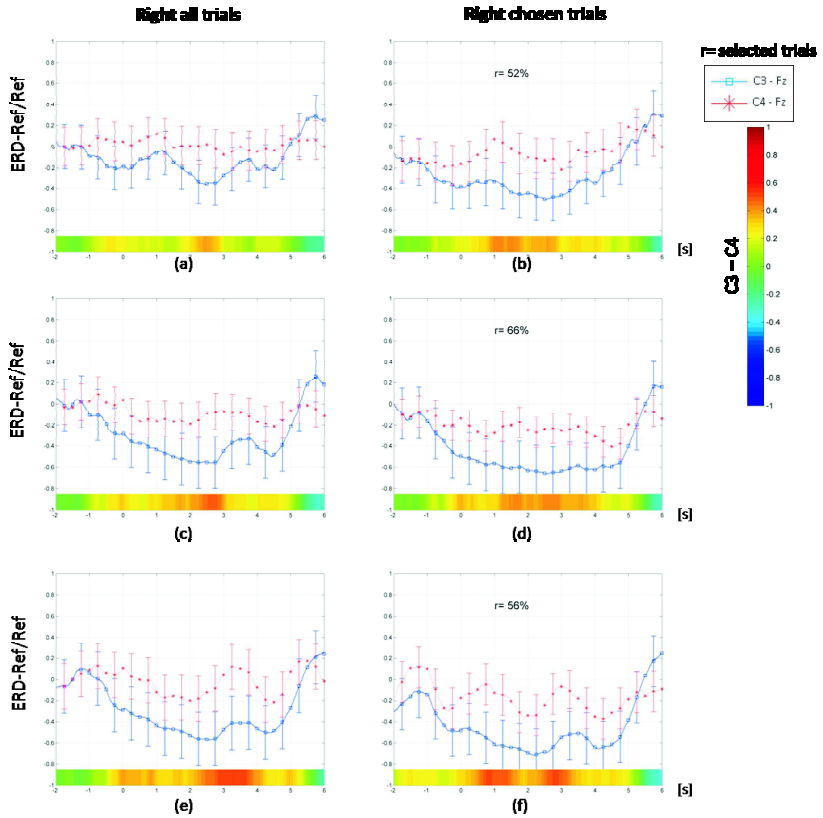

Figure D.16: Event-Related Desynchronization (ERD) and Synchronization (ERS) of subject 1 during real right Up & down movement, referenced to Fz scalp sensors using an auditory clue. (a)/(b) First Alpha. (c)/(d) Second Alpha. (e)/(f) High Alpha.

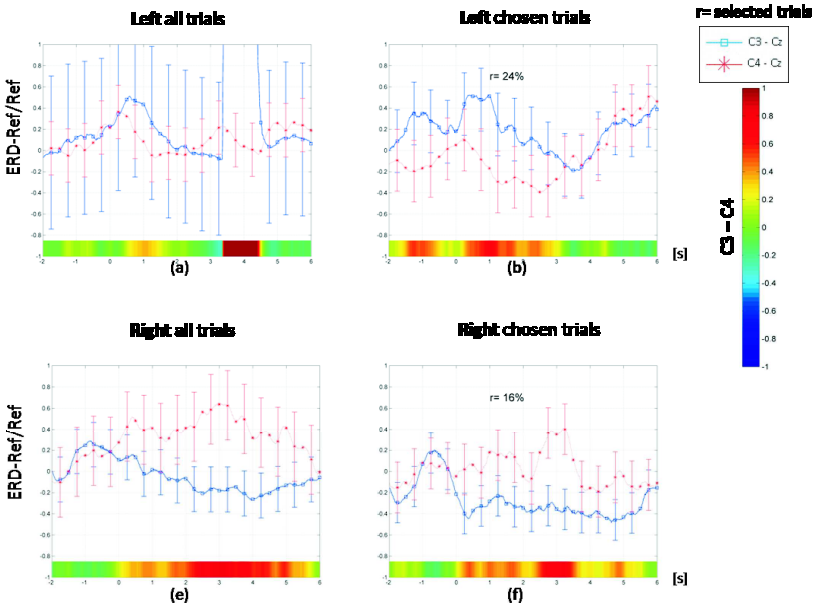

Figure D.17: Event-Related Desynchronization (ERD) and Synchronization (ERS) of subject 1 during real left imaginary visual movement, referenced to Cz scalp sensors using an auditory clue. (a)/(b) First Alpha. (c)/(d) Second Alpha. (e)/(f) High Alpha.

Subject 2: ERS/ERD in frequency bands

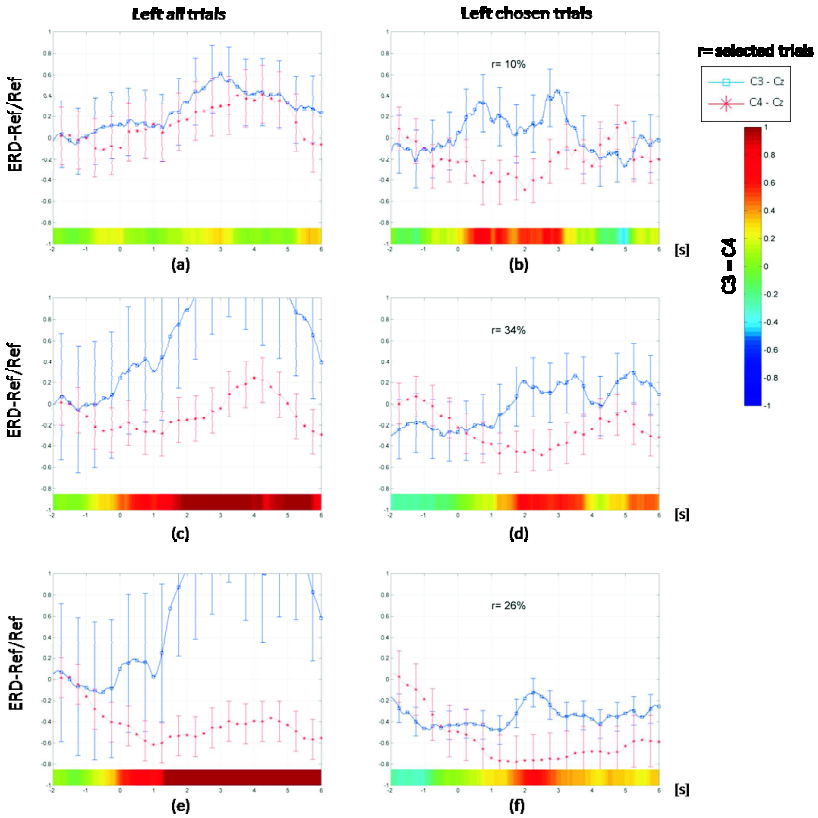

Figure D.18: Event-Related Desynchronization (ERD) and Synchronization (ERS) of subject 2 during real left Open & close movement, referenced to Cz scalp sensors using an auditory clue. (a)/(b) First Alpha. (c)/(d) Second Alpha. (e)/(f) High Alpha.

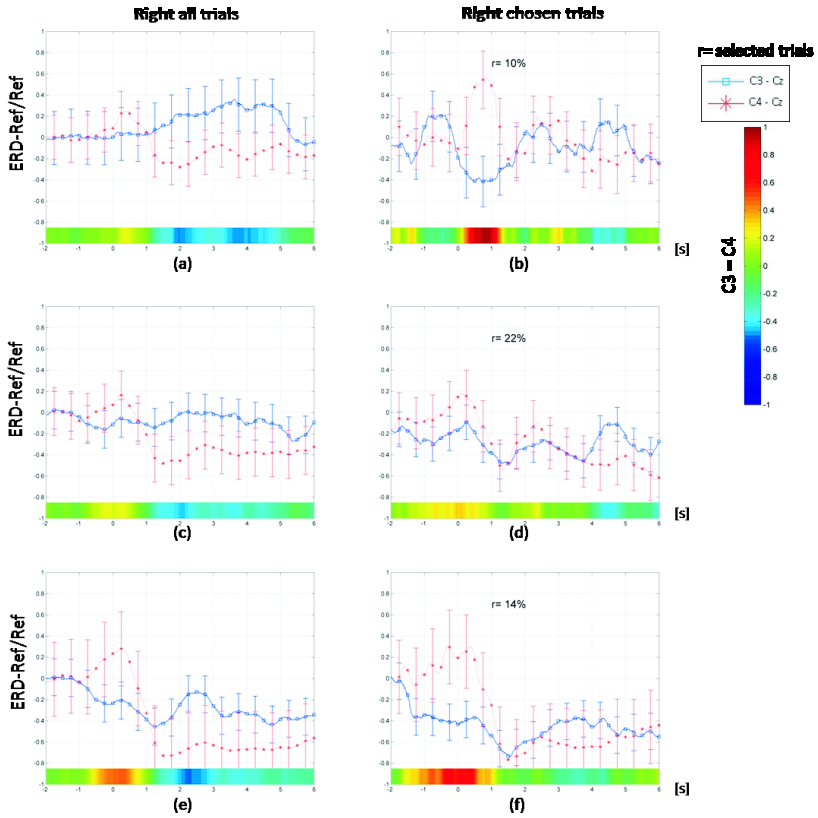

Figure D.19: Event-Related Desynchronization (ERD) and Synchronization (ERS) of subject 2 during real right Open & close movement, referenced to all scalp sensors using an auditory clue. (a)/(b) First Alpha. (c)/(d) Second Alpha. (e)/(f) High Alpha.

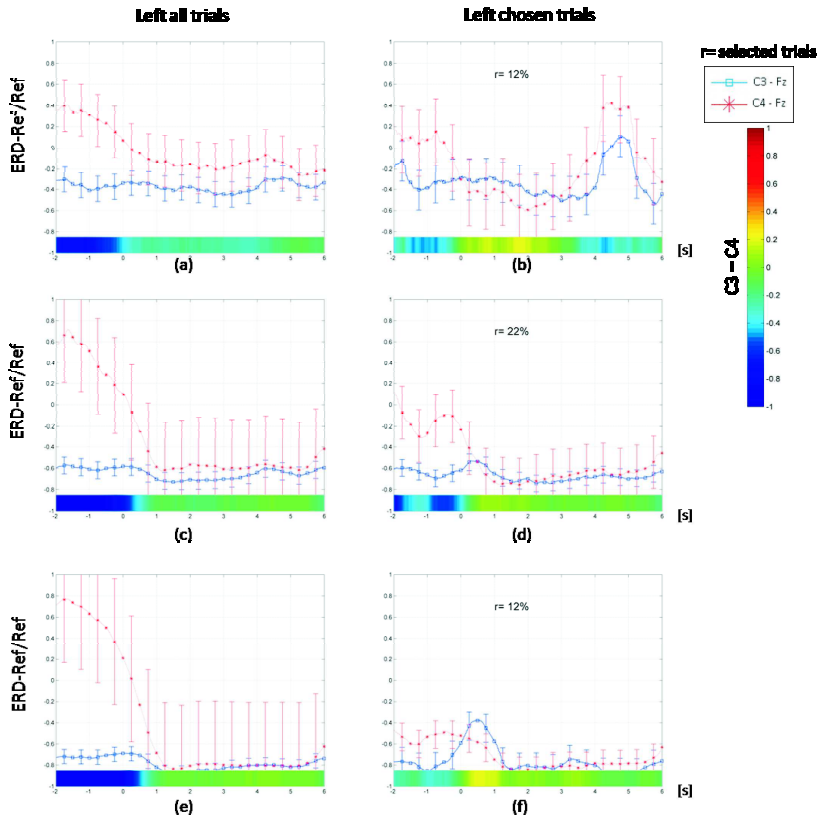

Figure D.20: Event-Related Desynchronization (ERD) and Synchronization (ERS) of subject 2 during real left Up & down movement, referenced to Fz scalp sensors using an auditory clue. (a)/(b) First Alpha. (c)/(d) Second Alpha. (e)/(f) High Alpha.

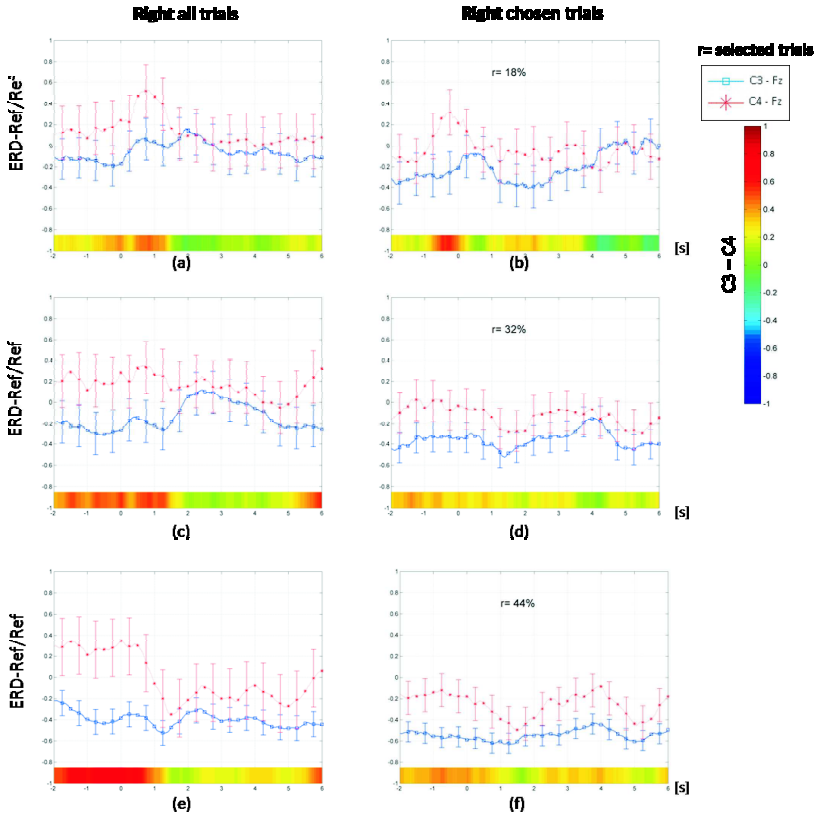

Figure D.21: Event-Related Desynchronization (ERD) and Synchronization (ERS) of subject 2 during real right Up & down movement, referenced to Fz scalp sensors using an auditory clue. (a)/(b) First Alpha. (c)/(d) Second Alpha. (e)/(f) High Alpha.

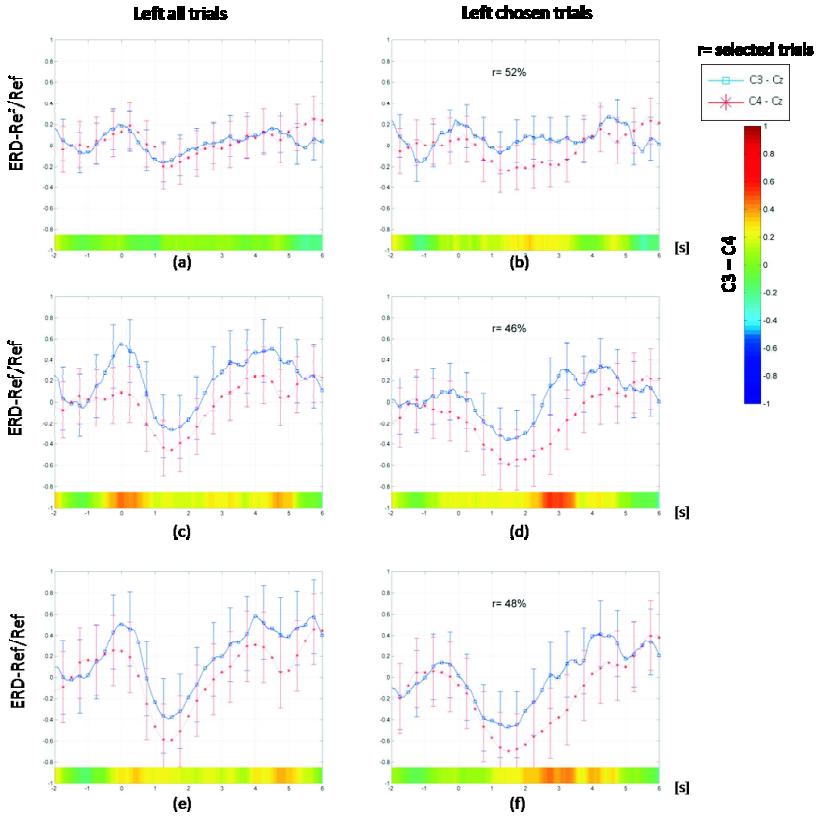

Figure D.22: Event-Related Desynchronization (ERD) and Synchronization (ERS) of subject 2 during imaginary left muscle movement, referenced to Cz scalp sensors using an auditory clue. (a)/(b) First Alpha. (c)/(d) Second Alpha. (e)/(f) High Alpha.

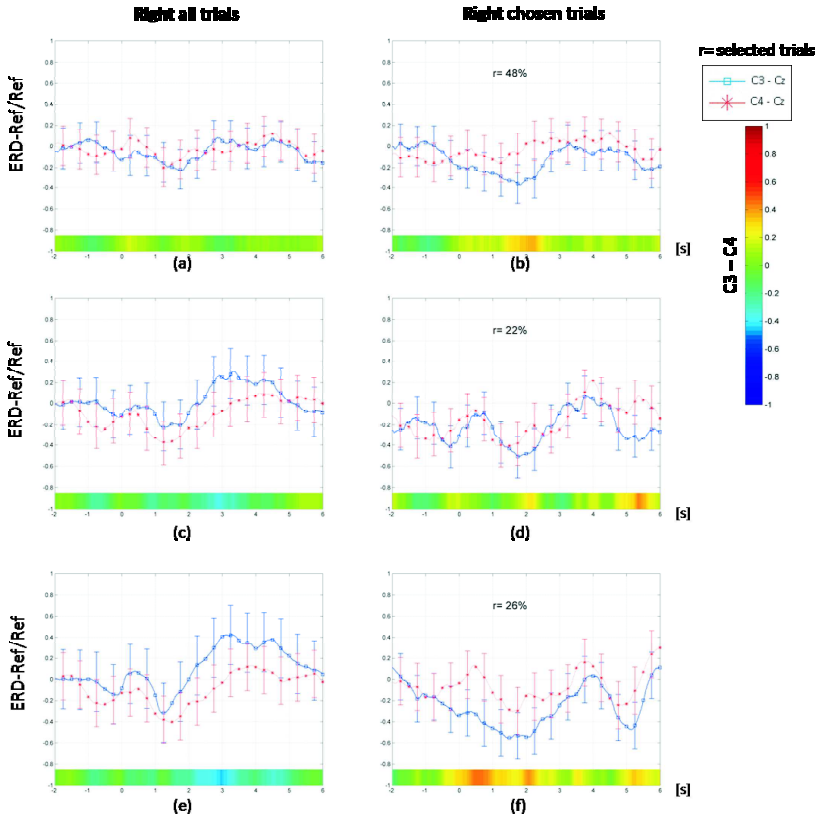

Figure D.23: Event-Related Desynchronization (ERD) and Synchronization (ERS) of subject 2 during imaginary right muscle movement, referenced to Cz scalp sensors using an auditory clue. (a)/(b) First Alpha. (c)/(d) Second Alpha. (e)/(f) High Alpha.

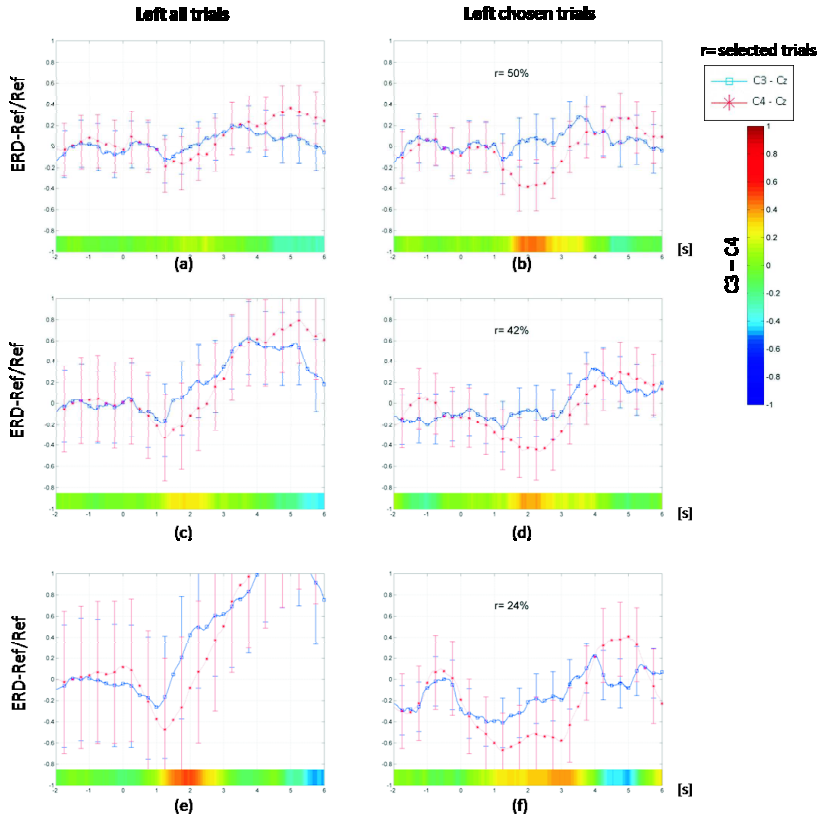

Figure D.24: Event-Related Desynchronization (ERD) and Synchronization (ERS) of subject 2 during imaginary left visual movement, referenced to Cz scalp sensors using an auditory clue. (a)/(b) First Alpha. (c)/(d) Second Alpha. (e)/(f) High Alpha.

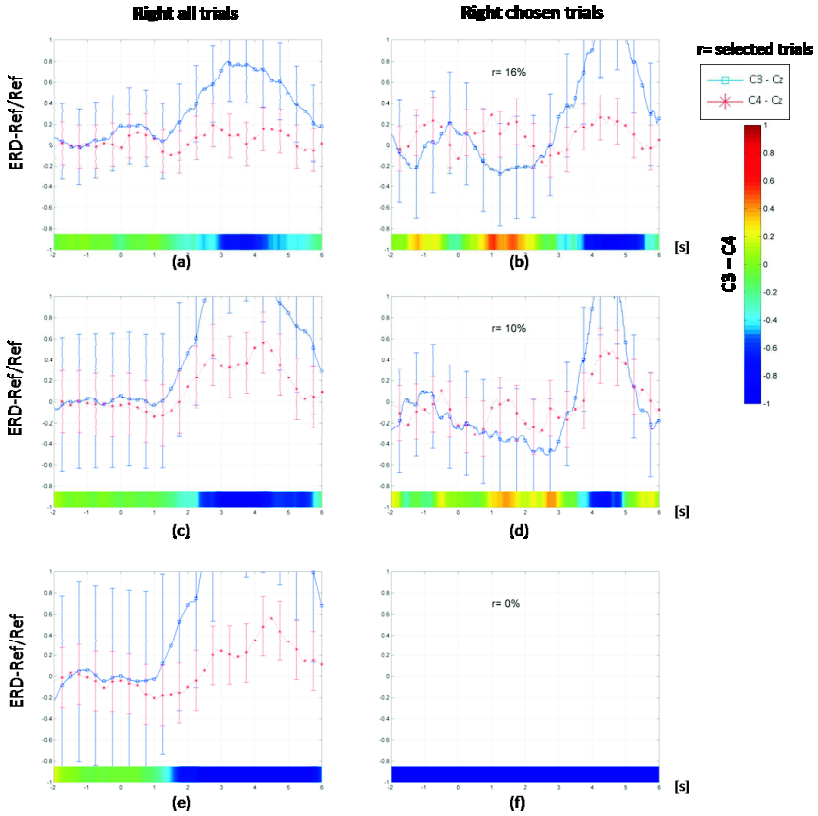

Figure D.25: Event-Related Desynchronization (ERD) and Synchronization (ERS) of subject 2 during imaginary right visual movement, referenced to Cz scalp sensors using an auditory clue. (a)/(b) First Alpha. (c)/(d) Second Alpha. (e)/(f) High Alpha.

Subject 3: ERS/ERD in frequency bands

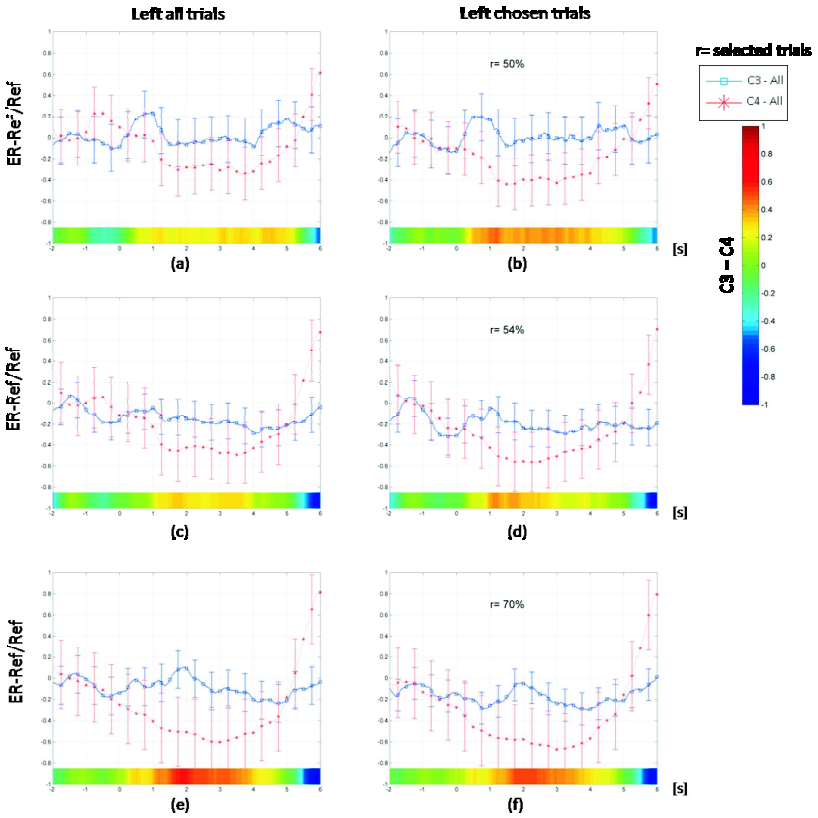

Figure D.26: Event-Related Desynchronization (ERD) and Synchronization (ERS) of subject 3 during real left Open & close movement, referenced to all scalp sensors using an auditory clue. (a)/(b) First Alpha. (c)/(d) Second Alpha. (e)/(f) High Alpha.

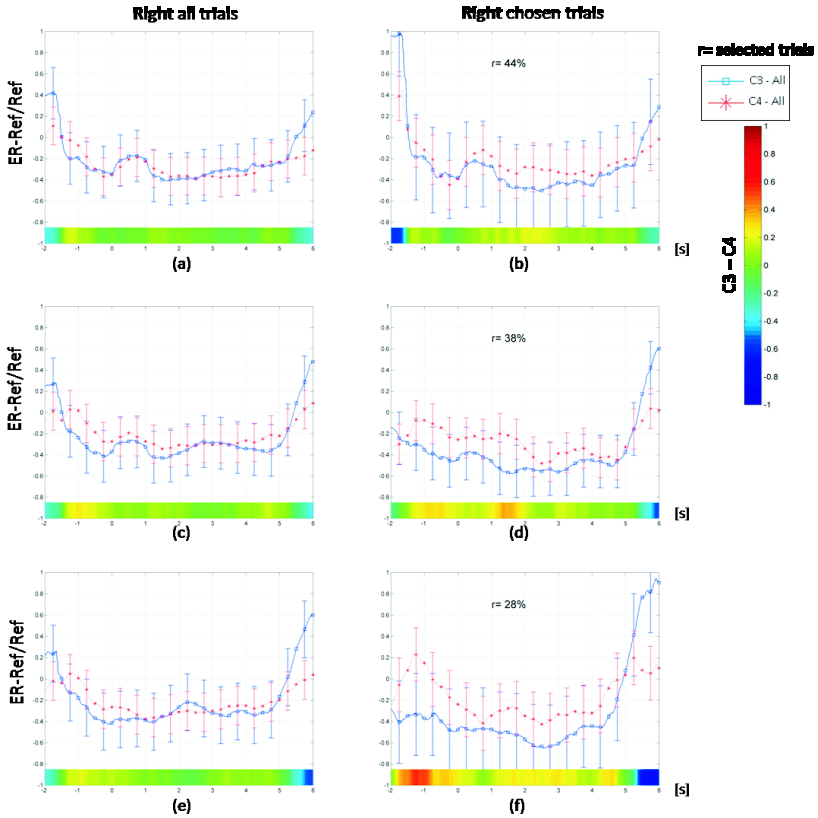

Figure D.27: Event-Related Desynchronization (ERD) and Synchronization (ERS) of subject 3 during real right Open & close movement, referenced to all scalp sensors using an auditory clue. (a)/(b) First Alpha. (c)/(d) Second Alpha. (e)/(f) High Alpha.

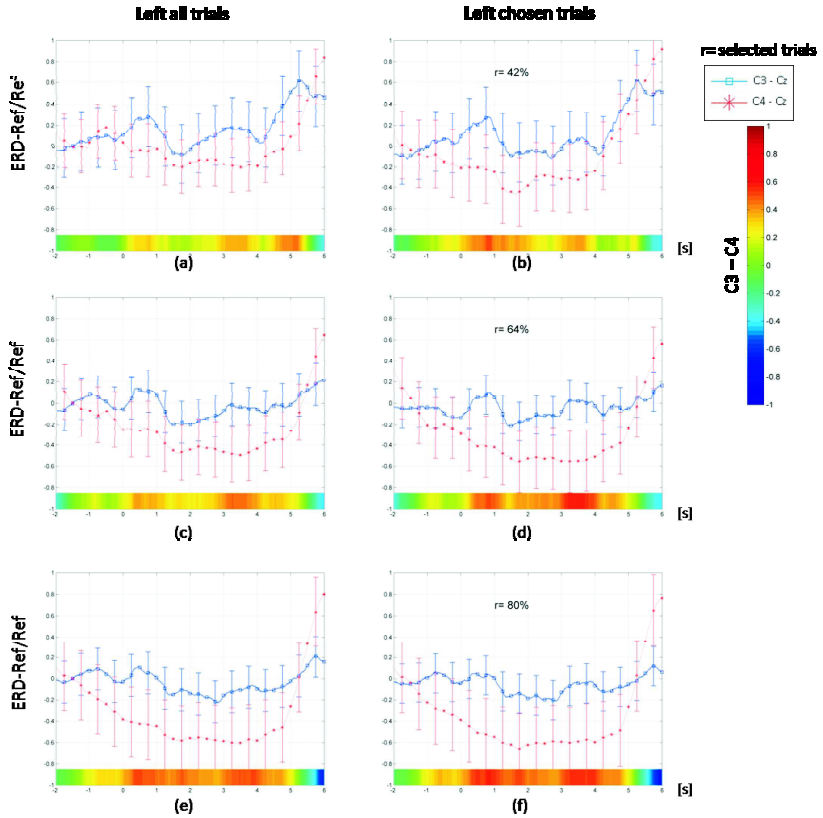

Figure D.28: Event-Related Desynchronization (ERD) and Synchronization (ERS) of subject 3 during real left Open & close movement, referenced to Cz scalp sensors using an auditory clue. (a)/(b) First Alpha. (c)/(d) Second Alpha. (e)/(f) High Alpha.

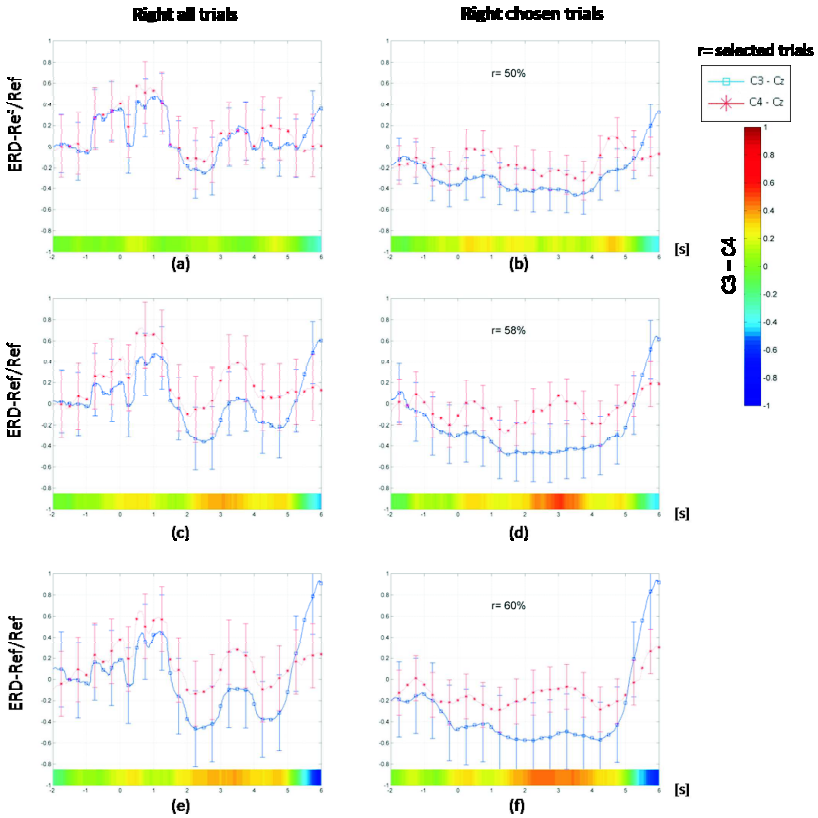

Figure D.29: Event-Related Desynchronization (ERD) and Synchronization (ERS) of subject 3 during real right Open & close movement, referenced to Cz scalp sensors using an auditory clue. (a)/(b) First Alpha. (c)/(d) Second Alpha. (e)/(f) High Alpha.

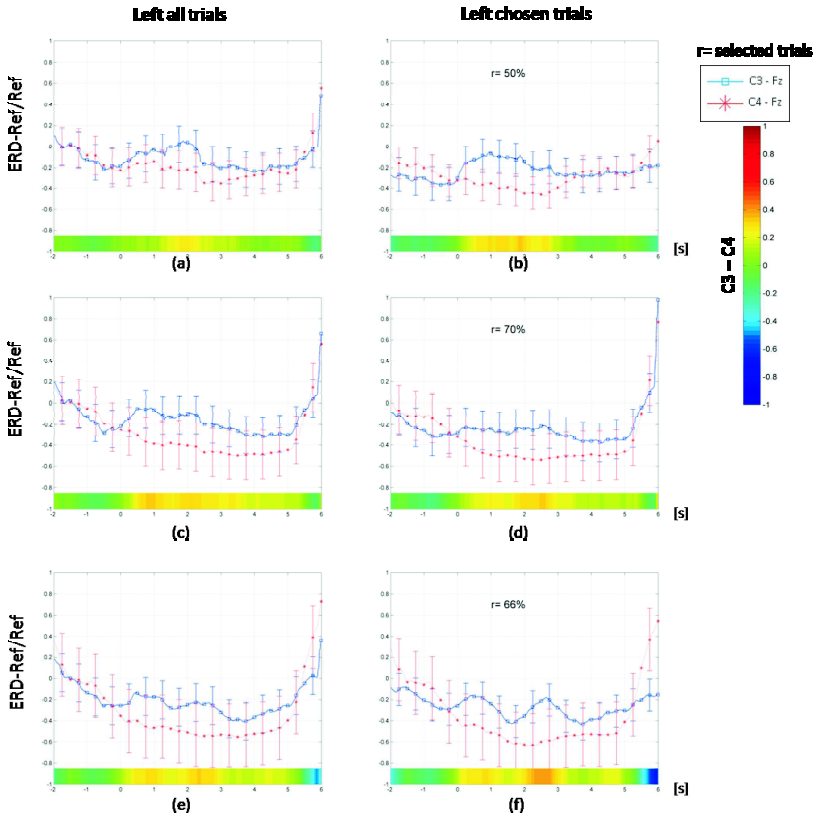

Figure D.30: Event-Related Desynchronization (ERD) and Synchronization (ERS) of subject 3 during real left Up & down movement, referenced to Fz scalp sensors using an auditory clue. (a)/(b) First Alpha. (c)/(d) Second Alpha. (e)/(f) High Alpha.

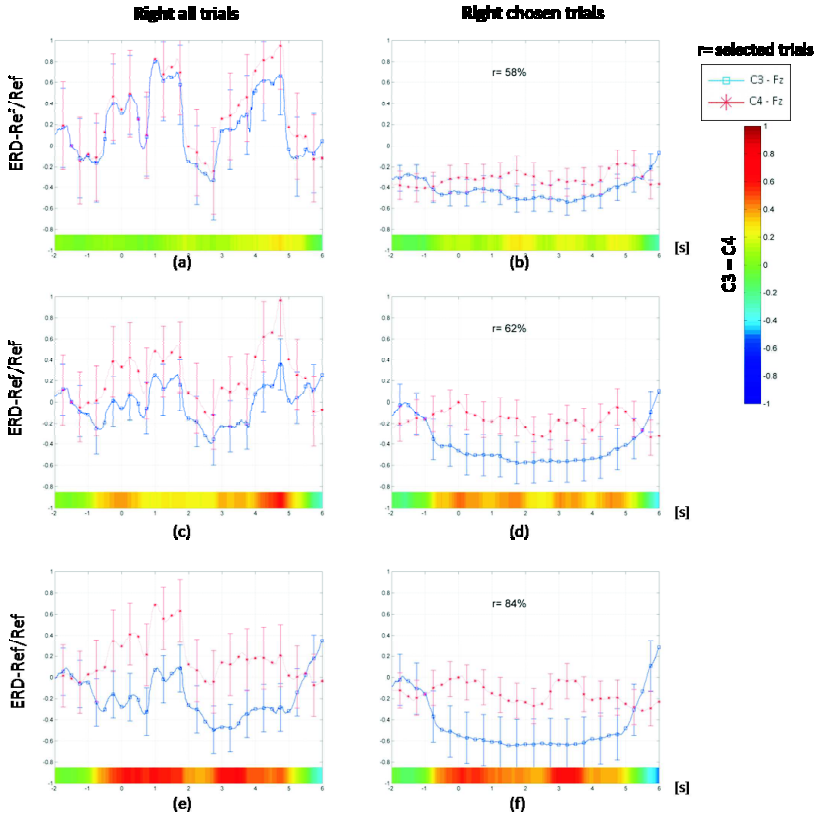

Figure D.31: Event-Related Desynchronization (ERD) and Synchronization (ERS) of subject 3 during real right Up & down movement, referenced to Fz scalp sensors using an auditory clue. (a)/(b) First Alpha. (c)/(d) Second Alpha. (e)/(f) High Alpha.

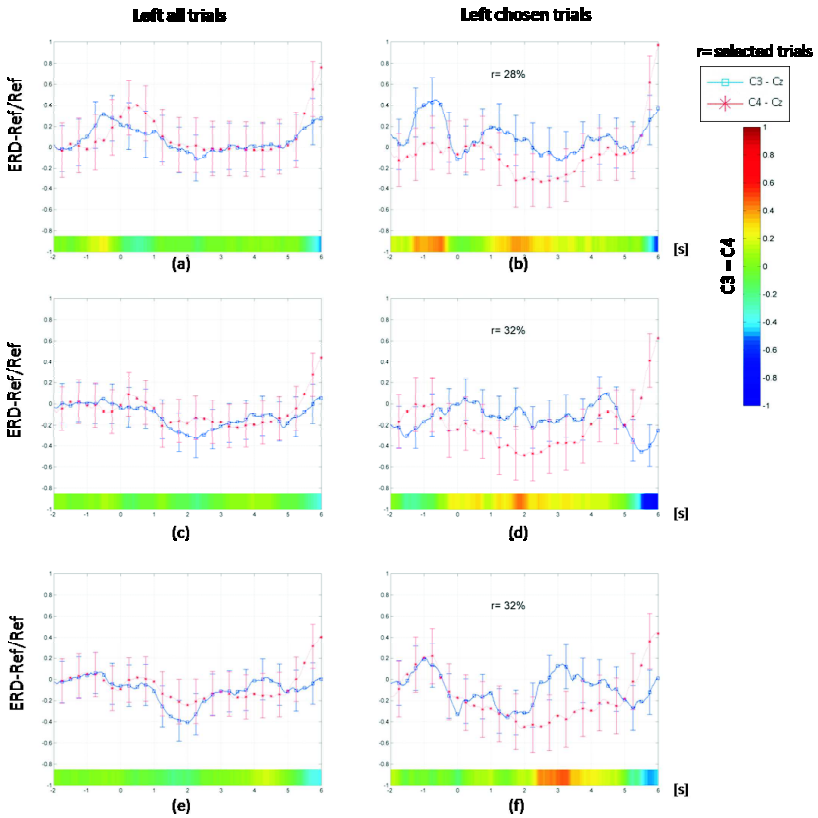

Figure D.32: Event-Related Desynchronization (ERD) and Synchronization (ERS) of subject 3 during imaginary left muscle movement, referenced to Cz scalp sensors using an auditory clue. (a)/(b) First Alpha. (c)/(d) Second Alpha. (e)/(f) High Alpha.

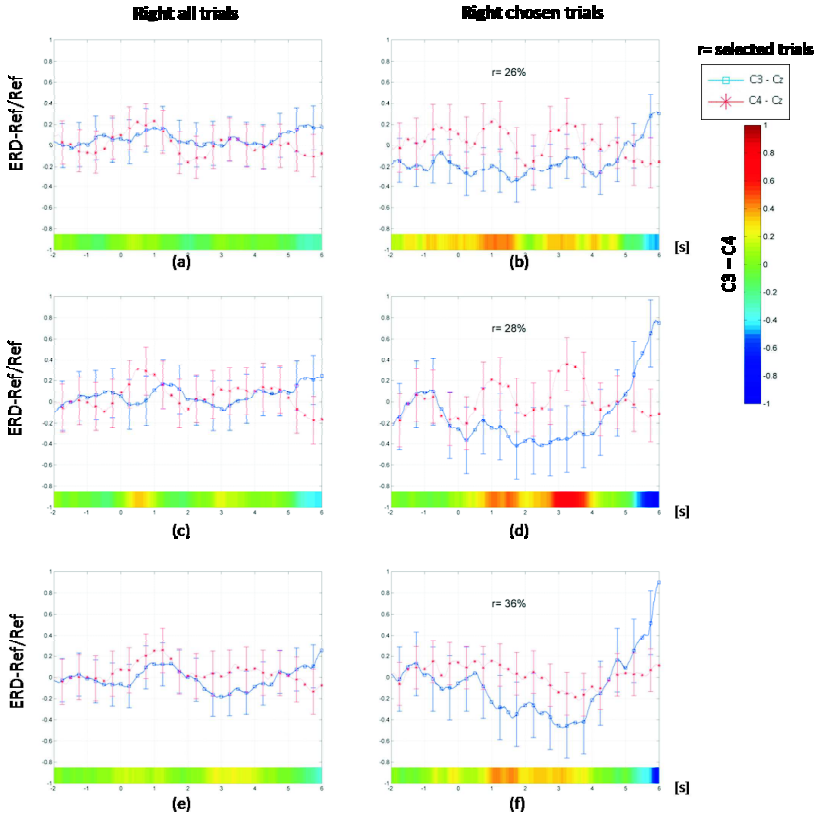

Figure D.33: Event-Related Desynchronization (ERD) and Synchronization (ERS) of subject 3 during imaginary right muscle movement, referenced to Cz scalp sensors using an auditory clue. (a)/(b) First Alpha. (c)/(d) Second Alpha. (e)/(f) High Alpha.

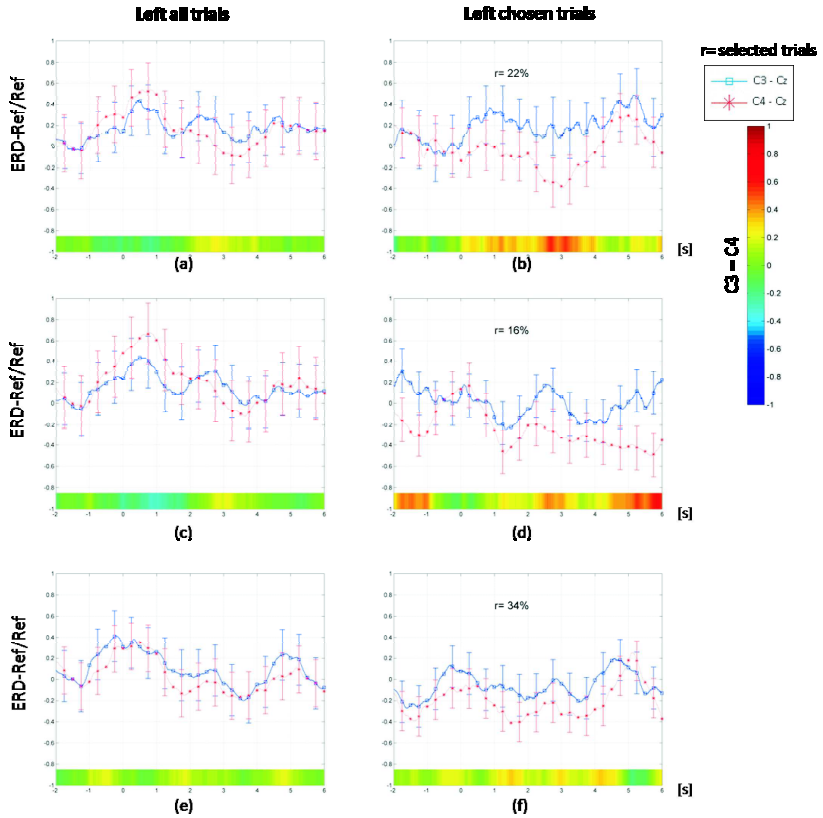

Figure D.34: Event-Related Desynchronization (ERD) and Synchronization (ERS) of subject 3 during imaginary left visual movement, referenced to Cz scalp sensors using an auditory clue. (a)/(b) First Alpha. (c)/(d) Second Alpha. (e)/(f) High Alpha.

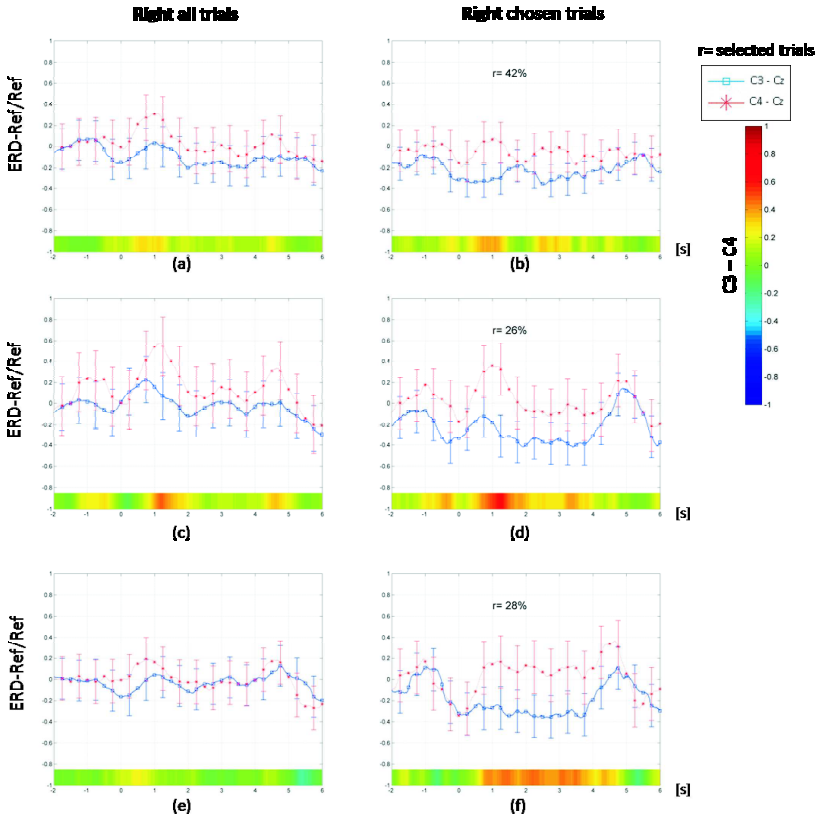

Figure D.35: Event-Related Desynchronization (ERD) and Synchronization (ERS) of subject 3 during imaginary right visual movement, referenced to Cz scalp sensors using an auditory clue. (a)/(b) First Alpha. (c)/(d) Second Alpha. (e)/(f) High Alpha.

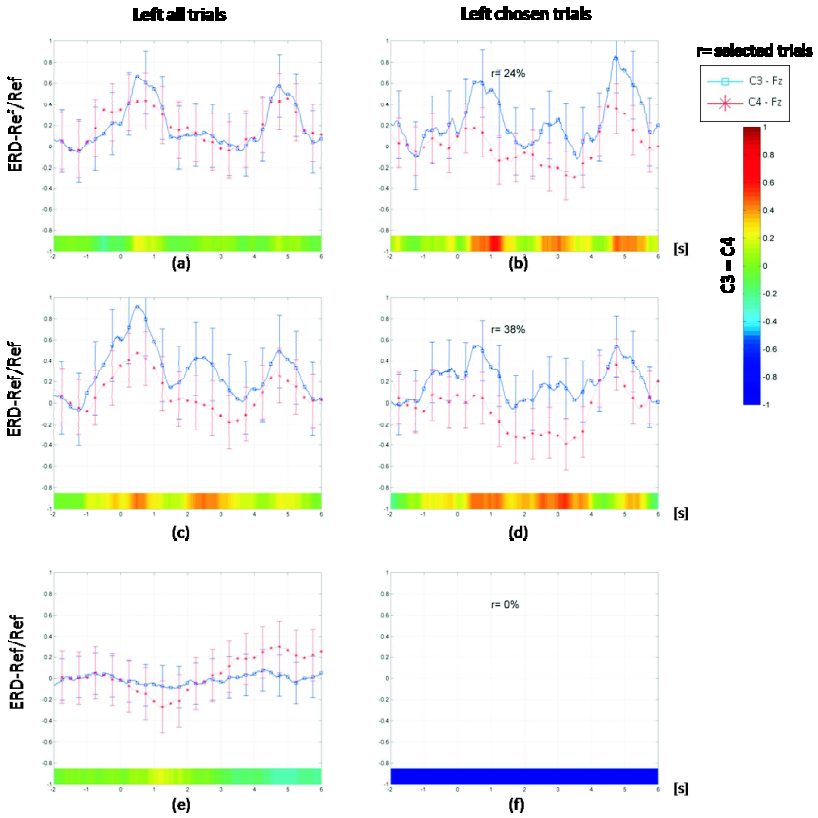

Figure D.36: Event-Related Desynchronization (ERD) and Synchronization (ERS) of subject 3 during imaginary left visual movement, referenced to Fz scalp sensors using an auditory clue. (a)/(b) First Alpha. (c)/(d) Second Alpha. (e)/(f) High Alpha.

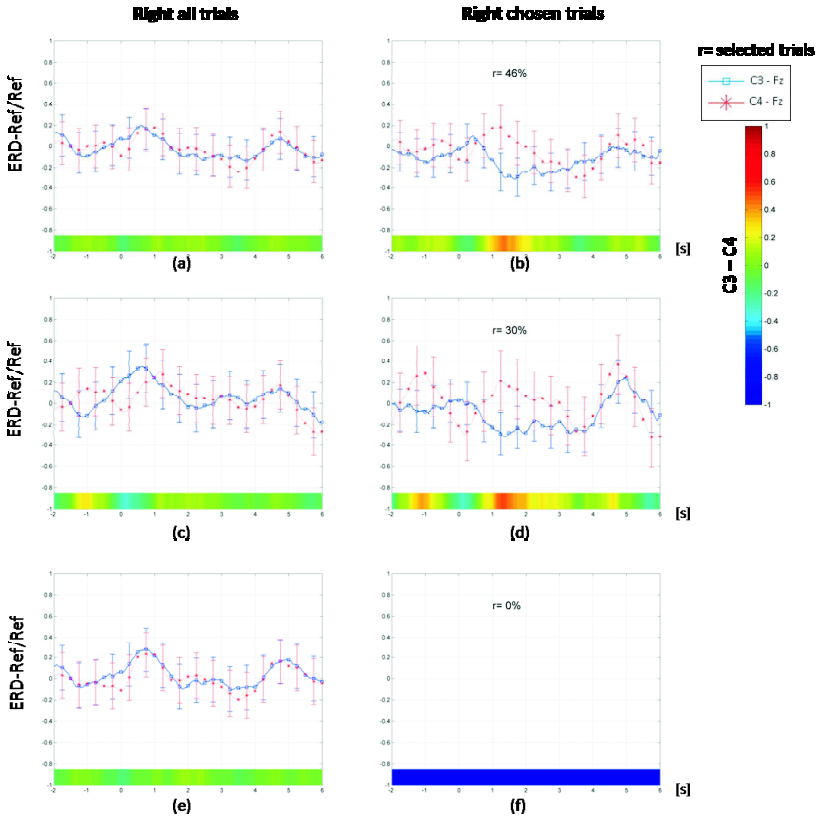

Figure D.37: Event-Related Desynchronization (ERD) and Synchronization (ERS) of subject 3 during imaginary right visual movement, referenced to Cz scalp sensors using an auditory clue. (a)/(b) First Alpha. (c)/(d) Second Alpha. (e)/(f) High Alpha.

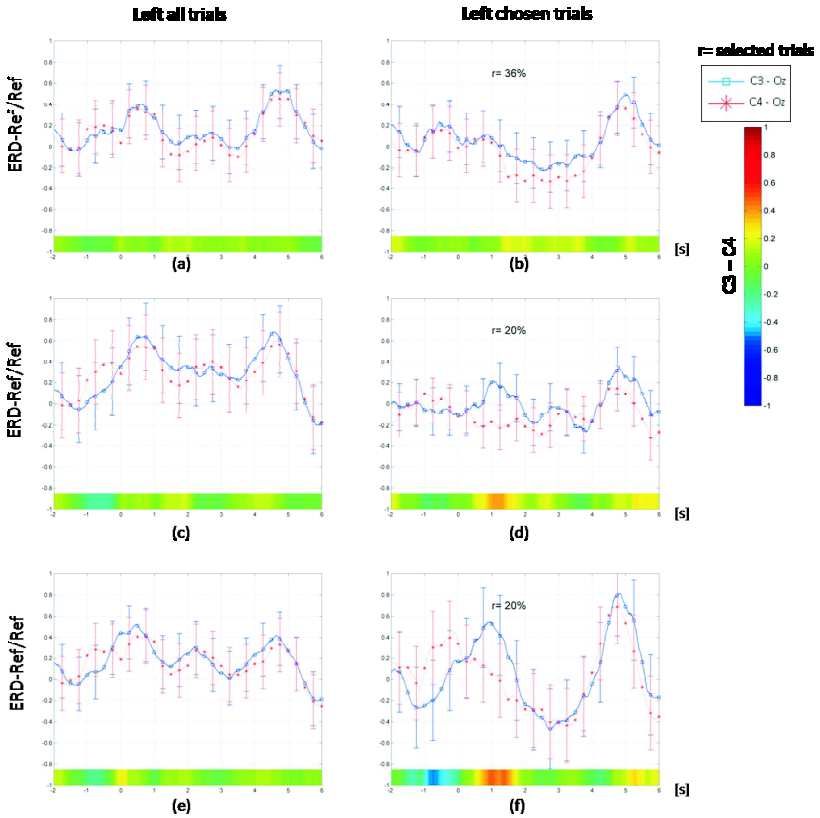

Figure D.38: Event-Related Desynchronization (ERD) and Synchronization (ERS) of subject 3 during imaginary left visual movement, referenced to Oz scalp sensors using an auditory clue. (a)/(b) First Alpha. (c)/(d) Second Alpha. (e)/(f) High Alpha.

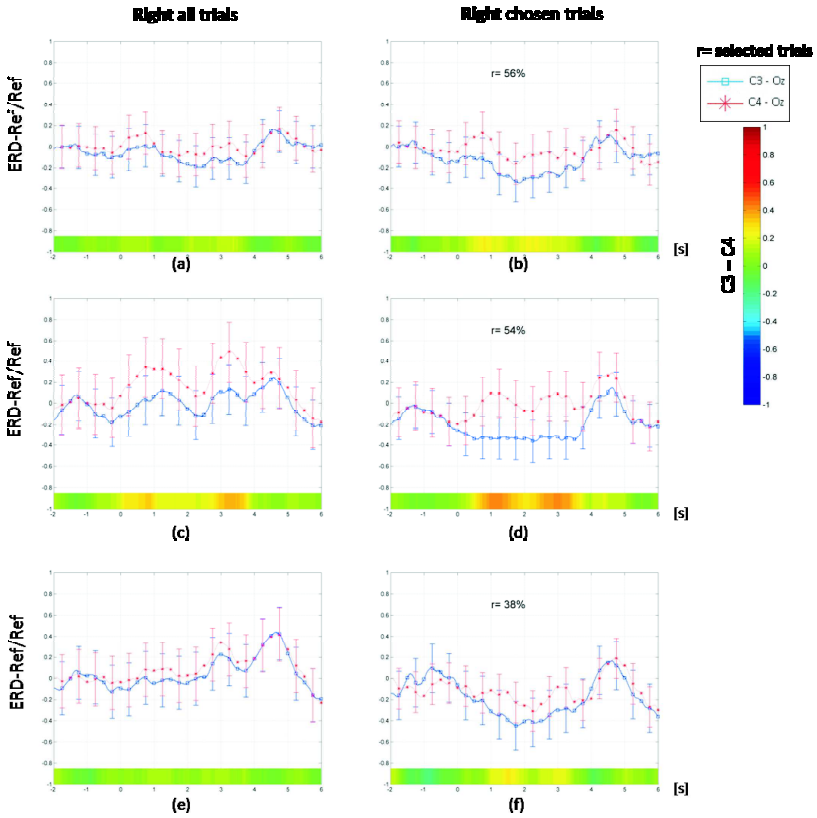

Figure D.39: Event-Related Desynchronization (ERD) and Synchronization (ERS) of subject 3 during imaginary right visual movement, referenced to Oz scalp sensors using an auditory clue. (a)/(b) First Alpha. (c)/(d) Second Alpha. (e)/(f) High Alpha.

Subject 4: ERS/ERD in frequency bands

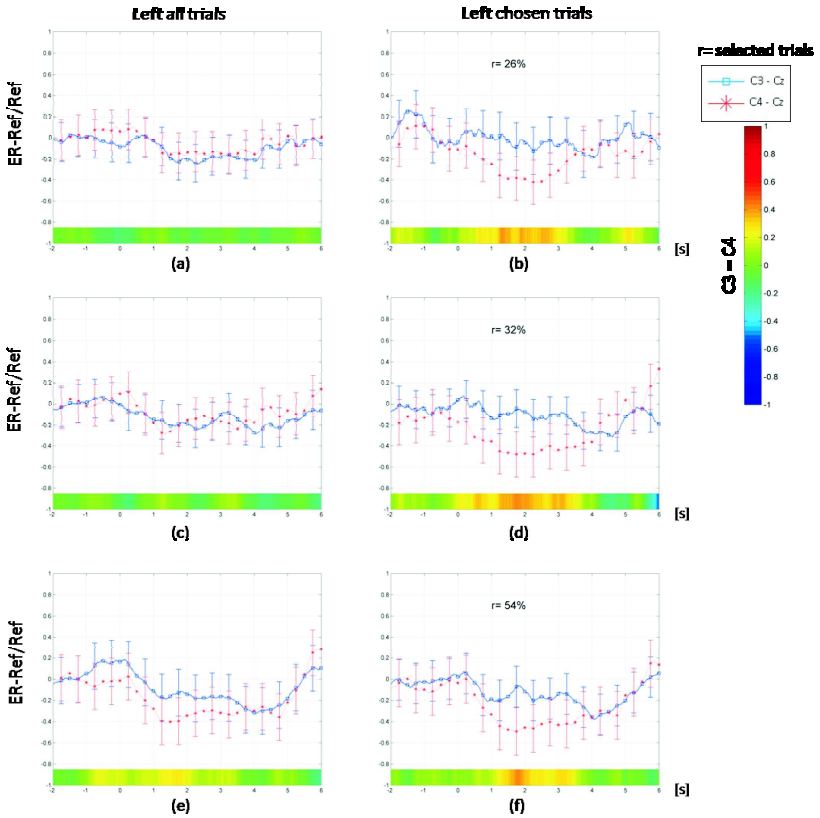

Figure D.40: Event-Related Desynchronization (ERD) and Synchronization (ERS) of subject 4 during real left Open & close movement, referenced to Cz scalp sensors using an auditory clue. (a)/(b) First Alpha. (c)/(d) Second Alpha. (e)/(f) High Alpha.

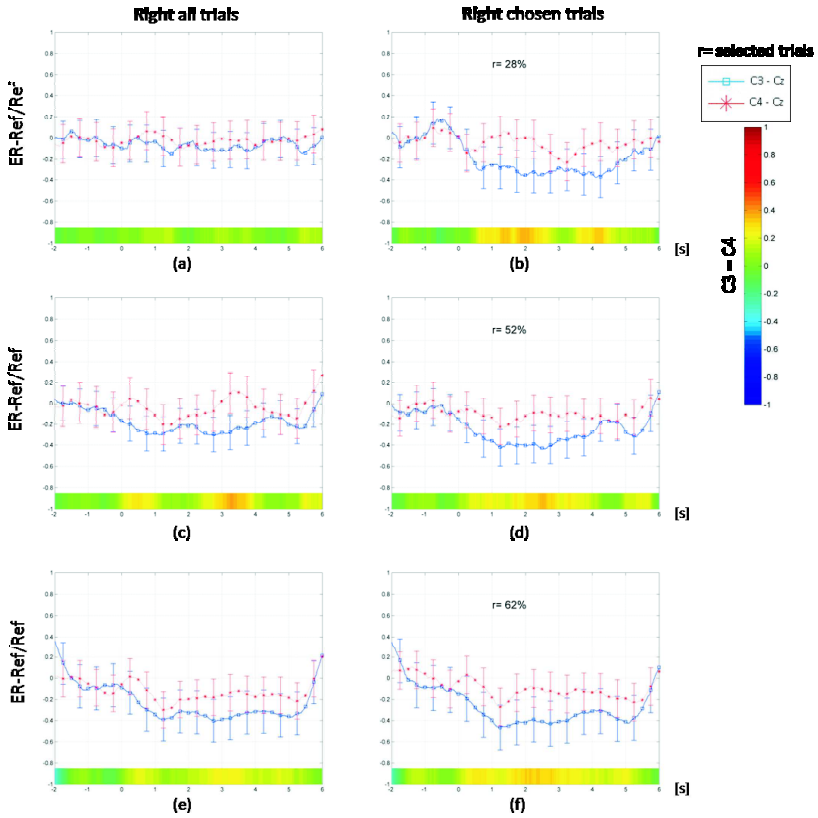

Figure D.41: Event-Related Desynchronization (ERD) and Synchronization (ERS) of subject 4 during real right Open & close movement, referenced to Cz scalp sensors using an auditory clue. (a)/(b) First Alpha. (c)/(d) Second Alpha. (e)/(f) High Alpha.

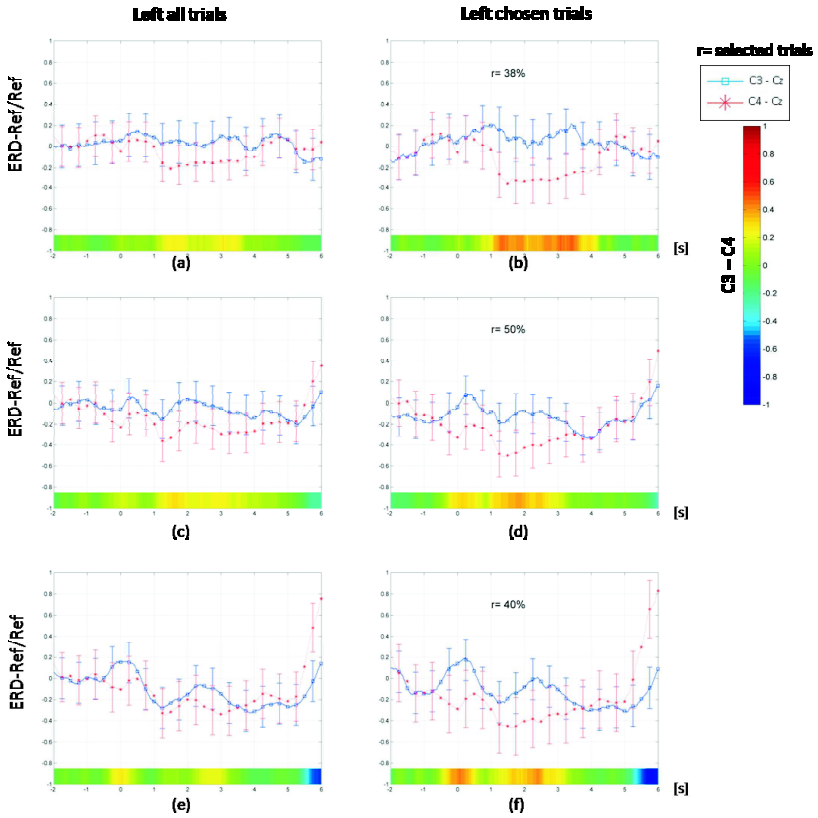

Figure D.42: Event-Related Desynchronization (ERD) and Synchronization (ERS) of subject 4 during real right Up & down movement, referenced to Cz scalp sensors using an auditory clue. (a)/(b) First Alpha. (c)/(d) Second Alpha. (e)/(f) High Alpha.

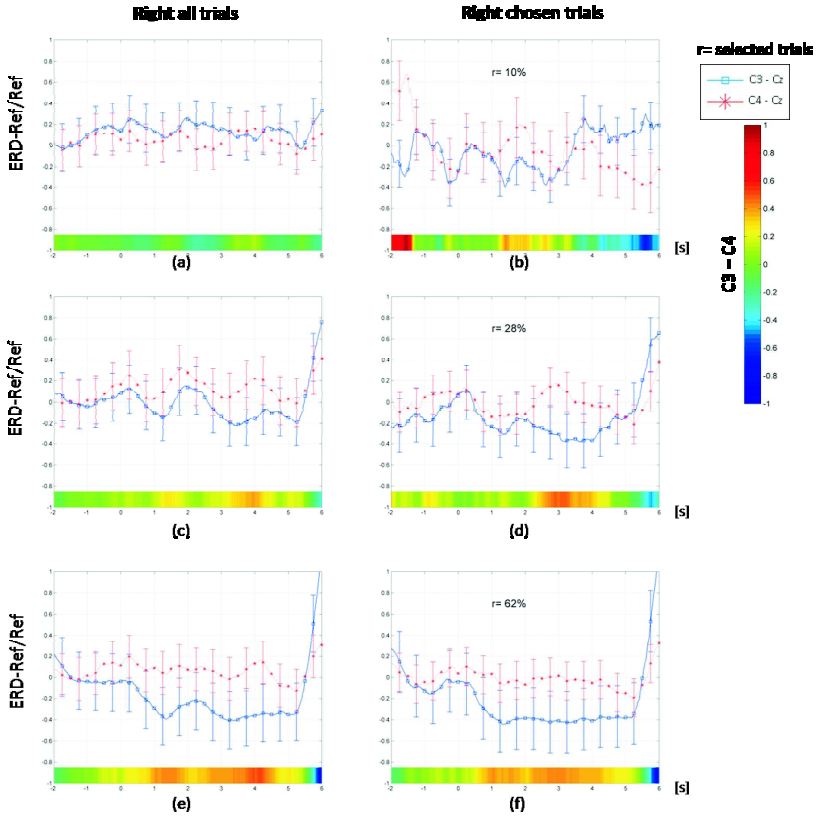

Figure D.43: Event-Related Desynchronization (ERD) and Synchronization (ERS) of subject 4 during real left Up & down movement, referenced to Cz scalp sensors using an auditory clue. (a)/(b) First Alpha. (c)/(d) Second Alpha. (e)/(f) High Alpha.

Appendix E

Data from BCI competition IV

E.1 Format of the Data

Given the continuous signals of 59 EEG channels and, for the calibration data, markers that indicate the time points of cue presentation and the corresponding target classes are given. This appendix explain the organization of the data given and the structure of it.

Data is provided in Matlab format (∗.mat) containing the following variables:

- cnt: the continuous EEG signals, size [time x channels]. The array is stored in datatype INT16. To convert it to uV values, use cnt= 0.1∗double(cnt); in Matlab.
- mrk: structure of target cue information with fields (the file of evaluation data does *not* contain this variable)
  - pos: vector of positions of the cue in the EEG signals given in unit *sample*, length # cues
  - y: vector of target classes (-1 for class one or 1 for class two), length # cues
- nfo: structure providing additional information with fields
  - fs: sampling rate,
  - clab: cell array of channel labels,
  - classes: cell array of the names of the motor imagery imaginary classes,
  - xpos: x-position of electrodes in a 2d-projection,
  - ypos: y-position of electrodes in a 2d-projection.
- As an alternative, data is also provided in zipped **ASC II** format:
  - ∗_cnt.txt: the continuous EEG signals, where each row contains the values for all channels at a specific time point
  - ∗_mrk.txt: target cue information, each row represents one cue where the first value defines the time point (given in unit *sample*), and the second value the target class (-1 for class one or 1 for class two). For evaluation data no ∗_mrk.txt file is provided.
  - ∗_nfo.txt: contains other information as described for the Matlab format.

Appendix F

Appendix: Intern day

Intern day

The Philips Intern Day is the main activity organized by the Philips Intern Committee together with the EMEA Recruitment Services (ERS) and is held for all interns who are currently doing their internship at a division of Philips in the Netherlands. During the day guest speakers discuss the latest news from a variety of interesting topics and give information about Philips and possible future careers at Philips. It is possible to participate in discussion workshops for any special working area in order to obtain information from recruiters and young employees about working at Philips. Also, it is useful to have plenty of time for more informal interaction. The Intern Day is a great way to meet interns and share experiences.

Figure F.1: Picture of the Intern Philips Day, 28 November 2008, during the presentation of "Electroencephalogram Processing in Brain-Computer Interfaces" by Arnau Espinosa.

Poster session

Background

One of the ingredients of the upcoming Philips Intern Day is a poster session. The session is an opportunity to present a project to other interns and show the knowledge gathered during an internship. It further gives a good change to find out more about the diversity of Philips. This can help to get better insights about opportunities within Philips. Last but not least, the poster sessions give the opportunity to learn how to make an appealing poster and how to present a topic efficiently.

The simple rules

A poster is a visual communication tool that is used to explain the main points to as many people as possible. It further provides the audience with a source of information, and of it is a nice way to start a conversation and meet other people. In order to keep the whole process very simple we included some general rules for creating an appealing poster which send out the message that we wanted to transmit. In this way, all the posters provide a common appearance and fulfill some simple layout rules. The poster will be printed in color, A1 size, and be presented at the intern day. During the intern day time is being scheduled for each poster session, in which is possible to talk about the poster with others in an informal way.

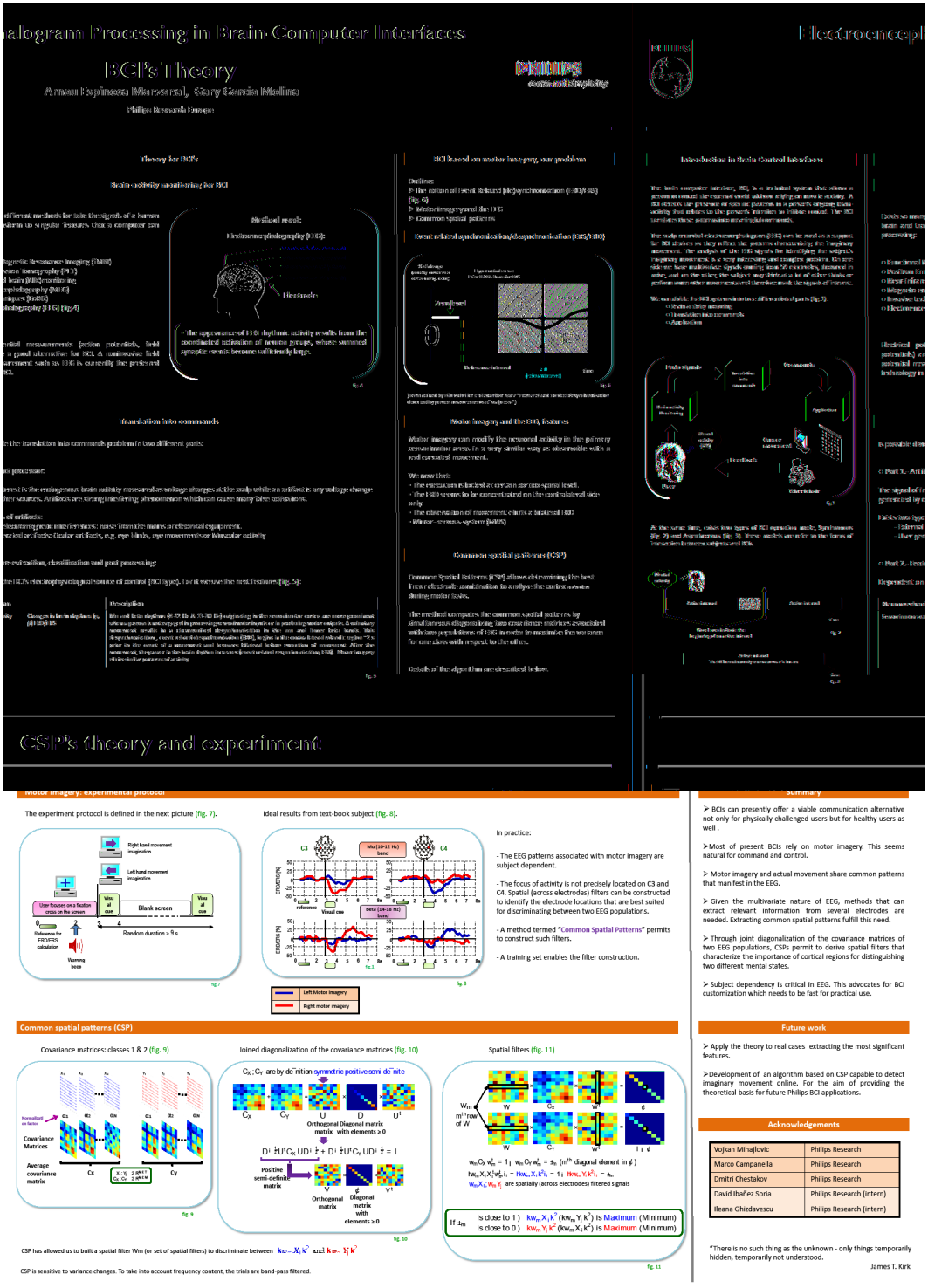

Figure F.2: Poster: "Electroencephalogram Processing in Brain-Computer Interfaces" by Arnau Espinosa and Gary Garcia

Bibliography

[1] H. Burger. Uber das electroencephalogram des menschen. *Archiv fur Psychiatrie und Nervenkrankheiten*, 87:527–570, 1929.

[2] E. R. Kandel, J. H. Schwartz, and T. M. Jessell. *Principles of neural science*. Appleton and Lange, 2000.

[3] A. C. Guyton and J. E. Hall. *Human physiology and mechanisms of disease*. Saunders Philadelphia, 1982.

[4] J. M. Stern and J. Engel. *Atlas of EEG patterns*. Lippincott Williams and Wilkins, 2004.

[5] G. H. Klem, H. O. LÃijders, H. H. Jasper, and C. Elger. The ten-twenty electrode system of the international federation. the international federation of clinical neurophysiology. *Electroencephalography and clinical neurophysiology. Supplement*, 52:3, 1999.

[6] G. Pfurtscheller and F. H. Lopes da Silva. Functional meaning of event-related desynchronization (erd) and synchronization (ers). *Handbook of Electroencephalography, Clinical Neurophysiology. Elsevier Science, Amsterdam*, 1999.

[7] B. Blankertz, R. Tomioka, S. Lemm, M. Kawanabe, and K. Muller. Optimizing spatial filters for robust eeg single-trial analysis. *IEEE Signal Processing Magazine*, 25(1):41, 2008.

[8] W. Klimesch. Eeg alpha and theta oscillations reflect cognitive and memory performance: a review and analysis. *Brain Research Reviews*, 29(2-3):169–195, 1999.

[9] G. E. Burch and N. P. DePasquale. *A history of electrocardiography*. Norman Publishing, 1990.

[10] C. Blakemore, Corporation British Broadcasting, and Commission Australian Broadcasting. *Mechanics of the Mind*. Cambridge University Press New York, 1977.

[11] D. J. McFarland, C. W. Anderson, K. Muller, A. Schlogl, and D. J. Krusienski. Bci meeting 2005-workshop on bci signal processing: feature extraction and translation. *IEEE Transactions on Neural Systems and Rehabilitation Engineering*, 14(2):135, 2006.

[12] R. O. Duda, P. E. Hart, and D. G. Stork. *Pattern classification*. Wiley New York, 2001.

[13] J. R. Wolpaw, N. Birbaumer, W. J. Heetderks, D. J. McFarland, P. H. Peckham, G. Schalk, E. Donchin, L. A. Quatrano, C. J. Robinson, and T. M. Vaughan. Brain-computer interface technology: A review of the first international meeting. *IEEE Transactions on Rehabilitation Engineering*, 8(2):164–173, 2000.

[14] E. Donchin, K. M. Spencer, and R. Wijesinghe. The mental prosthesis: assessing the speed of a p300-basedbrain-computer interface. *IEEE Transactions on Rehabilitation Engineering*, 8(2):174–179, 2000.

[15] T. M. Vaughan. Guest editorial brain-computer interface technology: a review of the second international meeting. *IEEE Transactions on Neural Systems and Rehabilitation Engineering*, 11(2):94–109, 2003.

[16] H. Wolosker, E. Dumin, L. Balan, and V. N. Foltyn. d-amino acids in the brain: d-serine in neurotransmission and neurodegeneration. *FEBS Journal*, 275(14):3514–3526, 2008.

[17] B. Hjorth. An on-line transformation of eeg scalp potentials into orthogonal source derivations. *Electroencephalogr Clin Neurophysiol*, 39(5):526–30, 1975.

[18] W. J. Freeman, M. D. Holmes, B. C. Burke, and S. Vanhatalo. Spatial spectra of scalp eeg and emg from awake humans. *Clinical Neurophysiology*, 114(6):1053–1068, 2003.

[19] B. He and R. J. Cohen. Body surface laplacian ecg mapping. *IEEE Transactions on Biomedical Engineering*, 39(11):1179–1191, 1992.

[20] T. I. Alecu, S. Voloshynovskiy, and T. Pun. Eeg cortical imaging: a vector field approach for laplacian denoising and missing data estimation. pages 1335–1338, 2004. IEEE International Symposium on Biomedical Imaging: Nano to Macro, 2004.

[21] T. L. Lee-Chiong. *Sleep: a comprehensive handbook*. Wiley-Liss, 2005.

[22] G. Pfurtscheller and F. H. Lopes da Silva. Event-related eeg/meg synchronization and desynchronization: basic principles. *Clinical Neurophysiology*, 110(11):1842–1857, 1999.

[23] G. Pfurtscheller, C. Neuper, G. R. Muller, B. Obermaier, G. Krausz, A. Schlogl, R. Scherer, B. Graimann, C. Keinrath, and D. Skliris. Graz-bci: state of the art and clinical applications. *IEEE Transactions on Neural Systems and Rehabilitation Engineering*, 11(2):1–4, 2003.

[24] G. Pfurtscheller, C. Brunner, A. SchlÃűgl, and F. H. Lopes da Silva. Mu rhythm (de) synchronization and eeg single-trial classification of different motor imagery tasks. *Neuroimage*, 31(1):153–159, 2006.

[25] M. Cheng, W. Jia, X. Gao, S. Gao, and F. Yang. Mu rhythm-based cursor control: an offline analysis. *Clinical Neurophysiology*, 115(4):745–751, 2004.

[26] H. Ramoser, J. Muller-Gerking, and G. Pfurtscheller. Optimal spatial filtering of single trial eeg during imagined handmovement. *IEEE Transactions on Rehabilitation Engineering*, 8(4):441–446, 2000.

[27] M. Pregenzer and G. Pfurtscheller. Frequency component selection for an eeg-based brain to computerinterface. *IEEE Transactions on Rehabilitation Engineering*, 7(4):413–419, 1999.

[28] B. Blankertz, G. Dornhege, M. Krauledat, K. R. MÃijller, and G. Curio. The non-invasive berlin brainâĂŞcomputer interface: fast acquisition of effective performance in untrained subjects. *NeuroImage*, 37(2):539–550, 2007.

[29] L. Rabiner. On the use of autocorrelation analysis for pitch detection. *IEEE transactions on acoustics, speech and signal processing*, 25(1):24–33, 1977.

[30] J. Muthuswamy and N. V. Thakor. Spectral analysis methods for neurological signals. *Journal of Neuroscience Methods*, 83(1):1–14, 1998.

[31] J. Cadzow. Digital notch filter design procedure. *IEEE Transactions on Acoustics, Speech and Signal Processing*, 22(1):10–15, 1974.

[32] S. C. Pei and C. C. Tseng. Two dimensional iir digital notch filter design. *IEEE Transactions on Circuits and Systems II: Analog and Digital Signal Processing*, 41(3):227–231, 1994.

[33] K. Hirano, S. Nishimura, and S. Mitra. Design of digital notch filters. *Communications, IEEE Transactions on [legacy, pre-1988]*, 22(7):964–970, 1974.

[34] C. C. Tseng and S. C. Pei. Stable iir notch filter design with optimal pole placement. *IEEE Transactions on Signal Processing*, 49(11):2673–2681, 2001.

[35] S. Romero, M. A. MaÃśanas, and M. J. Barbanoj. A comparative study of automatic techniques for ocular artifact reduction in spontaneous eeg signals based on clinical target variables: A simulation case. *Computers in Biology and Medicine*, 2007.

[36] S. Dastmalchi. *Functional brain imaging: extracting temporal responses of multiple cortical areas from multi-focal visual evoked potentials*. PhD thesis, UNIVERSITY OF CALIFORNIA, 2003.

[37] G. N. G. Molina. *Direct Brain-Computer Communication Through Scalp Recorded EEG signals*. Lausane: ÃL'cole Polytechnique FÃl'dÃl'rale de Lausane, 2004.

[38] V. Morash, O. Bai, S. Furlani, P. Lin, and M. Hallett. Classifying eeg signals preceding right hand, left hand, tongue, and right foot movements and motor imageries. *Clinical Neurophysiology*, 119(11):2570–2578, 2008.

[39] J. Shlens. A tutorial on principal component analysis. *Systems Neurobiology Laboratory, University of California at San Diego*, 2005.

[40] Y. Wang, Z. Zhang, Y. Li, X. Gao, S. Gao, and F. Yang. Bci competition 2003-data set iv: an algorithm based on cssd and fda for classifying single-trial eeg. *IEEE Transactions on Biomedical Engineering*, 51(6):1081–1086, 2004.

[41] K. Fukunaga. *Introduction to statistical pattern recognition*. Academic press, 1990.

[42] Y. Wang, P. Berg, and M. Scherg. Common spatial subspace decomposition applied to analysis of brain responses under multiple task conditions: a simulation study. *Clinical Neurophysiology*, 110(4):604–614, 1999.

[43] K. R. MÃijller, M. Tangermann, G. Dornhege, M. Krauledat, G. Curio, and B. Blankertz. Machine learning for real-time single-trial eeg-analysis: From brainâĂŞcomputer interfacing to mental state monitoring. *Journal of Neuroscience Methods*, 167(1):82–90, 2007.

[44] M. Welling. Fisher linear discriminant analysis. *Department of Computer Science, University of Toronto*, 2006.

[45] I. Nabney. *NETLAB: algorithms for pattern recognition*. Springer, 2002.

[46] K. R. Muller, C. W. Anderson, and G. E. Birch. Linear and nonlinear methods for brain-computer interfaces. *IEEE Transactions on Neural Systems and Rehabilitation Engineering*, 11(2):165–169, 2003.

[47] L. Mingyu, J. Hongbing, and Z. Chunhong. Event related potentials extraction from eeg using artificial neural network.

[48] Y. Wang, S. Gao, and X. Gao. Common spatial pattern method for channel selelction in motor imagery based brain-computer interface. 2005.

[49] P. M. T. Broersen and H. E. Wensink. Autoregressive model order selection by a finite sample estimator for the kullback-leibler discrepancy. *IEEE Transactions on Signal Processing*, 46(7):2058–2061, 1998.

[50] C. W. Anderson, E. A. Stolz, and S. Shamsunder. Multivariate autoregressive models for classification ofvspontaneous electroencephalographic signals during mental tasks. *IEEE Transactions on Biomedical Engineering*, 45(3):277–286, 1998.

[51] A. Kachenoura, L. Albera, L. Senhadji, and P. Comon. Ica: a potential tool for bci systems. *IEEE Signal Processing Magazine*, 25(1):57, 2008.

[52] B. Kamousi, Z. Liu, and B. He. Classification of motor imagery tasks for brain-computer interface applications by means of two equivalent dipoles analysis. *IEEE Transactions on Neural Systems and Rehabilitation Engineering*, 13(2):166–171, 2005.

[53] G. Besio, K. Koka, R. Aakula, and W. Dai. Tri-polar concentric ring electrode development for laplacian electroencephalography. *IEEE Transactions on Biomedical Engineering*, 53(5):926–933, 2006.

[54] M. J. Corinthios. Complex-variable distribution theory for laplace and z transforms. *IEEE Proceedings-Vision, Image and Signal Processing*, 152(1):97–106, 2005.

[55] B. He, D. Yao, J. Lian, and D. Wu. An equivalent current source model and laplacian weighted minimum norm current estimates of brain electrical activity. *IEEE Transactions on Biomedical Engineering*, 49(4):277–288, 2002.

